Groundwater quantity and quality assessment for Aquifer Recharge in Ohangwena region, Namibia

Prepared by:

Hilja Ndakola, BSc. Civil Eng.

Supervised by:

John Okedi. BSc.Civil Eng, MSc water Res. Eng, PhD

Dissertation submitted in fulfillment of the requirements for the degree of Masters of Science in Civil Engineering (MSc)

Department of Civil Engineering

University of Cape Town, Private Bag Rondebosch, 7700

South Africa

(14 September 2022)

Declaration

I know the meaning of plagiarism and declare that all the work in the document, for that which is properly acknowledged, is my own. This thesis/dissertation has been submitted to the Turnitin module (or equivalent similarity and originality checking software) and I confirm that my supervisor has seen my report and any concerns revealed by such have been resolved with my supervisor. I have used the Harvard convention for citation and referencing. Each significant contribution to and quotation in this report from the work or works of other people has been attributed and has been cited and referenced. I have not allowed and will not allow anyone to copy my work to pass it as his or her Work.

Signed: _Signed by candidate_____ Date: _____14/09/2022_____

Dedication

I would like to dedicate this report to my mother (Hileni Shetunyenga), my brother (Andreas Ndakola), and my sister (Selma Ndakola) who have been my main source of support and motivation throughout my years of study at the University of Cape Town, and everyone who has challenged me to be my very best.

Acknowledgment

First and foremost, I would like to thank the Lord Almighty God for the love and support he has shown, as well as the protection and guidance throughout this research project, and in my two years of study at the University of Cape Town. My sincere gratitude goes to everybody who offered me assistance and encouragement during my research project period, and during the compilation of this report. Many thanks go to the University of Namibia (UNAM) and GIZ for the financial support they have given me to pursue an MSc. Degree in Civil Engineering. It is through their valued support that I was able to come this far, and I highly appreciate it.

This project has been made successful through constant advice and guidance from my supervisor Dr. John Okedi. In this regard, I would like to pay my heartfelt gratitude to him for his time, constant encouragement, and supervision throughout the entire duration of the project.

Last but not least, I wish to tremendously thank my family and friends for their countless efforts, as well as my fellow students for their support during my studies at the University of Cape Town. I also appreciate the USGS for providing free MODFLOW software used in this study, and the Namibian Ministry of Agriculture, Water and Land Reform, and Ondangwa Meteorological Services for the data used in this study.

Abstract

The high population growth rate and changing climatic conditions for the Ohangwena region create increasing pressure on the local water balance. As groundwater demands increase and availability declines, sustainable groundwater management is required for the Ohangwena region. This thesis assessed the suitability of using runoff for aquifer recharge to augment groundwater in the Ohangwena region and minimize the lowering of water table. The Geographical Information System (GIS) and groundwater flow models were used in this study to assess the water resources in the study area.

A multicriteria approach using a weighted rating was used in this study to generate a map showing areas suitable for groundwater recharge. The resultant groundwater potential recharge zones map was produced based on the overall weights of seven influential factors for groundwater recharge namely lithology, land use/land cover, lineaments, drainage, slope, geology, and soil type. The results of the assessment indicated that 85% of the Ohangwena region is characterized by high groundwater recharge zones, while 25% is characterized by very high groundwater recharge zones. The very high groundwater recharge zones are mostly found in the central part of the region, on the far upper western side and the eastern side of the region.

The recorded recharge rates for the region in the range of 40 – 60 mm/year were introduced to an established model using the MODFLOW software, to assess the impact of Aquifer Recharge on the groundwater levels. The impact was assessed with both the steady-state model to approximate aquifer recharge under controlled conditions, and the transient state model for close representation of recharge in reality at four wells namely, WW201045, WW201637, WW201634, and WW20267, where it was evaluated by the hydraulic heads and water budget analysis. The steady state model results indicated a change in groundwater levels in the range of -0.10 - 0.70 m. In the same manner, the transient state model results show a gradual increase in groundwater levels in the range of 9.2 - 12.10 meters for the 350 m deep Ohangwena aquifer. The groundwater levels can be improved locally by infiltrating runoff into the KOH-II aquifer via the injection wells or infiltration basins during the rainy season (November to April) when there is plenty of runoff and flood in the region. The high soil infiltration rates in the region make runoff to be suitable for Aquifer Recharge implementation in the region. Transferring runoff to the aquifer aims at making use of the large aquifer storage space and limiting evaporation loss.

The study also employed particle tracking and MT3DMS to assess the transport of contaminants associated with runoff within the aquifer. This was assessed at two wells that served as injection wells in the model, and four contaminants namely chloride, Electrical Conductivity, Total Dissolved Solids, and *E-coli* were studied. The outcomes of this assessment indicated that both Chloride, Electrical conductivity, Total Dissolved Solids, and *E-coli* concentrations decrease from 1000 mg/l to 0.01 mg/l, 532 mS/s to 0.1, 478.56 mg/l to 0.01 mg/l, and 9.58 to 0.01 respectively as timesteps increase, and it takes 20 timesteps (94672800 seconds) for them to disperse further into the aquifer. The dispersion of Chloride, EC, TDS, and *E-coli* within the aquifer covers a maximum distance of 12.1, 9.6, 8.7, and 6.7 km respectively.

TABLE OF CONTENTS

List of Figures

List of Tables

List of Equations

Acronyms and Abbreviations

AHP	Analytical Hierarchical Processing Method
ADV	Advection Package
AR	Aquifer Recharge
ASR	Aquifer Storage Recovery
ASTR	Aquifer Storage Transfer Recovery
BGR	Bundesansalt fur Geowissenschaften und Rohstoffe-Federal institute (German Federal Institute for Geosciences and Natural Resources)
BTN	Basic Transport Package
CEB	Cuvelai Etosha Basin
CHD	Constant Head Boundary
CMB	Chloride Mass Balance
DEM	Digital ElevationModel
DPA	Discontinuous Perched Aquifer
DRN	Drainage Package
DSP	Dispersion Package
DWA	Department of Water Affairs
E	East
EC	Electrical Conductivity
ET	Evapotranspiration
EVT	Evapotranspiration Package
GCG	Generalized Conjugate Gradient Package Solver
GHB	General Head Boundary
GIS	Geographic Information System
GMS	Groundwater Modeling Software
GUI	Graphical User Interface
HOB	Head Observation Package
IGRAC	International Groundwater Resources Assessment Centre
IWRM	Integrated Water Resources Management

KOH	Kalahari Ohangwena Aquifer (Ohangwena multi – layered aquifer)
MAR	Managed Aquifer Recharge
MCDA	Multi-Criteria Decision Analysis
MDG	Millenium Development Goal
MMR	Mean Monthly Rainfall
MODFLOW	3 Dimensional finite difference numerical flow model
MODPATH	Numerical finite model
MSA	Main Shallow Aquifer
MT3DMS	Numerical finite model
NRMSE	Normalized Root Mean Square Error
NWT	Newton Solver
OMDEL	Omaruru Delta
PCG	Preconditioned Conjugate Gradient Package
PVGB	Pajaro Valley Groundwater Basin
RCH	Recharge Package
RMSE	Root Mean Square Error
SASSCAL	Southern African Science Service Centre for Climate Change and Adaptive Land Management
SAT	Soil Aquifer Transfer
S	South
SSM	Sink and Source Mixing Package
TDS	Total Dissolved Solids
UNAM	University of Namibia
UPW	Upstream Weighting Package
USA	United States of America
USGS	United States Geological Survey
3D	Three dimensional

1. Introduction

1.1 Background

Water is the most valuable natural resource that supports life on earth. It has become evident that because of the steadily increasing demand, freshwater scarcity is a threat to the sustainable development of human society (Alam *et al.*, 2021). It is believed that the ever-increasing demands of water for domestic, irrigation as well as industrial sectors have created a water crisis worldwide. In arid and semi-arid regions, the available surface water resources are scarce and groundwater resources are often over-used.

Ohangwena region lies in the northern part of Namibia, the most arid area south of the Sahara Desert. The average rainfall in Ohangwena is about 419 mm. This region depends on two sources of water *i.e.,* boreholes and the Calueque – Oshakati canal. The canal is approximately 150 km in length, with water from the Kunene River in Southern Angola. The western part of this region depends on potable water from the Calueque canal while the Southern and eastern part of the region depends on underground water through boreholes (Wallner *et al*., 2017). To enable a reliable, safe, and sustainable water supply in this area, there is a need to diversify future sources of water supply and storage.

Aquifer Recharge (AR) is considered an important technique that can increase the quantities of groundwater through recharge and storing surface water. Artificial recharge is a promising and important technology that mitigates water scarcity and drought situations in arid and semi-arid regions (Jovanovic *et al.,* 2017). This technique of storing water underground increases the groundwater levels, reduces evaporation losses, and utilizes the porous aquifer media for water conservation and decontamination. In artificial recharge, surplus water is transferred into aquifers through injection via boreholes or through surface ponding and infiltration (Steinel *et al.,* 2016). This technique has in several local and international studies been pointed out as an important measure to mitigate water scarcity and drought situations.

A variety of water sources are used to recharge aquifers around the world. According to (Grützmacher & Sajil Kumar, 2012), the water sources used for aquifer recharge are primarily selected depending on their local availability, and the quality that could be used with less pre-treatment effort. The water sources used for Aquifer Recharge globally are; surface runoff, stormwater, river/lake water, rooftop collected rainwater, and treated wastewater. The available raw water should be critically assessed for factors such as; sufficient amount (considering extreme droughts), impact on eco-systems, water table depth to avoid damage to buildings, and sewage effluent or industry outlet upstream (Grützmacher & Sajil Kumar, 2012).

Identification and assessment of suitable sites for AR was carried out before any decision of executing AR could be made. Computational tools play an important role in evaluating AR scenarios and screening potential sites (Zhang *et al.*, 2019). GIS-based methods and numerical modelling are some of the most used tools to identify suitable sites for AR and can be used to estimate the potential benefits of AR projects on regional hydrologic conditions under a range of future climate, water use, and management circumstances. Combining GIS-based methods

with numerical modelling gives a more detailed and quantitative assessment of AR opportunities and impacts (Russo *et al*., 2015).

1.2 Problem statement

The Ohangwena region faces major challenges due to water scarcity caused by growing demands. Groundwater in the area is pumped beyond sustainable levels, which has led to the rapid depletion of groundwater in some aquifers. Water scarcity in Ohangwena is not caused by lack of rainfall but largely due to uneven spatial and temporal distribution of rainfall. Rainfall occurs in the area in the monsoon seasons, and it is lost as runoff to the ephemeral streams and ponds. This runoff water could potentially be captured in AR structures to improve groundwater levels. This would help ease water scarcity problems during the dry season. This study assessed the potential for AR to secure and enhance water supply in the Ohangwena region.

1.3 Objectives of the study

The main objectives of this research are as follows:

1. To undertake an extensive literature review including case studies and data collection to be used in determining the potential for AR in securing and enhancing water supply in the Ohangwena area.
2. To identify and map locations with potential for AR using surface runoff in Ohangwena Region.
3. To assess the impact of AR using surface runoff on groundwater levels.
4. To assess the transport of runoff contaminants within the Ohangwena aquifer system.

1.4 Aim of the study

The main aim of this study is to provide Aquifer Recharge suitability maps that can guide decision making in the implementation of the AR technique in the study area, to assess the impact brought about by Aquifer Recharge using surface runoff on the groundwater levels, and to observe the dispersion of the contaminants associated with runoff, within the Ohangwena aquifer system.

1.5 Research hypothesis

Aquifer Recharge is looked at as a major part of integrated water and catchment management strategy along with surface water and soil management, soil erosion, pollution control, and environmental management. Thus, there is a great potential for Aquifer Recharge to increase security and quality water supplies in water-scarce areas.

1.6 Significance of the study

This desktop study was undertaken to assess the potential for AR to increase groundwater recharge, to facilitate increased water availability and accessibility in the study area, to reduce evaporation losses, to improve water security, and hence minimize the risk of water scarcity. A map was developed showing suitable sites to implement AR using surface runoff, the main source of water available in the area.

Therefore, this research focused on mapping the potential of AR using surface runoff as a water source. Despite the sporadic and seasonal availability of runoff, it has become a popular option for AR to augment and recharge aquifers (Beganskas & Fisher, 2017). Aquifer Recharge with runoff could help provide increased flexibility in water management, improve water security in areas with variable climatic conditions, decrease flooding, flood damage, and capture water that is lost as runoff. This study contributes to the local knowledge base, to assist in groundwater management in the study area.

1.7 Summary

This dissertation consists of 7 chapters. Chapter 1 (this one) provides an introduction including background, problem statement, objectives of the study, aim of the study, research hypothesis, and the significance of the study. Chapter 2 is a review of the available literature relating to groundwater quantity and quality assessment for aquifer recharge, Chapter 3 includes an overview, statement of the method, selection of the study area, characteristics of the study area, data required, the methods used in mapping potential sites suitable for Aquifer Recharge, modelling the impact of AR on groundwater levels, modelling the transport of runoff contaminants within the aquifer, and a summary of the method. Chapter 4 discusses the results of the study, Chapter 5 presents the conclusion and recommendations, Chapter 6 presents a reference list, and appendices are provided in Chapter 7.

2. Literature Review

2.1 Overview

This chapter discusses the relevant published work on similar studies done on mapping the potential for Aquifer Recharge. The approaches are discussed in 10 sections to provide a context of the study. Section 2.2 highlights water scarcity as the primary factor driving the need for AR and use. Section 2.3 discusses groundwater management, Section 4 focuses on the concept of Aquifer Recharge, including AR around the world, in Africa, and in Southern Africa including Namibia. Section 5 discusses the sources of water used for Aquifer Recharge, Section 6 looks at site assessment for Aquifer Recharge suitability, Section 7 looked at mapping the potential sites suitable for AR using GIS, Section 8 discusses modelling and simulation of groundwater systems, Section 9 discusses the groundwater flow and contaminant transport modelling, then Section 10 is a summary of the literature review.

2.2 Water scarcity

Water scarcity is defined as a situation whereby the available and easily accessible water resources in an area, are insufficient to meet the water demands of that specific area (Faures *et al*., 2012) The gradual population growth, economic development, and dietary shift have caused the ever-increasing water demand, and have placed pressures on water resources which have led to the depletion of water resources. Water scarcity is a major constraint to socio-economic development and a threat to livelihood in many parts of the world (Liu *et al.*, 2017).

Water scarcity is mainly characterized by three main dimensions which are: a physical lack of water availability to satisfy demand; the level of infrastructure development that controls storage, distribution, and access; and the institutional capacity to provide the necessary water services (Faures *et al.*, 2012).

Since the 1980s when water scarcity became an issue, many indicators have been developed to facilitate the assessment of the status of water scarcity across the world. (Liu *et al*., 2017) stated that these indicators consider the proportion of water supply of a country/area in question, from renewable freshwater resources available for human requirements, while accounting for existing water infrastructure such as desalination plants and water stored in reservoirs. According to (Faures *et al*., 2012), the best known national water scarcity indicator is per capita renewable water, where threshold values of 500, 100, and 1700 m^3/person /year are used to distinguish between different levels of water stress. This is shown in Table 2.1.

Table 2.1: Conventional definitions of water stress level (Faures *et al*., 2012)

Annual Renewable freshwater (m^3/pers.yr)	Level of water stress
<500	Absolute water scarcity
500-1000	Chronic water shortage
1000-1700	Regular water stress
>1700	Occasional or local water stress

The Sustainable Development Goal 6 (SDG) ensure sustainable withdrawal and supply of freshwater to address water scarcity and substantially reduce the number of sufferings from water scarcity (Faures *et al*., 2012). Different sectors are dependent on water, and where water resources are limited, conflicts arise over its use.

Water scarcity has a huge impact on food production which is gradually increasing in most parts of the world. It is reported that agriculture is one of the economic factors where water scarcity has the greatest significance (Faures *et al*., 2012). According to (Faures *et al*., 2012), agriculture currently accounts for about 70% of global freshwater withdrawals, and more than 90% of its consumptive use. The steady increase in demand for agricultural products to satisfy the needs of a growing population continues to be the main driver behind agricultural water use. In attempts to solve this ever-growing problem, many researchers have tried to come up with effective methods of water management.

Water scarcity is fundamentally dynamic and varies in time as a result of natural hydrological variability, but more so as a function of prevailing economic policy, planning and management approach, and the capacity of societies to anticipate changing levels of supply and demand (Faures *et al*., 2012).

2.3 Groundwater management

Groundwater currently contributes to the water demands of the rapidly increasing populations in Africa and around the world (Ebrahim *et al.*, 2020). It plays a key role in enhancing resilience, particularly in arid and rural areas. Groundwater resources are limited, and they are declining both in quantity and quality due to contamination and climate change. (Ajay Singh et al., 2019) stated that under the environment of increasing water demand for domestic, agricultural, and industrial uses, groundwater management is a challenging task worldwide.

According to (Ross & Hasnain, 2018), it is estimated that around the world, groundwater supplies provide 40% of potable water, 42% of irrigated agriculture water, and 24% of direct industrial water supply. However, these groundwater supplies are diminishing with an estimate of 20% of the world's aquifers being over-exploited, which often leads to serious consequences such as land subsidence and saltwater intrusion in coastal areas.

The usage of groundwater in many regions is less monitored than surface water resources. The impacts of groundwater overexploitation and pollution can remain undetected for decades or even centuries, presenting further challenges for managing water resources (Anthony *et al.*, 2016). At times, groundwater abstraction may exceed recharge over long periods and extensive areas. This causes a subsequent decline in water table level, which in turn may have harmful impacts on groundwater-dependent streams, wetlands, and ecosystems (Anthony *et al*., 2016). Therefore, groundwater recharge is essential for efficient and sustainable groundwater management due to the critical economic development of water resources.

2.4 Aquifer Recharge

2.4.1 Overview

Aquifer Recharge is the intentional recharge of groundwater for recovery or environmental purposes which includes monitoring of recharge water quality and the resulting impacts (Dillon *et al.*, 2009). It is commonly known as artificial recharge. This technique supports an increase in water resources, and it is an important tool for mitigating the economic, environmental, and public health impacts of water supply shortages. The technique is widely used in many countries to enhance water supplies, particularly those in semi-arid and arid areas, primarily for water quality management. AR captures available water (during wet periods, low demand, or water that would be lost) and moves this water under controlled conditions into underground reservoirs (aquifers).

There are various methods used for Aquifer Recharge internationally. The most commonly used method includes surface infiltration method which involves percolation of recharge from or near the ground surface, vadose zone infiltration methods which involve percolation of recharge water at some depth below the ground surface, but within the vadose zone, and direct injection method which involves direct injection of recharge water into the aquifer (Reddy, 2008). In addition to these common methods, a few other methods are also used such as *inter alia* Aquifer Storage Recovery (ASR); Aquifer Storage Transfer and Recovery (ASTR); infiltration ponds; infiltration galleries; Soil Aquifer Treatment (SAT); percolation tanks or recharge weirs; rainwater harvesting for aquifer storage; and recharge releases (Dillon *et al*., 2009). The selection of suitable sites and the choice of method for AR depends on the hydrogeology, topography, hydrology, and land use of the area.

The surface infiltration method involves the application of recharge water at the surface above an unconfined aquifer in man-made or natural depressions, which ultimately causes the water table to rise (Reddy, 2008). The different surface infiltration methods include infiltration ponds or basins, infiltration ditches, stream channels, land applications, and in-channel systems *i.e.*, percolation ponds, leaky dams and recharge releases, sand storage dams, and subsurface dams. This method is widely used due to lower cost, greater simplicity, and lower operation and maintenance costs. However, it requires that the soils from the infiltration location to the top of the aquifer have high vertical permeability (Reddy, 2008).

The vadose zone infiltration method is used when near-surface soils have low permeability or when other land uses are not compatible with surface infiltration (Reddy, 2008). In this method, recharge water is introduced beneath the land surface (in the vadose zone) and then allowed to infiltrate into the unconfined aquifer. The different vadose zone infiltration method includes trenches and galleries, dry wells, infiltration shafts, and infiltration pits. According to (Reddy, 2008) this method applies to unconfined aquifers containing alluvium, semi-consolidated sediments at outcrop, or highly fractured bedrock.

The direct injection method involves injecting water directly into an aquifer using vertical wells (Reddy, 2008). In these wells, recharge water can be directly injected into the saturated portion of the aquifer, and they may also be used for recovery purposes if desired. According to (Reddy, 2008), the injection wells reduce the vertical transit time of water to the aquifer and avoid unfavourable reactions between water and the soil or minerals in the unsaturated zone.

Aquifer Storage Recovery (ASR) and Aquifer Storage Transfer Recovery (ASTR), are direct injection methods that use injection wells, and they are the most used methods throughout the world. (Jakeman *et al*., 2016), defined ASR as the injection of water into an aquifer/well for storage and recovery by pumping from the same well at a later stage. This method is mostly used in aquifers that have brackish water, impermeable to a non-point source of pollution, and in which groundwater moves slowly. The method is also mainly for the seasonal storage of good quality water. Storage is the primary goal of ASR and water treatment is not much considered. ASTR involves the injection of water in one aquifer/well and recovery by pumping from a second well/aquifer that is located several meters down-gradient from the injection well (Jakeman *et al.*, 2016). ASTR helps to achieve extra water treatment in the aquifer by extending residence time in the aquifer beyond that of a single well (Dillon *et al*., 2009).

Infiltration basins are also one of the methods of AR, that facilitates the transfer of water to the aquifer. These basins are mainly used to recharge unsaturated zones or, in some cases they create hydraulic barriers (Jakeman *et al*., 2016). The infiltration ponds divert surface water into off-stream basins and channels that allow water to soak through the unsaturated zone to the underlying unconfined aquifer (Dillon *et al*., 2009). Through this method of infiltration, the basins also manage stormwater runoff, preventing flooding and downstream erosion, and improving the quality of water in the adjacent river or stream.

Three other methods of AR are the Soil aquifer treatment, percolation tanks/recharge weirs, and rainwater harvesting for aquifer storage as mentioned above. The soil aquifer treatment method deals with treating sewage effluent and infiltrates it through infiltration ponds to facilitate pathogens and nutrients removal in the route through the unsaturated zone for recovery by wells after dwelling for some time in the unconfined aquifer. This description is according to (Dillon *et al*., 2009). This method is a natural wastewater treatment process, where wastewater contaminants are removed through biological, physical, and chemical processes.

Percolation tanks constitute earthen dams that are built-in ephemeral streams that hold up water. According to (Page *et al*., 2018), this water is extracted down-valley, and it infiltrates

through the bed to increase storage in unconfined aquifers. This method enhances natural urban river infiltration. The rainwater harvesting method for aquifer storage involves diverting roof runoff into a well that is filled with gravel/sand, whereby this runoff is allowed to percolate to the water table, where it is later collected by pumping from a well (Page *et al*., 2018). This method is generally of a much smaller scale than other types/methods of AR, but it is very effective when it is widely used.

2.4.2 AR around the world

Artificial recharge is widely practiced in different countries around the world such as Germany, Finland, Israel, the USA, Australia, and many more. (Murray, 2004) reported that about 15% of Germany's drinking water is supplied from artificial recharge, whereby riverbank infiltration and infiltration basins are the most commonly used methods. He further stated that most of Finland's town's water supplies come from the underground of which 32% is artificially recharged. The USA has numerous infiltration and injection schemes; in the same manner, Australia has quite many injection schemes in hard-rock aquifers.

Many schemes around the world demonstrate the advantages of Aquifer Recharge. According to (Ross & Hasnain, 2018), recharge enhancement in India is the highest in the world with 3 km^3 produced annually, and 0.4 km^3 is produced by individual sites in Hungary, Slovakia, the Netherlands, Germany, Poland, and France. (Ross & Hasnain, 2018) further clarified that rooftop rainwater and urban stormwater have been used as sources of water to recharge the aquifers in Australia, Germany, India, Jordan, the USA, and other countries with permeable soils or karst aquifers. Treated sewage effluent has also been used to recharge the aquifers in countries like Australia, Germany, Israel, Italy, Mexico, South Africa, and Spain. The desalinated water has been used for recharge in the USA and the United Arab Emirates. In coastal areas such as California, China, and Bangladesh, the replenishment of aquifers using injection wells has protected urban and irrigation supplies from salination. Different sources of water used for Aquifer Recharge are further explained in Section 2.5 of this study.

Table 2.2 shows the summary of some of the AR schemes around the world (Dillon *et al*., 2009).

Table 2.2: Summary of AR schemes around the world (Dillon *et al*., 2009)

Country	Location	AR-type	Number of schemes	Water source	Scheme objective
Netherlands	Westland	Infiltration basins	10	Natural water	Seasonal storage
	Ovezande	Recharge wells	10	Natural water	Seasonal storage
India	Haridwar	Bank infiltration	1	Natural water	Multi-purpose use throughout the year
USA	Surprise Arizona	Infiltration basins	10	Natural water	Water security
	Surprise Arizona	Infiltration basins	10	Natural water	Water security
	Marana Arizona	Infiltration basins	10	Natural water	Water security
	Sahuarita Arizona	Infiltration basins	10	Natural water	Water security
	Queen creek Arizona	Infiltration basins	10	Natural water	Water security
	Tonopah Arizona	Infiltration basins	10	Natural water	Water security
	Texas - San Antonio	Recharge wells	10	Natural water	Drinking water
	Texas - Kerrville	Recharge wells	10	Natural water	Municipal water supply
	Texas - el paso water utility	Recharge wells	10	Recycled water	Multi-purpose use throughout the year
	California	Recharge wells	10	Natural water	Municipal water supply
	Florida	Recharge wells	10	Natural water	Drinking water
Australia	Mandurah, geraldton and esperance, WA	Infiltration basins	10	Recycled water	Irrigation supplies
	Perry lakes and floreat, WA	Infiltration basins	10	Recycled water	Ecological benefits
	Alice spring, NT	Recharge wells	10	Recycled water	Water quality
	Bolivar SA	Recharge wells	10	Recycled water	Irrigation supplies
	Anglesea, vic	Recharge wells	10	Recycled water	Water security
	Beenyup,WA	Recharge wells	10	Recycled water	Drinking water
New Zealand	Near ashburton, canterbury plains	Infiltration basins	10	Natural water	Ecological benefits

2.4.3 AR in Africa

AR was initially implemented in the 1960s and has increased over time. Aquifer Recharge in Africa was done as a Managed Aquifer Recharge (MAR). A review conducted by (Ebrahim *et al*., 2020) reported that, in 1965, the first AR projects in Africa were launched in Sourka, Tunisia, and Polokwane, South Africa. Two more followed in the 1970s, and three more in the 1980s. In the 1990s AR projects accelerated substantially, with seven implemented in that decade, followed by 16 more projects that were implemented in the 2010s. The historical development of AR cases in Africa where the starting date is known is shown in Figure 2.1, whereby the number of projects is given for each decade.

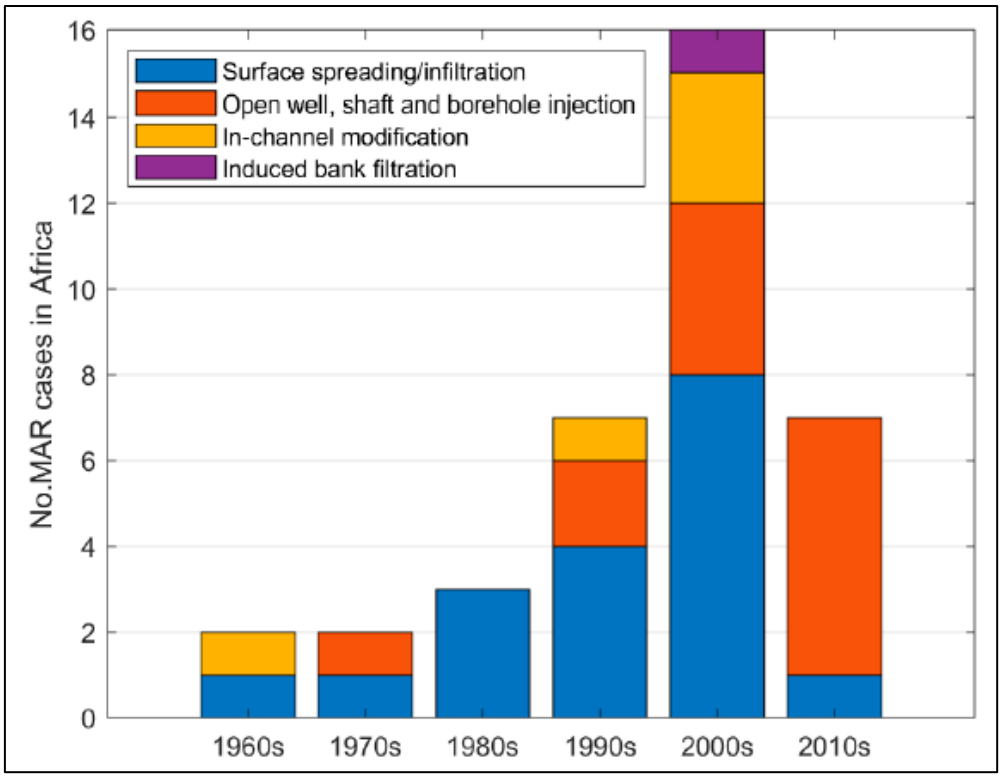

Figure 2.1: Historical development of MAR cases in Africa (Ebrahim *et al*., 2020)

MAR in Africa is mainly practiced to maximize the natural storage of water. The objectives of maximizing natural storage of groundwater include increasing groundwater availability to meet water demands during dry periods, summer peak demand, emergency and drought supplies, and water banking for seasonal peak demands and emergency supplies (Murray & Tredoux, 2004). A report by (Ebrahim *et al*., 2017) stated that MAR in Africa started in 1958, and Morocco was the first African country that used the technique as a source of water supply to Tanga city.

An overview of MAR progress in Africa was done by (Ebrahim *et al*., 2020), to inform the potential for future use of this approach in the continent. The overview indicated that there are 52 recorded cases of MAR in Africa, of which 44 cases are listed on the Global MAR portal and 8 were identified through (Ebrahim *et al*., 2020) literature search. The results of this review

showed that the extent of MAR practice in Africa is quite limited, and the main objective of MAR in Africa is mainly for securing and augmenting water supply, and to balance variability in supply and demand. (Ebrahim *et al*., 2020), further justified that the total annual recharge volume is about 158 Mm3 per year.

The MAR implementation cases in Africa are concentrated in nine countries. According to (Ebrahim *et al*., 2020), in South Africa, there have been 17 reported cases of MAR, followed by Tunisia with 11 cases, Kenya with 8 cases, and Algeria with 5 cases. In addition, there is evidence of MAR implementation in five other African countries (Egypt, Ethiopia, Morocco, Namibia, and Nigeria), with up to 4 cases per country. MAR appears to be more prevalent in some of Africa's wealthier yet drier countries or in certain areas where a certain type of MAR technology is popular.
Figure 2.2 shows the summary of African countries that practice Managed Aquifer Recharge.

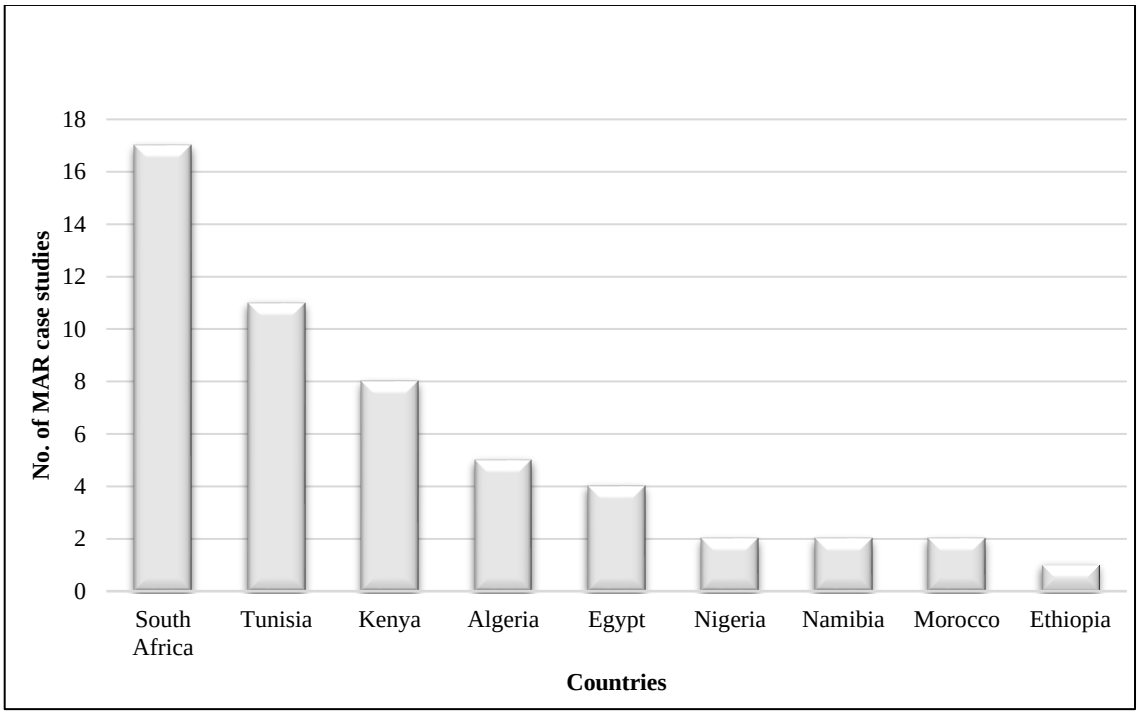

Figure 2.2: MAR studies in Africa (Ebrahim *et al*., 2020)

According to (Ebrahim *et al*., 2020) The most common method of MAR and the main MAR type in Africa is the surface spreading/ infiltration method, the second most common is the open well shaft, borehole injection and in-channel modification is ranked third. In Kenya, the most common MAR method is an in-channel modification with sand dams, spreading/infiltration is mostly used in Tunisia, while the open well shaft and borehole injection are mostly used in South Africa. The riverbank filtration case in Egypt is the only one reported in Africa. Rainwater and runoff harvesting have not been reported used for MAR in Africa. Figure 2.3 shows the number of MAR cases in Africa per main MAR type, modified from (Dillon *et al*., 2009), and Table 2.3 shows the number of main MAR types per country, also modified from (Dillon *et al*., 2009).

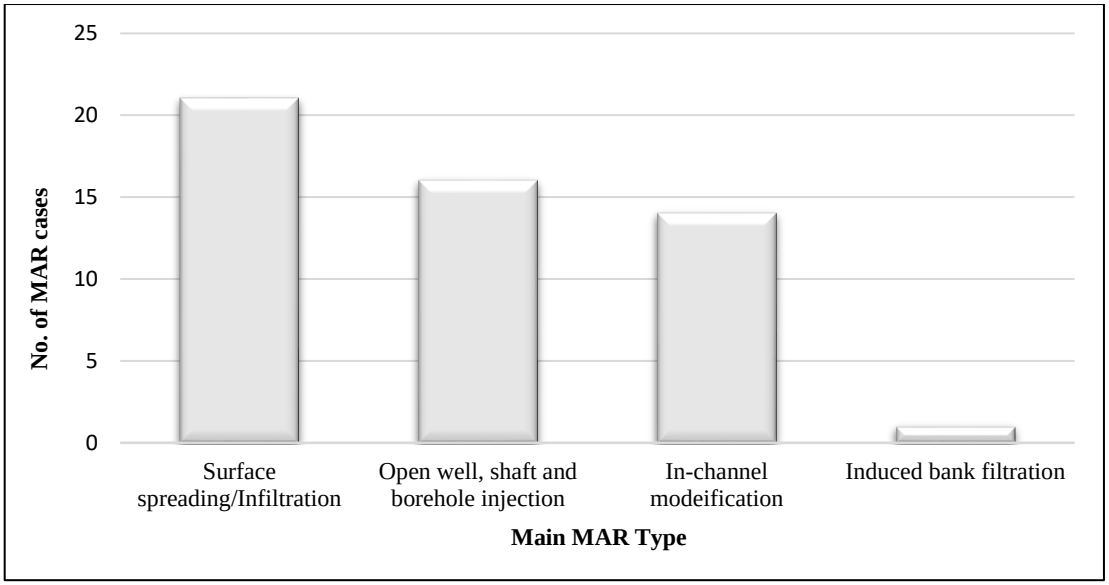

Figure 2.3: Main types of MAR methods in Africa (Dillon *et al.*, 2009)

Table 2.3: Number of main MAR types per country (Dillon *et al.*, 2009)

Country	Surface Spreading/Infiltration	Open Well, Shaft and Borehole Injection	In-Channel Modification	Induced Bank Filtration
Algeria	5			
Egypt	3	-	-	1
Ethiopia	-	-	1	-
Kenya	-	-	8	-
Morocco	1	-	1	-
Namibia	1	1		
Nigeria	1	1	-	-
South Africa	4	12	1	-
Tunisia	6	2	3	-
Total	21	16	14	1

As reported by (Ebrahim *et al.*, 2020), the development of MAR implementation, as well as the potential for its out-scaling is evident in urban and rural Africa. In addition, these MAR schemes at present in Africa tend to be found in areas where water availability varies considerably from year to year. And if properly planned, implemented, managed, maintained, and adapted to the local conditions, the MAR schemes have a large potential for securing water and increasing resilience in Africa.

The review by (Ebrahim *et al.*, 2020) reported that the main source of water for AR schemes in Africa is surface water. Out of 52 cases of AR in Africa, 32 cases use river water as a water source, 11 cases use treated wastewater, and other schemes use several sources of water such as groundwater, stormwater runoff, and rooftop runoff. Out of 33 cases that use river water, 19 cases use ephemeral rivers for their water source, while 8 of the 33 cases depend on perennial rivers. Egypt has three of the eight cases using perennial rivers as the source of their water, using Nile River water. Treated wastewater is mostly used in countries with limited

water resources such as South Africa, Namibia, and Tunisia. Five Artificial Recharge cases in Africa that rely on groundwater as their water source, are found in South Africa with four cases, and Ethiopia with one case. The summary of the number of Artificial Recharge cases in Africa per water source is shown in Figure 2.4.

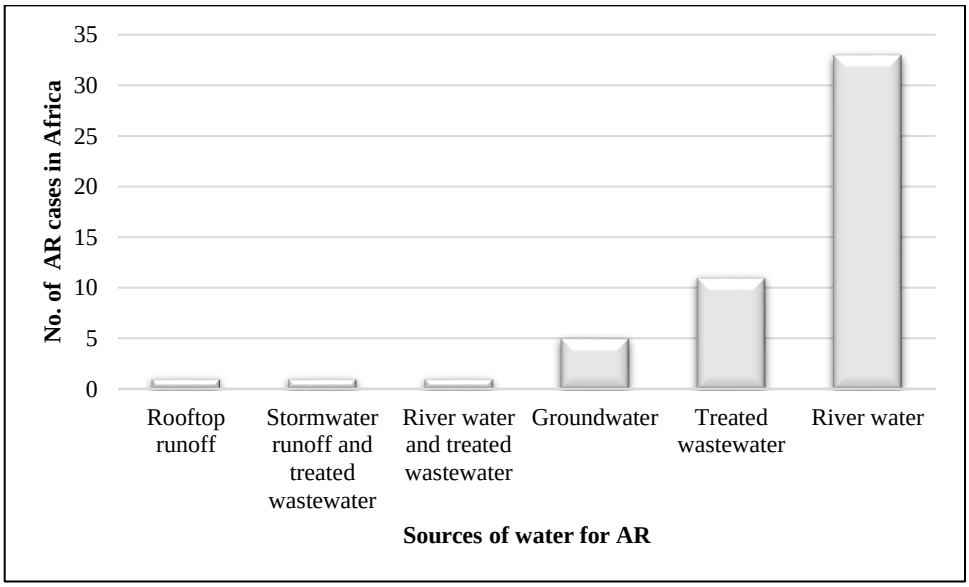

Figure 2.4: Number of MAR cases in Africa per water source (Ebrahim *et al*., 2020)

2.4.4 AR in Southern Africa

The concept of water banking and sub-surface storage of water is gaining popularity in Southern Africa, as an efficient and cost-effective method for both shorter and longer-term management of water resources. Aquifer Recharge in Southern Africa is practiced as Managed Aquifer Recharge (MAR). The main uses and importance of artificial recharge in Southern Africa are for conserving water for future use, improving water quality, and preventing saline water intrusion (Murray, 2004).

A booklet covering key issues that affect the success of artificial recharge schemes and provides case studies from Southern Africa by (Murray, 2004), indicated that there are six (6) artificial recharge sites in Southern Africa that have been studied in-depth and a few more where feasibility studies have been carried out. The six sites where artificial recharge is practiced in Southern Africa are summarised in Table 2.4 and shown in Figure 2.5:

Table 2.4: Summary of MAR sites in Southern Africa

Country	MAR site	Year of construction	Period of operation	Source of water
Namibia	Windhoek	2005	Over 5 years of operation	Surface water
	OmDel	1997	Over 5 years of operation	Floodwater
South Africa	Atlantis	1979	Over 40 years of operation	Stormwater & Wastewater
	Polokwane	1994	Over 20 years of operation	Stormwater & Wastewater
	Karkams	1995	Over 5 years of operation	Surface runoff
	Calvinia	Recently tested	Recently tested	Treated surface water

Figure 2.5: Southern Africa MAR sites locations (Murray, 2018)

Managed Aquifer Recharge in Namibia is practiced at two sites namely: Windhoek in Khomas region and Omdel in Erongo region. The Windhoek MAR scheme is one of the largest schemes of the Southern African Schemes, started in 1996. It is comprised of injecting fully treated surface water into a quartzite aquifer and recovering it from nearby boreholes. The aquifer recharge scheme was implemented to provide security of water supply during droughts, to meet seasonal peak demands, and to provide emergency water supplies in case of problems with the other bulks supplies or the treatment works. According to (Murray *et al.*, 2018) the recharge rate of this scheme in 2009 was recorded to be 2 mm^3/a, compared to the natural recharge which

was 1.7 mm^3/a. The city of Windhoek opted to implement artificial recharge prior to other options because it is the most cost-effective option for the city, and it will provide the water supply security needed.

The city of Windhoek primarily depends on surface water but due to unreliable rainfall, the reserves in the three supply dams regularly run low (Murray, 2004). As reported by (Murray, 2004), 10% of the city's water need is currently accounted for by groundwater, and with a large scale of artificial recharge practice, it could be increased significantly to the extent that the aquifer becomes the city's main source of water during droughts. A different study conducted by (Murray & Tredoux, 2004) indicated that the groundwater levels around the city of Windhoek have dropped drastically in the wellfield areas by tens of meters, and they are steadily dropping in the natural recharge areas in the southern direction of the city. Thus, to rapidly replenish the aquifer, artificial recharge was implemented in the wellfield and the natural recharge areas. A three-phased approach was adopted by the city of Windhoek to implement a large-scale artificial recharge. The phases consisted of several boreholes used for both injection, and abstraction of water into and from the aquifers.

The coastal towns of Namibia (Swakopmund, Henties Bay, and Walvis Bay) solely depend on groundwater due to their low rainfall. The mean annual rainfall in these towns is about 50 mm/a (Murray, 2004). The natural groundwater recharge in these areas is very low and only occurs when the ephemeral river of Omaruru gets flooded. According to (Murray, 2004), the area experienced an over-abstraction in the mid - 1970s, causing the groundwater levels to drop by tens of meters. The study showed that the three coastal towns are supported by two boreholes schemes that are associated with groundwater in paleochannel systems, of which the OMDEL aquifer is used for abstraction and artificial recharge. The Artificial recharge technique was introduced in this area to rapidly replenish the aquifer when river runoff is available and to reverse the negative trend of groundwater levels dropping.

Atlantis has been practicing artificial recharge for more than 20 years by using infiltration basins. This town was initially fully dependent on groundwater, but since the reserves were insufficient, artificial recharge was introduced to augment local groundwater supplies (Murray & Tredoux, 2004). The recharge system uses urban stormwater runoff and high-quality treated domestic wastewater, as the sources of water for the system in the area. The natural recharge of Atlantis is estimated to be in the order of 15 – 30% of the annual rainfall which is about 450mm (Murray & Tredoux, 2004). From the year of operation of this system, the artificial recharge has been effective, with the infiltration rates recorded in the basins to be ranging from 0.01 to 0.16 m/day. The infiltration rates largely depend on the thickness of the unsaturated zone (Murray, 2004).

Polokwane is also one of the towns in South Africa that have been practicing artificial recharge for over 10 years. This town largely depends on surface water; however, the town also has an elaborate groundwater abstraction infrastructure that can supply domestic water in times of surface water shortages and during periods of peak demand (Murray, 2004). The main source

of water for this scheme is treated municipal wastewater that infiltrates into alluvial and gneissic aquifers in Polokwane.

Another operational Artificial recharge scheme in Southern Africa is found in Karkams, which is a small-scale borehole injection in Namaqualand. It is reported that Karkams village has a mean annual rainfall of about 250 mm, with about 1700 inhabitants, and the village solely depends on groundwater (Murray, 2004). Similar to the OMDEL case study, Karkams also have a very low natural groundwater recharge rate, and as a result of over-abstraction that occurred in the area in the mid-1990s, the groundwater levels are reported to have dropped tens of meters, and the salinity of the water has deteriorated significantly (Murray & Tredoux, 2004). To reverse the negative trend of abstraction in the area, an artificial recharge scheme was set up to replenish the aquifer rapidly when the river runoff is available.

Regarding the above-mentioned six case studies, it can be concluded that, even in arid areas, artificial recharge either through infiltration basins or other methods, can significantly increase the stored water reserves, and surface water that could be lost to evaporation can be safely stored underground. The case studies also show that this technique is not only applicable to large-scale schemes but can also be effectively used in small-scale operations.

2.5 Sources of water used for Aquifer Recharge

Water availability with sufficient quantity and quality is one of the main prerequisites for AR implementation. Water to be recharged for AR may be sourced from rainwater, stormwater, treated wastewater, perennial streams, intermittent streams, storage dam, urban stormwater, groundwater, and rooftop rainwater harvesting (Ebrahim *et al*., 2017). The most used sources of water are surface water (rivers and lakes), stormwater, wastewater, and groundwater. According to (Alam *et al*., 2021), surface water such as rivers and lakes are the main source of most AR in all climate regions; stormwater and recycled water are the second and third most common sources of water for AR; contaminated groundwater is commonly used in semi-arid, dry sub-humid, and humid regions. In coastal areas, desalinated seawater can serve as a reliable source of water for AR. Specific AR types are identified based on the type of water source available at a site.

2.5.1 Treated wastewater effluent for Aquifer Recharge

In recent years, there has been a great interest in the use of treated wastewater as a source of water for AR particularly in arid regions where freshwater resources are limited (Ebrahim *et al*., 2017). The advantage of using municipal wastewater as a source of water is that it has a predicted quantity, and it is available even during dry periods although it may require substantial treatment before it is used for recharge. Wastewater can serve as a reliable source of water for AR in hyper-arid areas (Alam *et al*., 2021b). About 11 cases of AR in Africa use wastewater as a water source, with Atlantis being one of them using both treated wastewater and urban stormwater runoff (Ebrahim *et al.*, 2020). Windhoek is also one of the AR schemes

using treated wastewater and river water as sources of water. Treated wastewater is used for recharge systems whose objective is to significantly increase the volume of groundwater, and those whose objective is to improve groundwater quality (Jakeman *et al*., 2016).

2.5.2 Ephemeral streams as a water source for Aquifer Recharge

In arid and semi-arid regions, ephemeral streams may be valuable sources of water for aquifer recharge, although recharge water may contain a lot of suspended sediments that may require pre-treatment or sedimentation (Ebrahim *et al*., 2017). According to (Ebrahim *et al*., 2020), 33 out of 52 cases of AR in Africa use river water as a water source, and about 19 cases use ephemeral rivers as their water source. Surface water is mostly used due to the following reasons: the chemical and microbiological quality of surface water is acceptable which permits its use for both quantitative and qualitative purposes. Secondly, surface water can be used with different existing AR techniques, from infiltration or indirect injection to direct injection. And thirdly, the laws that permit the use of surface water for recharge systems already exist (Jakeman *et al*., 2016).

2.5.3 Stormwater as a water source for Aquifer Recharge

Stormwater is defined as water that originates from rain, including snow or ice melt, that can either infiltrate into the soil, be stored on the land surface such as ponds, evaporate or contribute to surface runoff (Luthy *et al*., 2019). Stormwater runoff from urban areas is harvested by collecting, treating, and storing. Stormwater harvesting differs from rainwater harvesting as the runoff is collected from drains and not roofs. In this case, stormwater is temporarily stored in stormwater ponds, which are designed to function as infiltration cells with specific features that allow groundwater aquifers to be recharged for future abstraction and supply (Wu *et.al*. 2012). Enhanced Aquifer Recharge and recovery, allows the use of groundwater storage for Stormwater harvesting.

Stormwater represents a valuable alternative urban water source to reduce pressure on freshwater resources, supplement traditional urban water supplies, and mitigate the environmental impact of urban stormwater runoff (Inamdar *et al*., 2013). The changing precipitation patterns due to climate change in most areas brought new opportunities to develop AR projects using stormwater. (Murray & Tredoux, 1998), regarded stormwater as highly variable in quantity and quality. AR and Stormwater infiltration systems are largely developed in urban areas to prevent flooding and to compensate for reduced groundwater recharge due to the road surface and structure coverings. These systems involve collecting stormwater runoff and infiltrating them through porous medias to recharge the aquifers.

Usage of stormwater for recharging aquifers is associated with quality risks, particularly during the onset of the runoff, due to contaminants from many sources such as industrial and agricultural chemicals (Ebrahim *et al*., 2017). According to (Luthy *et al*., 2019), pollution coming from industrial areas and fuel stations are major sources of pollution that endanger the

quality of stormwater in urban areas. The availability of stormwater is linked to rainfall, and in most cases, pre-treatment of stormwater is required before recharge to ensure a sustainable recharge rate, protection of the aquifer, and post-treatment is also required for the recovery of water to meet human health and environmental risk requirements (Page *et al.*, 2018). Stormwater flows into rivers, creeks, and stormwater drains to form part of freshwater that flows to oceans and estuaries. The recovered water from the aquifers may be used for drinking, other household use, and agriculture.

2.6 Site Assessment for Aquifer Recharge suitability

Several studies have been conducted around the world on assessing sites that are suitable for the practice of Aquifer Recharge to address water shortage and scarcity. To assess the suitability of a certain site for AR, detailed three-dimensional (3D) information about the subsurface materials and their hydraulic properties of the study area is needed (Behroozmand *et al.*, 2019). Computational tools such as; GIS and numerical modeling and Geophysical Imaging Methods have been used to assess the suitability of sites for Aquifer Recharge. These assessments are often made on a regional basis, within which there may be limited data on complex surface and subsurface conditions and flows. The computational tools play a major role in the evaluation of AR circumstances, and screening potential sites because they can be applied on a regional spatial scale. This allows testing of operational scenarios and hydrologic conditions, combined with other management options (Russo *et al*., 2015).

In a case study of central coastal California in the Pajaro Valley Groundwater Basin (PVGB), an assessment of Aquifer Recharge site suitability was done on this area using GIS and modeling (Russo *et al*., 2015). In this study, a two-step regional analysis of a coastal groundwater basin was done to assess the regional suitability for aquifer recharge and to quantify the relative impact of Aquifer Recharge activities on groundwater and seawater intrusion (Russo *et al*., 2015). Geographical Information System (GIS) was employed in this study to analyze the surface and subsurface hydrologic properties and conditions of the study area. A regional groundwater numerical model was then used together with the analysis results of GIS, to assess the hydrologic impact of potential AR placement and operating cases. According to the results of this study, the GIS analysis showed that about 7% of the basin may be highly suitable for AR. The results from the modeling also suggested that simulated AR projects that are placed near the coast help in reducing seawater intrusion more rapidly, but these projects also increased groundwater flows to the ocean (Russo *et al*., 2015).

In a different case study of North-Western Himalaya, India, geospatial techniques and groundwater modeling were employed to delineate suitable sites for artificial recharge to groundwater (Jasrotia *et al.*, 2019). In this study, a weighted index overlay method in GIS was used to prepare the artificial recharge zone map of the study area. In the same manner, groundwater modeling for artificial recharge to groundwater was carried out using MODFLOW software, to determine the modeling zones for artificial recharge to groundwater (Jasrotia *et al*., 2019). The artificial recharge zones were validated, by comparing the GIS-

based artificial zones map with groundwater modeling recharge zones. The impact of discharge and artificial recharge on the surrounding aquifers was also determined. The results of this study proved the proficiency of geospatial technology and groundwater modeling techniques for defining suitable sites and zones for artificial recharge to groundwater and their implementation in the field (Jasrotia *et al*., 2019).

Another site assessment for artificial recharge suitability was carried out in North Jordan (Steinel *et al*., 2016). The investigation of this study was done to increase the available water resources using AR, via infiltration of captured surface runoff for two basins in northern Jordan. This study used Boolean logic to combine thematic maps to constraint maps and weighted linear combinations to create suitability maps. These two methods were used to evaluate the general suitability of the catchments, to generate sufficient runoff, and to identify promising sites to harvest and infiltrate runoff into the aquifer for later recovery. According to the evaluation results, non-committed source water availability is the most factor that is preventing successful water harvesting in regions with a rainfall of less than 200 mm (Steinel *et al*., 2016). The experiences with the existing aquifer recharge structures in Northern Jordan displayed that sediment loads of runoff are relatively high. Hence, if maintenance is not undertaken, the usefulness of any existing Aquifer Recharge scheme will decrease rapidly to the point where it results in an overall undesirable effect due to increased evaporation.

In Southern Africa, site assessment for AR was done in West Coast, South Africa *(*Zhang *et al.*, 2019). Aquifer Recharge was considered as a solution to improve water security in towns along the West Coast of South Africa, that are facing water shortages due to climate change and increasing day by day water demand. The implementation of AR in this area was planned to be practiced with water from Berg River and other sources during the rainy season. This assessment was done using a two-step method of combining GIS-based analysis with numerical modeling, to select sites that are suitable for the implementation of the AR scheme. In GIS-based analysis, many factors such as regional characteristics, heterogeneities in surface and subsurface characteristics, and variable groundwater qualities were taken into consideration to generate an initial map for suitable sites. A groundwater flow model was then adopted in this study to verify and optimize the suitable sites that were selected by the GIS-based analysis. The combination of GIS-based analysis with numerical modeling in this study allowed a more detailed and quantitative assessment of AR opportunities and impacts. The results showed that the map for suitable sites produced by GIS-based analysis was reasonable from a spatial aspect, but not necessarily the optimal choice, due to the lack of groundwater seepage information that is missing (Zhang *et al*., 2019).

In a different case study of Central Valley California, a new geophysical imaging method (tTEM) was used to provide the coverage and resolution that are optimal for the assessment of AR sites (Behroozmand *et al*., 2019). According to the study, a new geophysical imaging system is a towed-domain electromagnetic system that is efficient for acquiring data at a significantly improved resolution and a scale needed for AR. This method can advance the ability to identify important areas for natural recharge and inform the selection of sites for AR

or on-farm recharge. Besides that, this method provides a high-resolution 3D image of the sub-surface down to a depth greater than 60 m. The results of this study suggested that five of the seven sites assessed are appropriate for AR.

In a different study of Hanoi, Vietnam, the study evaluated the feasibility of AR as a remediation technique to restore the aquifer system in the urban area of Hanoi, by using MODFLOW-NWT to study the groundwater flow system of the area. The study also conducted a GIS-based Multi-Criteria Decision Analysis (MCDA) to identify the possible areas that are suitable for AR, and it also simulated the implementation of AR measures into the transient groundwater flow model to understand the potential effects on the groundwater.

The methods used for classifying and weighing sites for AR suitability differ significantly from study to study. This is caused by differences in data availability, local geology, and the importance of individual datasets to groundwater recharge (Russo *et al.*, 2015). According to the study, these methods can be refined from time to time when new data becomes available, provided that the mapping tools remain available for later use, and the methods used, and the values assigned are documented.

Suitability maps for Aquifer Recharge (AR) are increasingly used worldwide and hold the potential to be integrated into sustainable groundwater management plans (Sallwey *et al*., 2019). According (Sallwey *et al*., 2019), despite the increase in popularity of these maps, their quality strongly depends on the input data quality, and they are commonly derived through GIS-based Multi-Criteria Decision Analysis (MCDA). (Sallwey *et al*., 2019) further states that there is no common understanding of how suitability mapping should be conducted because there is considerable variability concerning GIS data used and MCDA methodology. It is also reported that the majority of the studies have used the GIS-based integration approach in combination with numerical groundwater modeling, to produce quality maps for the assessment of AR worldwide (Russo *et al*., 2015).

2.7 Mapping the potential sites suitable for groundwater recharge using GIS

The entry of water from the unsaturated zone into the saturated zone below the water table level, as well as the associated flow away from the water table within the saturated zone, is referred to as groundwater recharge (Yeh *et al*., 2016). Groundwater recharge occurs when water flows past the groundwater level and infiltrates into the saturated zone. Determining the distribution of groundwater recharge potential zones is an essential component of sustainable groundwater management, and it is required to map groundwater resources, and plan for future water supply to overcome the problem of limited water supply and increasing demand.

A study by (Alaa *et al*., 2021) explained that traditionally, the Groundwater Recharge Potential zones are identified using hydrogeological, geological, physical investigations, and soil moisture modeling. However, most in-situ investigation methods are costly, time-consuming, and require skilled personnel, making them infeasible for determining recharge

potential at the catchment scale. (Alaa *et al*., 2021) further elaborated that in today's world, Remote Sensing (RS) and Geographical Information Systems (GIS) technology are mostly used to identify the various factors relevant to the Groundwater recharge potential faster, more accurately, and with greater cost-efficiency.

According to (Yeh *et al*., 2016), lithology, topography, geological structures, depth of weathering, degree of fractures, primary porosity, secondary porosity, slope, drainage patterns, landform, land use/cover, and climate, are all factors that affect the occurrence and movement of groundwater in a particular region. These factors have been used in several studies explained in section 2.7.1 to identify the possible groundwater potential zones that are suitable for Aquifer Recharge using the Geographical Information System (GIS).

The factors used in this study to identify the zones that are suitable for Aquifer Recharge in Ohangwena Region are lithology, land use/ land cover, lineaments, drainage, and slope. According to (Alaa *et al*., 2021), the impact of these factors varies from one location to another. *i.e.,* the linear features such as fractures and faults constrain groundwater flow. Therefore, these factors are significant in identifying recharge potential zones. The suitable groundwater recharge potential zone's distribution was determined using the GIS's space integrating tool to coordinate it. The weights criteria for prospective groundwater recharge, as well as the scores achieved under various characteristics in this study, were referred to the study methodologies of (Yeh *et al*., 2016).

2.7.1 Establishing potentially related groundwater recharge factors

2.7.1.1 Lithology as a groundwater recharge potential factor

Lithology is important in the occurrence and distribution of groundwater because it influences groundwater recharge by controlling water flow percolation. According to (Fagbohun, 2018), groundwater occurrence and movement depend on the type of rock in which it occurs, and the rock type of any area has a significant effect on the availability of groundwater and its recharge. This study involves lithology to help determine lineaments and drainage.

2.7.1.2 Land use/ Land cover as a groundwater recharge potential factor

Land use/cover is another important factor in groundwater recharge. Land cover refers to the physical characteristics of the land such as vegetation cover, open water sources, and distribution of residential areas, whereas land usage refers to how people use the land. According to (Yeh *et al*., 2016), evapotranspiration, runoff, and groundwater recharge are all affected by land use and land cover. The knowledge of land use/cover is required to assist in quantifying the water budget (Yeh *et al*., 2016). Land uses with a high amount of vegetation have a high potential for groundwater infiltration than land uses with little or no vegetation (Aryanto & Hardiman, 2018). Land use/cover is included in this study as an important factor because it represents the influence of humans on groundwater recharge.

2.7.1.3 Lineaments as a groundwater recharge potential factor

(Yeh *et al*., 2016) defined lineaments as simple and complex linear properties of geological structures that are arranged in a straight line or a slight curve such as faults, cleavages, fractures, and various discontinuity surfaces. They are faulting and fracturing zones that result in secondary porosity and permeability. Lineaments are crucial in hydrogeology because they provide pathways for groundwater movement (Aryanto & Hardiman, 2018). Equation (1) is the most widely used to calculate the lineament-length density (L_d), which represents the total length of lineaments in the unit area.

$$L_d = \frac{\sum L_i}{A} \quad (1)$$

Where $\sum L_i$ denotes the total length of lineaments (L), and (A) denotes the unit area (L^2). The lineament density was reclassified into three classes (low, moderate, and high). A high lineament density (L_d) value denotes a zone with high secondary porosity, indicating a zone with high potential groundwater recharge.

2.7.1.4 Drainage as a groundwater recharge potential factor

Drainage density refers to the efficiency with which water is carried across the landscape. Mathematically, drainage density is calculated by dividing the total length of all rivers in a drainage basin by the drainage basin's total area (Yeh *et al.*, 2016). Because drainage density is a measure of surface runoff, it indirectly indicates groundwater recharge. A drainage network's structural analysis can help in determining the characteristics of a groundwater recharge zone, and the quality of a drainage network is determined by lithology, which serves as an important indicator of percolation rate (Yeh *et al*., 2016). The length density (D_d) is calculated using Equation (2) (Achu *et al*., 2020).

$$D_d = \frac{\sum S_i}{A} \quad (2)$$

Where $\sum S_i$ indicates the total length of drainage (L) and (A) denotes the unit area. The drainage density of the study area was reclassified into three different groups (low, moderate, and high). According to (Yeh *et al*., 2016), the drainage density is highly correlated with groundwater recharge. For instance, whereby a zone with a high drainage density (D_d) is described to have a high level of groundwater recharge.

2.7.1.5 Slope as a groundwater recharge potential factor

The slope is defined as the rate of elevation change and is an important factor in determining groundwater recharge potential zones (Aryanto & Hardiman, 2018). The slope directly controls the surface flow velocity, which determines infiltration and thereby groundwater recharge. According to (Achu *et al.*, 2020), a smaller recharge is produced by steeper and larger slopes because water runs quickly off the surface of a steep slope during rainfall, and it does not have enough time to infiltrate the surface and recharge the saturated zone. The slope of the study

area is generally obtained from the Digital Elevation Model (DEM), and it is assessed using the GIS tool.

2.7.2 Establishment of relationships among potential groundwater recharge factors

Groundwater recharge factors have varying degrees of influence, and none of them are independent. According to (Yeh *et al*., 2016), in calculating potential groundwater recharge, these factors are evaluated, and weight accumulation is applied to determine a recharge potential score. The recharge potential is expressed by Equation (3) as:

$$P_R = \sum w_i r_i \quad (3)$$

Where:

P_R - the potential recharge,

w_i - the *ith* factor weights

r_i – is the *ith* factor rate,

The subscripts *i* refer to the individual features of a theme.

The weight of a factor indicates its proportional value in the potential recharge scale. According to (Yeh *et al*., 2016), in a large study area, the recharge potential cannot be tested and verified, thus the score weight of the recharge potential must be subjectively determined based on the relative importance of each factor in the recharge process. In terms of groundwater recharge, each of the contributing variables/factors have a good or negative impact. The five major descriptive levels of potential groundwater recharge zones are given ranging from very high to very low, and the proposed weighting of these levels ranges from a maximum of 10 to a minimum of one point. The factor that has a large influence on groundwater recharge, is assigned a higher recharge weight.

The weights criteria for prospective groundwater recharge, as well as the scores achieved under various characteristics in this study, were referred to the study methodologies of (Yeh *et al.*, 2016).

2.7.3 Spatial Analysis of potential groundwater recharge zones

The factors affecting groundwater recharge identified for any study area are evaluated for the aim of estimating potential groundwater recharge, and weight accumulation is applied to obtain a recharge potential score. These factors are then combined and integrated with GIS to demarcate the potential groundwater recharge zones. According to (Yeh *et al*., 2016) The total weights of various polygons in the integrated layer are calculated using the following weighted linear combination method, shown by Equation (4).

$$P_R = LD_W LD_R + DD_W DD_R + LG_W LG_R + SG_W SG_R + LC_W LC_R + GG_W GG_R + ST_W ST_R \quad (4)$$

Whereby:

P_R – Groundwater recharge potential index

LD – Score of lineament density

DD – Score of drainage density

LG – Score of lithology

SG – Score of slope gradient

LC – Score of Land cover

ST – Score of soil type

GG – Score of geology

The subscripts *w* and *r* refer to the weight of a theme and the rate of individual features of a theme respectively. The resultant score values of the integrated map are then reclassified into five classes with groundwater recharge zones potentiality from very low to very high.

2.8 Modeling and simulation of groundwater systems

Groundwater models are conceptual descriptions and approximations that describe groundwater flow and transport processes using mathematical equations based on certain simplifying assumptions (Kumar, 2003). A model is seen as an approximation rather than an exaggeration because of the simplifying assumptions incorporated in the mathematical equations and the many uncertainties in the values of data required by the model. These assumptions include the direction of flow, aquifer geometry, the heterogeneity of the sediments or bedrock within the aquifer, the contaminant transport processes, as well as the chemical reactions (Kumar, 2003). According to (Asmael *et al.*, 2015), these models have been widely used to better understand flow patterns and explore groundwater system dynamics.

The performance of groundwater artificial recharge is evaluated through groundwater modeling. According to (Chitsazan *et al*., 2018), to use and develop a new numerical model, it is not only necessary to understand the physical and chemical processes relating to artificial recharge and groundwater movement, but also to comprehend the mathematics fundamental principles.

For a groundwater model to be employed in any kind of predictive role, it must be shown that the model is capable of accurately simulating observed aquifer activity, widely known to be model calibration. Model calibration is defined as a procedure in which particular model

parameters, such as recharge and hydraulic conductivity, are changed systematically and the model is run until the computed solution matches field-observed values within an acceptable margin of error (Khadri & Pande, 2016). The calibration of a groundwater model is done to match hydraulic head observations, and during calibration, the heads are adjusted to reduce the errors. This requires field conditions at a site to be properly characterized, and a lack of proper site characterization may result in a model that is calibrated to a set of conditions that are not representative of actual field conditions (Khadri & Pande, 2016).

According to (Khadri & Pande, 2016), the calibration process involves calibrating the model to steady-state and transient conditions. For the field conditions being modeled, the steady-state simulations show no changes in hydraulic head or pollutant concentration over time, while the transient simulations simulate the change in the hydraulic head or pollutant concentration over time. However, models may be calibrated without simulating the steady-state conditions. The simulations are very important in modeling as they are required to narrow the range of variability in model input data because there are numerous choices of model input data values that may result in similar steady-state simulations.

(Khadri & Pande, 2016) further enlightened that model calibration should at a minimum include comparisons of model-simulated and field conditions for data such as hydraulic head, groundwater flow direction, hydraulic head gradient, water mass balance, contaminant concentrations (if applicable), contaminant migration rates (if applicable), migration directions (if applicable), and degradation uses. Graphs, maps, and tables are more appropriate to present these comparisons. There are not widely acknowledged “fitness-of-fit” criteria that apply in every situation. However, it is critical and very important to reduce the discrepancy between model simulations and field measurements. The recommended discrepancy between simulated and actual field conditions should be less than 10% of the field data variability over the model domain (Khadri & Pande, 2016).

A conceptual Modelling approach is widely used worldwide, and it is also used in this study, and the two main steps to this conceptual model is the creation of the Groundwater Modelling System (GMS), and the calibration of the model using measured water levels from the boreholes/wells in the study area. The main parameters involved in the regional groundwater modeling are the construction of the model, Boundary conditions, model grid, time step, groundwater recharge, and model calibration.

2.8.1 Different types of groundwater modeling software

There are a variety of groundwater simulation codes available, each with its capability, operation characteristics, and limitations. Therefore, if modeling is required for a project or study, it is important to determine whether a particular code will be suitable, or if a code that can perform the simulations required exists. The common different types of groundwater numerical modeling software are; MODFLOW, PMWIN (Processing Modflow for Windows), mflab, Visual Modflow Flex, GMS (Groundwater Modelling System), Groundwater vistas, Modflow-Surfact, MODHMS, FEFLOW, and PEST (Kumar, 2019).

The above-listed groundwater modeling software's were studied attentively, and MODFLOW was chosen to be suitable for this study considering the following points: what code is the best in solving the particular problem, what are the data requirements for both code and problem, what computer hardware and supporting staff are required, how much will the computer code cost, and how accurate will the code be in representing the real world. These guidance points for selecting the appropriate software are according to (Kumar, 2019). MODFLOW is further discussed in detail in Section 2.8.2.

2.8.2 MODFLOW as a suitable tool for groundwater modeling for the Ohangwena region

MODFLOW is the most widely used numerical flow model which was originally developed in the US. (Kumar, 2019) defined MODFLOW as a three-dimensional finite-difference groundwater flow modeling program that allows a person to create a numerical representation of the hydrogeologic environment at a site being investigated. MODFLOW uses a block-centered finite difference technique to simulate groundwater flow within the aquifer. Different layers of the aquifer can be simulated as confined, unconfined, or a combination of the two. This tool also models the external stresses such as flow to wells, areal recharge, evapotranspiration, flow to drains, and flow through riverbeds.

(Harbaugh *et al*., 2000) developed this deterministic numerical model based on Darcy's law and the mass conservation idea. This model is well documented and widely used all over the world, based on the horizontal and vertical discretization of the modeling domain which solves the groundwater flow equation for each cell. It can easily be incorporated into future studies for optimal water resource management.

MODFLOW involves a conceptual modeling approach and a numerical model approach of groundwater flow. Model conceptualization is defined as the process of systematically assembling data describing field conditions to describe groundwater flow and contaminant transport processes at a site (Kumar, 2003). The model conceptualization assists in deciding on a modeling approach and the software to employ. While the mathematical model of groundwater flow is made up of the governing equation, appropriate boundary conditions, initial conditions, annual averaged infiltration and groundwater extraction amounts, and the spatial distribution of the hydrogeological parameters that affect the flow.

The three-dimensional (3D) groundwater flow in MODFLOW is mathematically represented using the water balance and Darcy's law governing equation (5):

$$q_s = S_S \frac{dh}{dt} - [\frac{\partial}{\partial x}\left(K_x \frac{\partial}{\partial x}\right) + \frac{\partial}{\partial y}\left(K_y \frac{\partial h}{\partial y}\right) + \frac{\partial}{\partial z}\left(K_z \frac{\partial}{\partial z}\right)] \quad (5)$$

Where h is the hydraulic head, S_s is the specific storage, q_s is the sink/source, K_x K_y K_z is the hydraulic conductivity in x, y, and z directions, respectively.

Various models were studied, and MODFLOW software was chosen to simulate the Ohangwena Multi-layered Aquifer's 3-D groundwater flow system based on the availability of data and accessibility of the model. In this study, the three-dimensional steady groundwater flow was simulated using MODFLOW-NWT with Model MUSE version 3.10. as the graphical user interface (GUI).

2.8.3 Case studies of groundwater modeling using MODFLOW

Several studies have used the MODFLOW program in simulating surface-water and groundwater flows, and also modeling managed aquifer recharge. In a case study of the West Coast, South Africa by (Zhang *et al*., 2019), a groundwater flow model of the study area was developed using ModelMuse (Graphical User Interphase of MODFLOW) to analyze the groundwater flow system and to verify the suitable sites for AR developed in GIS. The model was divided into four layers with varied thicknesses, and it was then calibrated using the groundwater level data of 59 boreholes which were adopted across the study area. It was calibrated for steady-state conditions, which represent the flow regime before 2014 when there was no major decrease in rainfall. The calibration process of this model continued until the best fit between the simulated and observed piezometric heads was achieved, during which the hydraulic conductivities were required to be maintained within certain ranges. In the comparison of the observed and simulated piezometric heads denoted by (h_{obs} and h_{sim}) respectively, the goodness of fit of the model was calculated using the Root Mean Square Error (RMSE) and the Normalized Root Mean Square Error (NRMSE) shown by Equation (6) and (7), with h_{max} and h_{min} as the maximum and minimum observed piezometric head, respectively.

$$RMSE_{\cdot} = \sqrt{\frac{\sum(h_{obs} - h_{sim})^2}{n}} \tag{6}$$

$$NRMSE_{\cdot} = \frac{RMSE}{h_{max} - h_{min}} \tag{7}$$

The calculation of the goodness of fit of the model shows that between the observed and simulated piezometric heads, an RMSE of 5.4m and an NRMSE of 5.3% were achieved, with a correlation coefficient value of 0.95, which represents an acceptable calibration for the intended modelling purpose.

In a different case study of Pajaro Valley Groundwater Basin, California by (Russo *et al*., 2015), MODFLOW was used to simulate the surface and subsurface hydrological processes. The model of this study was developed with 6 layers that vary in thicknesses across the basin and corresponding to the aquifer and confining layers. About 1000 active production (agricultural, municipal, and domestic groundwater wells, were included in this model. The simulations used in the study span 34 years (from 1976 to 2009) and are divided into 408 monthly stress periods with two times steps each.

In another study of Neishaboor plain, Iran done by (Izady *et al*., 2015) stated that during the last few decades there was increased irrigation in the watershed which has caused serious groundwater depletion. In this study, SWAT and MODFLOW programs were used to integrate and simulate surface-water and groundwater flows, respectively. The geographic and temporal distributions of hydrologic components were computed repeatedly using these tools. To predict the groundwater flow, fully transient simulations were run for the 2000-2012 period, and the model calibration and validation were done for October 2000 to September 2010, and October 2010 to September 2012 periods, respectively. The time-varying constant head bounds were prescribed using monthly measured groundwater level data from existing observation wells on the model boundary. To understand the model's responsiveness to parameter changes, the model was first calibrated by trial and error. After that, using 48 observation wells as a control point, the PEST algorithm was employed to establish optimal calibrations. The efficiency of the model and its ability to make predictions for the calibration and validation periods were assessed using a variety of criteria. The results of this study show that the simulated 10-year mean annual recharge rate calculated with the combined model ranged from 0 to 960 mm, with an average of 176 mm. This result was in good agreement with an earlier study's independently determined annual recharge rate.

In a case study of east-central Tunisia by (Lachaal *et al.*, 2012) MODFLOW and GIS tools were used to implement a 3-D groundwater flow model of this semi-arid region. To explore the hydrological processes in the Zeramdine-Beni Hassen Miocene aquifer and to confirm groundwater properties derived from the geophysical, hydrodynamic, and hydrochemical studies conducted in the region, an integrated methodology was developed using coupling of groundwater flow model MODFLOW 2000 code with Geographic Information System (GIS) tools. The three-dimensional groundwater flow was mathematically represented with Darcy's law Equation (5) based on the water mass balance.

The mathematical model of the groundwater flow is composed of the governing Darcy's law Equation (5), appropriate boundary conditions, initial conditions, annual-averaged infiltration, and groundwater extractions amounts, and the spatial distribution of the hydrogeological parameters that affect the flow. According to the evaluated data, the modeling period of this study is 27 years, from 1980 to 2007, and the data sets during this period were used to calibrate and validate this groundwater flow model. The results show that the ZBH aquifer is most sensitive to changes in water infiltration and hydraulic conductivity, and the model simulation shows a good understanding of aquifer hydrogeology. The results of the aquifer groundwater dynamics simulation show that the calculated water levels are close to the observed values. This model can be used to analyze the hydrological processes in complex groundwater with similar geological and hydrogeological circumstances, as well as to provide a management rescue plan for the assessed aquifer, which is particularly relevant for aquifer characterization in arid and semi-arid regions.

In another case study of Hanoi, Vietnam (Glass *et al*., 2018), stated that urban development in the area has caused a severe decline in groundwater levels. This study assessed

the current situation of the study area and analysed whether Aquifer Recharge (AR) is a viable option for preventing additional groundwater depletion. To analyse the groundwater flow system and examine the feasibility of using AR as a solution for sustainable water management, a hypothetical groundwater flow model was set up. MODFLOW-NWT was used to create a numerical transient flow model that was calibrated for the years 2005-2007. The model was divided into four layers with varying thicknesses. The goodness of fit of the model was calculated using the Root Mean Square Error (RMSE) and the Normalized Root Mean Square Error (NRMSE) by comparing the observed and simulated hydraulic heads. Equations (6) and (7) similar to the ones used in the study by (Zhang *et al.*, 2019), were used to calculate the Root Mean Square Error and the Normalized Root Mean Square Error. The calibration of this study's model was regarded as acceptable with an overall Root Mean Square Error of less than 2m and a Normalized Root Mean Square Error of less than 10%. According to the simulation results of this study's model, it shows that AR can only make a minor contribution to the city of Hanoi's overall water budget. However, using AR to efficiently relocate wells towards the Red River to induce riverbank filtration can help address the city's current massive groundwater depression cones. Groundwater simulations show that groundwater levels can be raised locally, preventing future land subsidence, and ensuring adequate water supply, particularly during the dry season.

GIS and groundwater flow model tools were again used to manage the groundwater resources in the arid area of Tunisia (Chenini *et al*., 2019). This study focused on characterizing hydrogeological and aquifer recharge mapping for groundwater resources management. A multicriteria method with a weighted-rating procedure was adopted in the study to create a map displaying locations appropriate for groundwater recharge. The map showing areas that are suitable for an artificial recharge was developed in GIS, which integrated and analyzed different thematic layers. The groundwater recharge susceptibility map was also generated using the same tool. The groundwater rechargeability index map that was produced in GIS was validated using the numerical model MODFLOW. The assessment of the impact of the recharge process and the phreatic aquifer behavior under different conditions were also done with the model, while the hydraulic heads simulation and water budget analysis for Tunisia were then used to assess the impact of groundwater recharge. The results of this study show that the medium rechargeability index covers only 29% of the overall shallow aquifer extension, while the high rechargeability index covers 45%.

In another study carried out by (Chenini & Ben , Mammou, 2010) in the Maknassy basin, located in Central Tunisia, made use of the GIS techniques and numerical modeling to demarcate the suitable sites for artificial recharge of groundwater aquifers in this arid area. Thematic maps were prepared using a Hydrogeological Information System, and all the thematic layers were then integrated into ArcView based model, which generated a map showing artificial recharge zones. MODFLOW-2001, a groundwater model, was used to estimate the impact of water recharge on the hydrological system's piezometric behaviour. These simulations have aided in the management of groundwater resources in the study area. The groundwater flow modeling results show that the recharge rate in the study area was 24%

of the total annual rainfall in 2004/2005, and the weight of recharge on groundwater storage was illustrated by the piezometric behaviour of the three aquifer levels, which was simulated based on the artificial recharge zone map.

MODFLOW is regarded as a powerful numerical code for representing groundwater flow regimes and their related physical processes, and it is an excellent tool for the simulation of future requirements to groundwater resources. The numerical modeling done by this tool gives a higher level of understanding groundwater flow processes and quantification of groundwater balance. Because it is an open source, it promotes transparency, and it is therefore preferred for litigation. MODFLOW is also supported by USGS with a continuous development of packages, solvers, engines, and visualization tools.

2.9 Groundwater flow and contaminant transport modeling

Groundwater is the major water source for domestic and industrial uses in many rural and urban settlements around the world, and therefore its quantity and quality have to be carefully managed. In a study by (Zulfiqar *et al*., 2013), it was reported that groundwater is in most cases contaminated by industrial effluents, accidental spills, and leaks from the surface and underground tanks. Groundwater contamination is a growing concern and is poorly understood compared to freshwater contamination. The extent of groundwater contamination can be assessed using an appropriate mathematical model, and develop strategies to mitigate the problem accordingly (Sharma *et al*., 2020). According to (Zulfiqar *et al*., 2013), the extent of groundwater contamination can also be determined by taking samples from several points within time and budgetary constraints, which in general requires the installation of several observation wells. The cost of this operation is very high, especially when more precise measurements are required.

Aquifer recharge can ensure a sustainable level of groundwater, while strict quality control of the water intended for recharge can minimize contamination both of groundwater and aquifers (Díaz-Cruz & Barceló, 2018). Aquifer Recharge has been achieved using a variety of water sources including surface water, reclaimed wastewater, urban and rural stormwater runoff as outlined in section 2.5. However, all these sources are vulnerable to contamination by a wide variety of chemicals that can adversely affect groundwater and the entire aquifer system over some time. These water sources are affected by industrial, agricultural, and domestic contamination (Díaz-Cruz & Barceló, 2018).

The transport of contaminants in groundwater is generally governed by three processes which are: advection, dispersion, and retardation. (Zulfiqar *et al*., 2013) defined advection as the movement caused by the flow of groundwater, and it is calculated based on Darcy's law. According to (Zulfiqar *et al*., 2013), several studies have used Particle tracking (a numerical method that places a particle into the flow field and numerically integrates the flow path) to calculate advective transport paths.

Dispersion is another process governing groundwater transport contaminant, which is defined by (Sharma *et al*., 2020) as it represents the spread of contaminants as they flow through the subsurface. (Zulfiqar *et al*., 2013) also reported that the contaminant plume is gradually diluted by dispersive spreading within and transverse to the main flow direction. The dispersion process causes contaminated water to mix with uncontaminated groundwater, resulting in a dilution effect. Furthermore, this technique is also used to predict transport away from point sources of contamination as well as influence the spread of nonpoint source contaminants. According to (Zulfiqar *et al*., 2013) the aquifer heterogeneities such as variations in hydraulic conductivities and porosity cause contaminant plumes to disperse.

Retardation is also another process governing groundwater contaminant transport which determines how fast a contaminant moves in relative to the groundwater. It is reported by (Zulfiqar *et al*., 2013) that the contaminant movement in groundwater is retarded by two mechanisms, sorption, and biodegradation.

In groundwater contaminant transport modeling, two partial differential equations are solved simultaneously, with appropriate initial and boundary conditions. The first partial differential equation (8) relates to the flow of groundwater in saturated porous media, while equation (9) relates to the transport of dissolved solutes.

$$\Delta_V = \Delta(-k\Delta h) = -S_S\frac{\partial h}{\partial t} \pm Q \tag{8}$$

Where: -

v = Darcy's velocity

k = hydraulic conductivity (LT^{-1})

h= hydraulic head (L)

Δ = Differential operator

S_S= Specific storage (S/b) (L^{-1})

S = storage coefficient of the aquifer

b = thickness of the aquifer (L)

Q = specific source (-) or sink (+) as volumetric flow rate per unit aquifer area (T^{-1})

The solute transport is expressed by equation (9)

$$\frac{\partial}{\partial \mathrm{x}}\left(\mathrm{D_x}\frac{\partial \mathrm{C}}{\partial \mathrm{x}}\right)+\frac{\partial}{\partial \mathrm{y}}\left(\mathrm{D_y}\frac{\partial \mathrm{C}}{\partial \mathrm{y}}\right)+\frac{\partial}{\partial \mathrm{z}}\left(\mathrm{D_z}\frac{\partial \mathrm{C}}{\partial \mathrm{z}}\right)-\frac{\partial}{\partial \mathrm{x}}(\mathrm{V_xC})-\frac{\partial}{\partial \mathrm{y}}(\mathrm{V_yC})-\frac{\partial}{\partial \mathrm{z}}(\mathrm{V_{zz}C})=\mathrm{R}\frac{\partial \mathrm{C}}{\partial \mathrm{t}} \tag{9}$$

Where: -

C= solute concentration in a liquid phase (M/L^3)

V= pore velocity components

D= hydrodynamic dispersion coefficient (L/T^2)

R= (1+ρK_d)/Θ represents the retardation factor

ρ = bulk density of the soil media

K_d= distribution coefficient

Θ = porosity of the soil media

Modeling groundwater flow and contaminant transport begin with the development of a conceptual model, selection of a computer code, and design of the model (Zulfiqar *et al*., 2013). (Zulfiqar *et al*., 2013) further explained that numerical groundwater flow models are defined by the following parameters: sources and sinks of water, the available geohydrologic system, system geometry, the spatial and temporal structure of the hydraulic properties, and boundary conditions. MODFLOW and MT3DMS solute transport codes are the most widely used to simulate the transport of contaminants within the aquifers. And according to (Zulfiqar *et al*., 2013) these codes use finite difference schemes as their numerical algorithms, and they are very reliable.

2.9.1 Case studies of groundwater flow and contaminant transport modeling

Various types of transport models have been used to simulate the movement of contaminants within the aquifers. A study by (Sharma *et al*., 2020) discussed the sources of contaminants, their movements within the aquifer system through mathematical modeling, and remedial measures to stop further contamination of groundwater in India and Australia. This study employed MODFLOW and MODPATH to simulate and track the movement of contaminants within the aquifer system at an injection well. The model of this study predicted that groundwater flow at the injection site would move to the South-east towards Lake Decatur, and based on the forward simulation with MODPATH, it was estimated that the contaminant particles (gas plume) placed at the injection site reached Lake Decatur in 80 days.

2.10 Previous studies conducted in Ohangwena region in relation to groundwater recharge

Few studies have been done in the Ohangwena region regarding groundwater recharge in the area. A study conducted by (Masule, 2019) looked at the age dating of groundwater in a perched aquifer of Ohangwena region to help determine the recharge dynamics using stable isotopes method at four different sampling sites. The study found out that at the first site, the groundwater age was 7 years, at the second site it was 5 years, at the third site it was 10 years and at the last site it was 1 year. It also found that the groundwater in the perched aquifer is higher proportion of younger water compared to old water, and this shows that there is more recharge taking place to the perched aquifer, although it contains predominantly blackish water.

Another study was conducted by (Wallner *et al*., 2017) on the KOH-II aquifer of the region to identify the recharge from rainfall to the aquifer. The study used Satellite radar interferometry (InSAR) for the analysis of ground uplifts and subsidence processes on the regional scale, which can be used to study groundwater recharge or aquifer depletion. The study found that the recharge to this aquifer from the Namibian side is less than 1 percent of the mean annual rainfall in the area, which is very low, and yielding recharge volumes of very few cubic metres to sustain the aquifer. However, (Wallner *et al*., 2017) stated that there is a possibility that this aquifer is recharged on the Angolan side, although not proven. Further research was suggested to be carried out on the Angolan side.

In another study conducted by (Lindenmaier *et al.,* 2014) established an exploration strategy of groundwater and followed in the northern Namibian Cuvelai-Etosha Basin (CEB). In this study, further exploration was made on the recharge of the KOH-2 aquifer, and several solutions were found that the recharge of the aquifer may be occurring through a top-down recharge via geological windows to the north or east of the area, this was due to the freshwater zone recorded by the TEM soundings. Another possible recharge path would be regional lateral discharge from the recharge areas in the Angolan highlands, although it is not proven. Recommendations were made that strict measures need to be applied to ensure that the water in the aquifer is exploited sustainably.

2.11 Summary

Based on the detailed literature review, it was determined that the methods used in the case studies of the West Coast South Africa (Zhang *et al*., 2019) and coastal central California (Russo *et al*., 2015) were the most suitable for this study. Accordingly, a combination of GIS and numerical modeling was used to give a more detailed and quantitative assessment of Aquifer Recharge's suitability in the study area. The study made use of the available data in Ohangwena, which included the surface, subsurface, and hydrologic data. The study also assessed the dispersion of the contaminants associated with runoff, within the Ohangwena aquifer system.

The combination of both the GIS-based integration method and numerical modeling would give a detailed and quantitative assessment of Aquifer Recharge opportunities and impacts. and it can assure consistency of data used for GIS and numerical modeling studies (Russo *et al*., 2015). The numerical modeling is an important tool for identifying sites that are amenable for AR and estimating the potential benefits based on regional hydrologic conditions under a range of future climates, water use, and management scenarios.

3. Method

3.1 Overview

In this study, the potential of using runoff for Aquifer Recharge was investigated in Ohangwena, Namibia. The various opportunities of aquifer recharge in Ohangwena were explored to determine potential and likely challenges. The method used in this study follows that used in the Western coast, South Africa case study (Zhang *et al*., 2019), and Central Coast California (Russo *et al*., 2015). The overall research framework flowchart is presented in Figure 3.1.

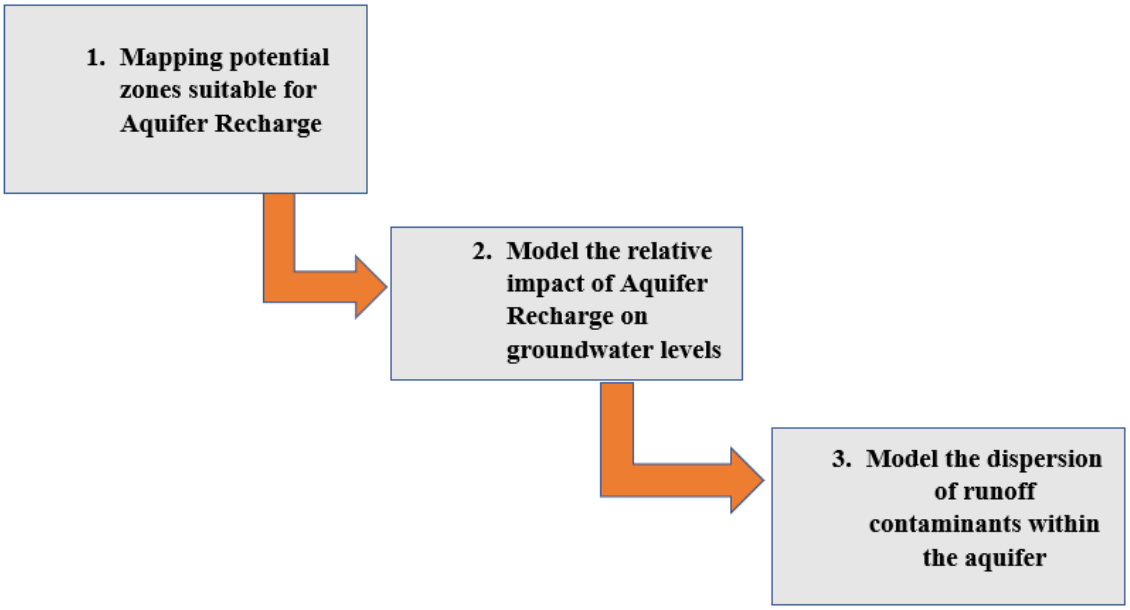

Figure 3. 1: Overall research flowchart

This chapter consists of nine sections which include an overview, statement of the method, selection of the study area, characteristics of the study area, data required, mapping the potential sites suitable for groundwater recharge, modelling the relative impact of AR on groundwater levels, modelling the transport of runoff contaminants in the aquifer, and a summary of the method.

3.2 Statement of the method

The method used for assessing the site suitability for AR using runoff in the study area is a two-way approach, comprising of GIS-based analysis and numerical modeling. The first step involves GIS-based analysis to produce an initial map of suitable sites in the study area. Groundwater modeling was then employed in step two, to determine the impact of aquifer recharge on the groundwater levels at some wells in the study area. Using a model, a simulation was run in the recommended sites to assess the impact of the AR scenario on the groundwater

levels of the study area. The model simulation was also used to assess the dispersion and movement of the runoff contaminants within the aquifer in the study area.

3.3 Selection of the study area

The essential pre-requisites for AR assessment are as follows.

i. The presence of a suitable aquifer in which to store water,

ii. Availability of water source, and

iii. Availability of data to model the hydrological and hydrogeological processes.

A preliminary investigation was undertaken to determine the availability of storage for water and the linked available data such as rainfall and sources of water. Several studies conducted in the study area that are linked to this research identified the presence of an aquifer and available water bodies and ponds in various catchments of Ohangwena (Lindenmaier *et al*., 2014), and (Wallner *et al.*, 2017). The local hydrogeological knowledge was also used to identify the presence of aquifers and their suitability for Aquifer Recharge.

3.4 Characteristics of the study area

Ohangwena region is in the Northern part of Namibia, lying in the Cuvelai-Etosha basin. It is located at 17˚56’20” S, 17˚23’28” S, 15˚32’49” E, and 17˚59’55” E with minimum and maximum elevations of 1071m and 1198m respectively. Cuvelai-Etosha Basin (CEB) is an extensive sedimentary basin that is part of the much larger Kalahari Basin covering parts of Namibia, Angola, Zambia, Zimbabwe, Botswana, and South Africa (Altchenko & Villholth, 2013). According to the 2011 census, the Ohangwena region houses 11.6% of the total population of Namibia. The projected population figures for the Ohangwena region for the year 2021 at 0.7% growth rate per annum is estimated at 319932 (Namibia Statistics Agency, 2014), and this population mainly depends on groundwater for domestic water supply. Rainwater ponds and hand-dug wells are used as sources of water for domestic use and livestock watering. The hand-dug wells have depths ranging between 0 to 30 m, and they draw water from the shallow aquifers. Figure 3.2 shows the location of the study area in Namibia.

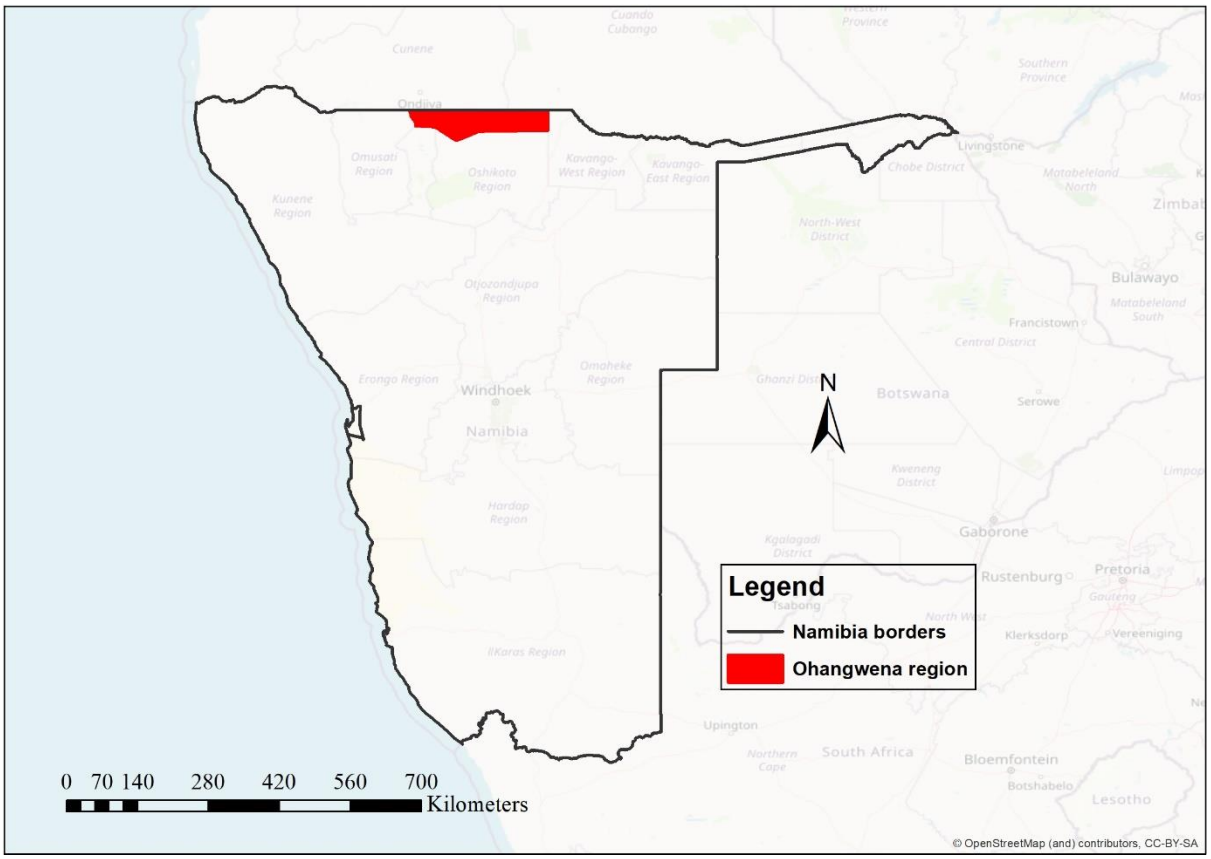

Figure 3.1: Ohangwena region location on the Namibian map

3.4.1 Suitability of Ohangwena region as a study area

Ohangwena was chosen from other catchments within the northern part of Namibia because it has several ponds and several shallow lakes. This has the potential to be adapted to act as a storage body for surface water, and as a location for the injection wells of runoff to augment the groundwater in the region. The region has an aquifer system, there is availability of water source (runoff), and there is available data to model the hydrological and hydrogeological processes which are mandatory requirements for Aquifer Recharge assessment, and this allows AR to store runoff as groundwater for later recovery. The sources of water in the area are shown by figure 3.5 in section 3.4.4.

3.4.2 Water storage in the area

Ohangwena region lies in a transboundary aquifer (Cuvelai - Etosha basin) that has a three-layered aquifer system and is mostly dominated by fine-grained, well-sorted, unconsolidated aquifer sands and fine-grained, unsorted, and clayey to silty sand. The high population density within this area, is made possible by the Oshana drainage system with periodic surface water flows, which recharge groundwater, renew grazing and bring fish into the area. Although there is a high population density, this area is frequently affected by drought. The most essential

natural resources that people depend on are freshwater (rainwater, ephemeral surface water, and groundwater), grazing, and suitable soils for crop cultivation and trees. The recharge of groundwater from rainfall and ephemeral floods is very limited due to high evaporation rates and pumping of groundwater leads to lowering of the groundwater table, with resulting adverse effects on vegetation and water supply in the long run.

According to (Wallner *et al*., 2017), There are three main aquifers in the area with intervening aquitards. The aquifer system is made up of an upper perched aquifer (KDP or KOH-0) which is seasonal, temporally, and generally not deeper than 11m. Below the upper perched aquifer lies the semi-confined aquifer (KOH-I) which is 60 – 180m deep, and the confined aquifer (KOH-II) which lies below the semi-confined aquifer and has a depth that ranges between 200 and 350m below ground level. The upper perched aquifer is also referred to as the Discontinuous Perched Aquifer (DPA), and the semi-confined aquifer is also referred to as the Main Shallow Aquifer (MSA).

The uppermost perched aquifer is discontinuous and appears mainly in the Aeolian sheet sands and is of local importance (Dierkes, 2011). KOH-I is semi-confined with varying water quality, becoming more and more brackish in the direction of the Etosha pan located on the southern side of the region. KOH-II extends to the west and south, however with decreasing water quality as it gets more brackish. In the past, the unperched aquifer (KOH-0) and the upper perched aquifer (KOH-I) were the most used aquifers by the inhabitants of the region, which led to their water levels dropping drastically, and in most cases, they get depleted especially during the dry season (Dierkes, 2011). However, many boreholes have now been drilled into the KOH-II aquifer, which holds a large capacity of water. This study assessed KOH-II as a storage facility.

The KOH-II aquifer has a large amount of fresh water and has a very high potential to compensate for water shortages during droughts if properly maintained (Wallner *et al.*, 2017). According to (Wallner *et al.,* 2017), three boreholes were first drilled in this aquifer by BGR (German Federal Institute for Geosciences and Natural Resources), which yielded good water, and they are currently supplying Eenhana town with water. After then, many boreholes have been drilled into this aquifer, to supply the inhabitants of the region with water. According to (Dierkes, 2011), the boreholes and wells drilled in the area are equipped with windmills, diesel-driven pumps, or solar power pumps, due to the depth of the water table. In some locations, the groundwater is used concurrently with pipeline water to minimize the high fluoride and Sodium content. Figure 3.3 shows the conceptual model of the Ohangwena Aquifer System.

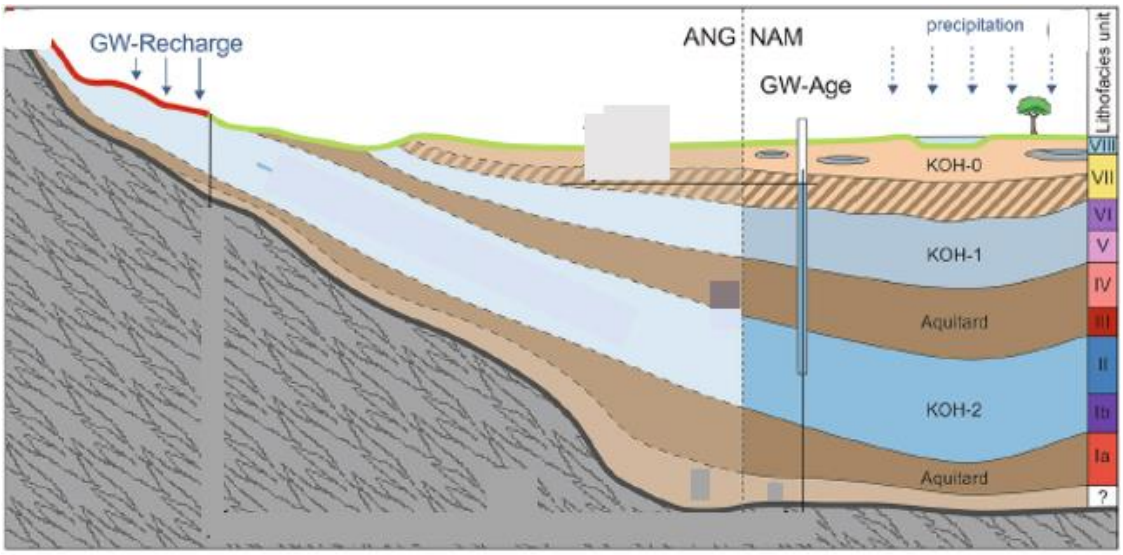

Figure 3.2: Conceptual model of Ohangwena aquifer system (Wallner, 2017)

3.4.3 Climatic conditions

Ondangwa Meteorological Services Weather station (located west of the region) is considered as the representative weather station of the region. According to a report by (The Department of Water Affairs Republic of Namibia, 1994), the mean annual rainfall in the region is about 419 mm, increasing from the west to east. The rainfall in the area occurs between October and May, concentrating on the period of January to March. The temperature in the area ranges from 17.5 ˚C to 26 ˚C, and humidity values are relatively low with a range between 50% in March and 17% in September. There is a high rate of evaporation due to strong solar radiation, low humidity, and high temperatures. With the high evaporation rates, most pans and ephemeral rivers dry up around August which results in precipitation of salts and increased salinity of shallow aquifers in waterlogged areas, and areas comprising of low permeable lithologies. The mean monthly rainfall for the Ohangwena region for six years period (2014-2019) is shown in Table 3.1 and Figure 3.4.

Table 3.1: Mean Monthly Rainfall (MMR) for Ohangwena region (2014-2019)

Month	Jan	Feb	Mar	Apr	May	Jun	Jul	Aug	Sep	Oct	Nov	Dec	**Total**
MMR (mm)	72	83	102	48	15	2	0	0	6	13	24	54	**419**

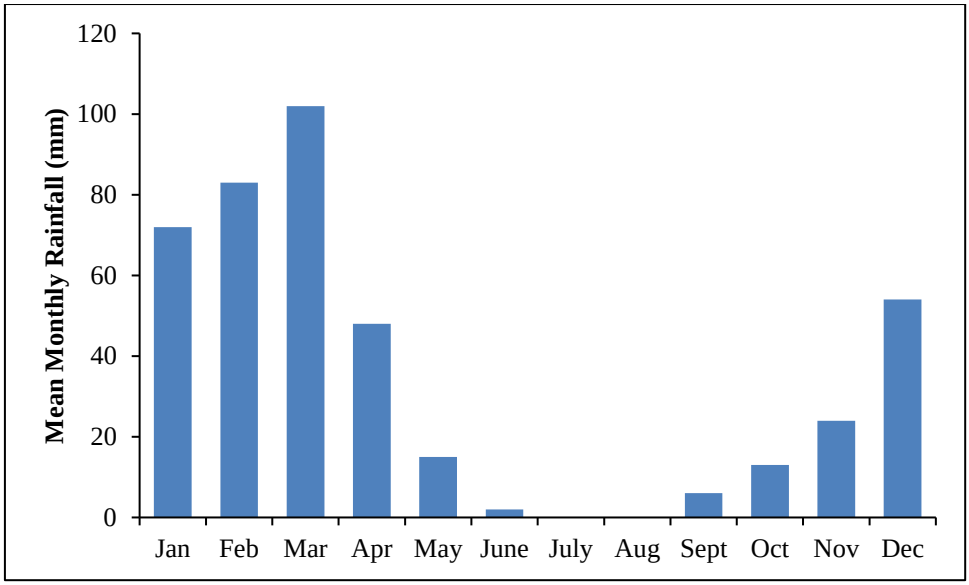

Figure 3.3: Mean Monthly Rainfall for Ohangwena region (2014-2019)

3.4.4 Sources of water in the study area

There are no perennial rivers and no permanent rivers or lakes in the area, but the western region is part of the Cuvelai delta drainage system, consisting of shallow ephemeral drainage basins (Oshana's). The shallow ephemeral drainage basins cover 35% of the region. There are also two main rivers passing through the region, one serves as the draining channel from Angola, and passes through the region, discharging water to the Etosha pan located south of the region. The second river also drains water from Angola and discharges to the eastern part of the region, which belongs to the Okavango delta. The nearest perennial rivers are the Kunene River in the northwest, flowing from Angola along the border to the Atlantic Ocean, and the Okavango River which forms part of the Angola-Namibia border, flowing south-eastward from central Angola to the Kalahari in northern Botswana, where it terminates in an immense inland delta known as the Okavango swamp. These two rivers are considered important sources of water for the whole of northern and central Namibia.

The main water source available for the inhabitants and their livestock in the area is rainfall during the rainy season. The rainwater is collected at the household level from roofs and as surface runoff from the catchment area flowing into reservoirs and ponds. Surface and flood water is another water source in the study area, which flows during the rainy season in ephemeral rivers and Oshana's and collects in natural pans. The floodwater originates from Angola and flows along the drainage channels and streams that pass through the region, discharging into the Etosha pan. This water can be channelled and stored in ponds and reservoirs. Groundwater is another water source in different types of aquifers, and some of the aquifers in the region contain saline groundwater which is unsuitable for human consumption. Lastly, river water is also another source of water that is transported using canals from the Kunene River to major settlements within the Owambo including the Ohangwena region,

although it only covers a small portion of Ohangwena. The sources of water in the area are well documented by (Sorensen, 2013) and are shown in Figure 3.5.

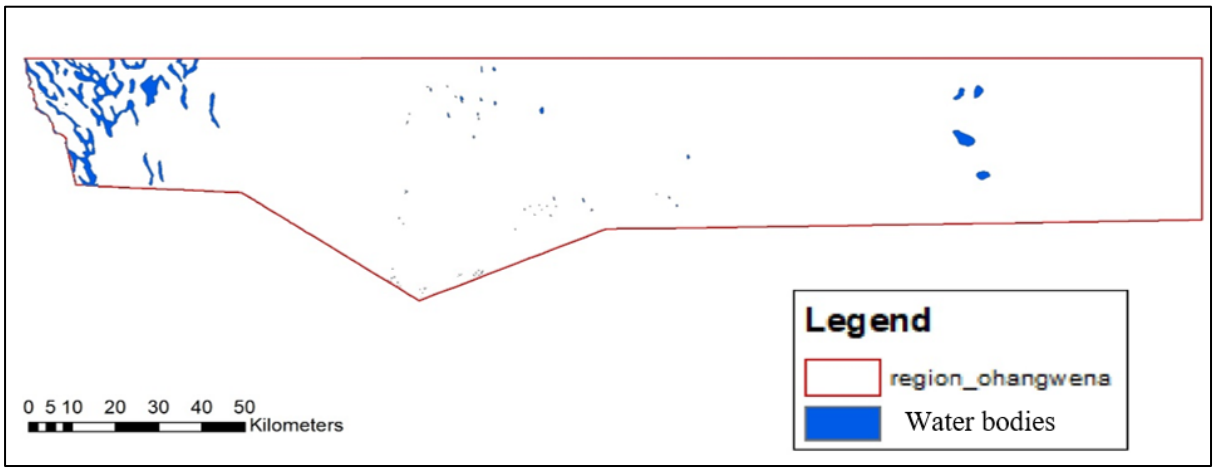

Figure 3.4: Ohangwena region water bodies (Sorensen, 2013)

As shown in Figure 3.5, most of the water bodies are situated in the central and western region which is part of the Cuvelai drainage system. There are four large ponds located on the central-eastern side of the region. These water bodies are located in the areas of small-scale agricultural systems, where most of the people in the region live (see land use map in Figure 3.7).

3.4.5 Water quality of Ohangwena region

Water in Ohangwena is mostly of good hygienic quality, but standing water collected in dams and ponds gets easily polluted from human and animal waste. Domestic animals contaminate the water directly by wading and with droppings and urine, and contamination from human waste is transported during heavy rains with surface flow from nearby places used as open-air toilets. Groundwater in the area is naturally saline, with salinity varying at different depths of the aquifers.

3.4.6 Soil data

The soils of the Ohangwena region are broadly classified into four groups which are mainly; aeolian, sands, and fluviatile origin showing poor water-holding capacity and low nutrients (Altchenko & Villholth, 2013). The ephemeral rivers in the area which discharge into the Etosha pan consist of highly variable fluviatile lithology, that comprises a mixture of gravel, sand, silt, and clay with frequently inter-bedded hardpan layers. Tall woodlands forests grow on the deep infertile sands of this region which has extremely little water holding capacity. These sands are not suitable for crop production, and during the wet season, many small pans are formed in this area. According to (Altchenko & Villholth, 2013), the soils around these pans consists of more clay particles that hold more water during rainy seasons with a greater concentration of nutrients. Most people live in clustered villages on these soils and grow crops

around the pans, and in a few towns that are established within the region. The known soil infiltration rates in the region are shown in Table 3.2.

Table 3.2: The soil infiltration rates in the region

Soil type	Infiltration rate (mm/hr)		
	Western side	The central and northern side	Southern side
Sand	21,00	26,00	23,19
Sandy silt	18,15	22,34	21,08
Silt	12,11	11,41	10,86
Clay	3,00	4,32	2,13

3.4.7 Land-use system

(The Department of Water Affairs Republic of Namibia, 1994) documented the land-use system of the study area and shows that the communities of Ohangwena depend on rain-fed subsistence agricultural farming in which small-scale activities such a pearl millet (Omahangu) cultivation and livestock rearing are practiced. Pearl millet is the main staple food in the area, and it is more drought-tolerant thus and better suited for semi-arid conditions. In addition to field crops, the community also keeps small vegetable gardens within the homesteads. This land-use system also consists of the management of trees that provide edible fruits. The tree component of the system is important for maintaining vegetation cover during the long dry season, and for the reduction of soil erosion and improvement of rainwater infiltration into the soil. A combination of these three components is essential to maintain the productivity of the system. The detailed map of the land use of the Ohangwena region is well shown in Figure 3.7, in section 3.6.1.2 of this report.

3.5 Data Required

For Aquifer Recharge site suitability selection, different types of data sets are required for the assessment, and considerations are given to data availability. The assessment involved surface and subsurface data as follows

i. The surface analysis data include surficial geology, soil infiltration capacity, land use, topographic slope, hydrological data, and measured recharge rates from observational studies;

ii. Subsurface analysis data aquifer thickness, aquifer hydraulic conductivity, aquifers layers thicknesses, aquifer storability, the type of aquifer, and historical changes in the water table elevation.

This study used both primary and secondary data. The secondary data was obtained from previous studies which were done in the study area. The data was obtained from the University of Namibia (UNAM), SASSCAL portal, and BGR databases. The secondary data used in this study were soil infiltration capacity, measured recharge rates, aquifer thickness, aquifer hydraulic conductivity, layers thicknesses, aquifer storativity, and runoff contaminants concentrations. The historical changes in water table elevation data used in this study are primary data obtained from the Namibian Ministry of Agriculture Water and Land Reform. Part of the weather data is obtained from Ondangwa Meteorological Services, while some weather data are obtained from different weather stations in the study area, through the Southern African Science Service Centre for Climate Change and Adaptive Land Management (SASSCAL) weather portal. The topographic slope and the land use data were obtained from the Diva-GIS portal. The surficial geology data and the shapefile of the study area were obtained from the SASSCAL data and information portal.

3.6 Mapping the potential sites suitable for groundwater recharge

In this study, mapping the potentially suitable zones for an Aquifer Recharge was done based on the characteristics of the study area, whereby appropriate weights were assigned to different factors that affect groundwater recharge. The factors influencing groundwater recharge, and their relative importance were compiled from different literature, explained in section 2.7 of the literature review. The seven main significant factors affecting the potential of groundwater recharge used in this study are Lithology, land use/cover, lineaments, drainage, slope, geology, and soils. GIS technology was used to digitize the hydrologic and geographic data, and a basic database was built. For each factor, appropriate scores were assigned, and lastly, the spatial analysis function was used to determine the potential groundwater recharge zone of the study area. Figure 3.6 illustrates the flowchart used in identifying the suitable groundwater recharge zones in this study.

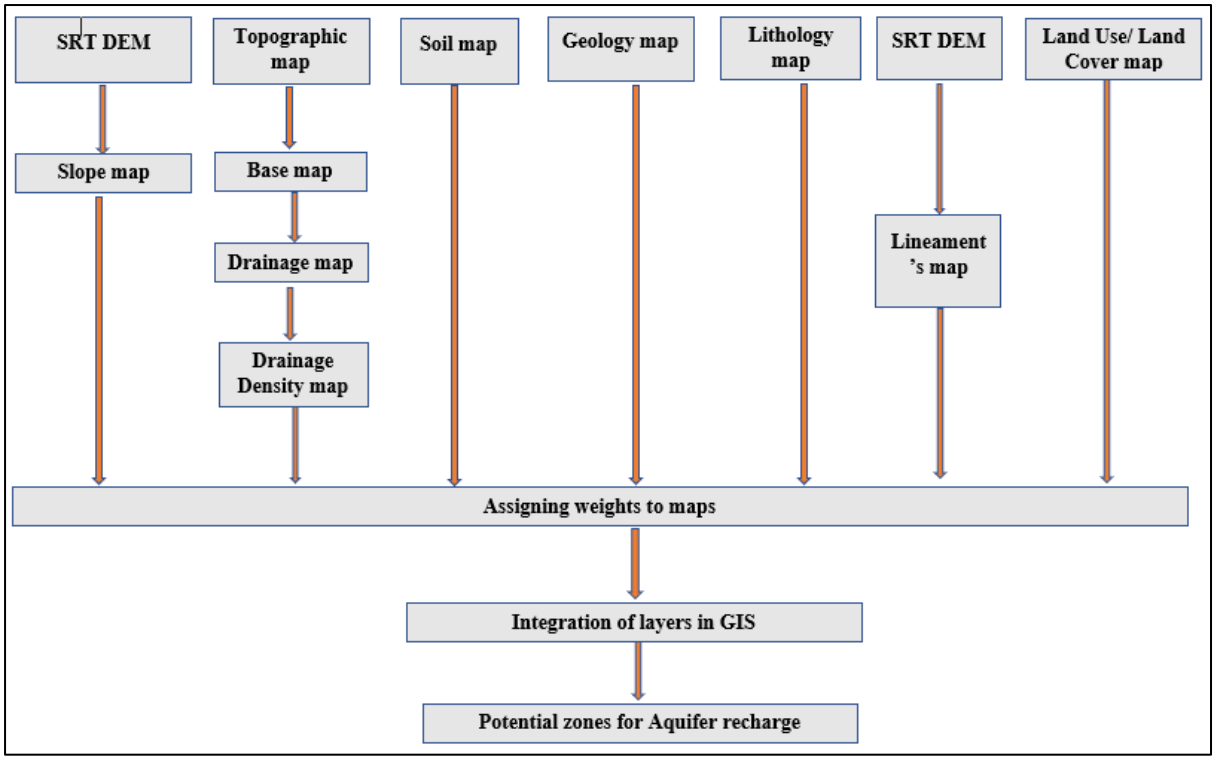

Figure 3.5: Flowchart for mapping the zones suitable for Aquifer Recharge

The parameters illustrated in Figure 3.6 for determining the potential groundwater recharge zones in the Ohangwena region are further discussed in detail in Section 3.6.1.

3.6.1 Factors that influence groundwater recharge

3.6.1.1 Lithology

Lithology is a factor that has a major role in the occurrence and distribution of groundwater in the Ohangwena region. Thus, it was considered in determining the potential sites that are suitable for aquifer recharge, to reduce the uncertainty in determining lineaments and drainage. The lithology map of the Ohangwena region was developed from the lithological and geological maps of Namibia which were obtained from the Digital Atlas of Namibia, and it was digitized using ArcGIS.

The lithology of the Ohangwena region is characterized by sand and calcrete. Sand is a granular material composed of finely divided rock and mineral particles, with high permeability, making it an ideal choice for groundwater recharge. It is supported by (Wang *et al.*, 2009) that sandy soils make areas to be very important for groundwater recharge. While calcrete is a type of soil formed from calcareous materials.

3.6.1.2 Land Use/Land Cover

The development of land typically alters flood peak and infiltration properties, thereby affecting the entire hydrological environment of the area. This also affects the groundwater

recharge of the area in general. This study also considered Land Use/Land Cover factor, in identifying the potential recharge zones in the area. The Land Use/Land Cover map for the Ohangwena region was developed from the Namibian land use/cover maps which were obtained from the DIVA-GIS portal, and the Digital Atlas of Namibia. These maps were used to digitize the Land Use/Land Cover map for the Ohangwena region in ArcGIS. Figure 3.7 shows the types of land use/Land cover distribution in the study area, while Table 3.3, shows the percentage of the area covered by different Land Use/Land Cover types.

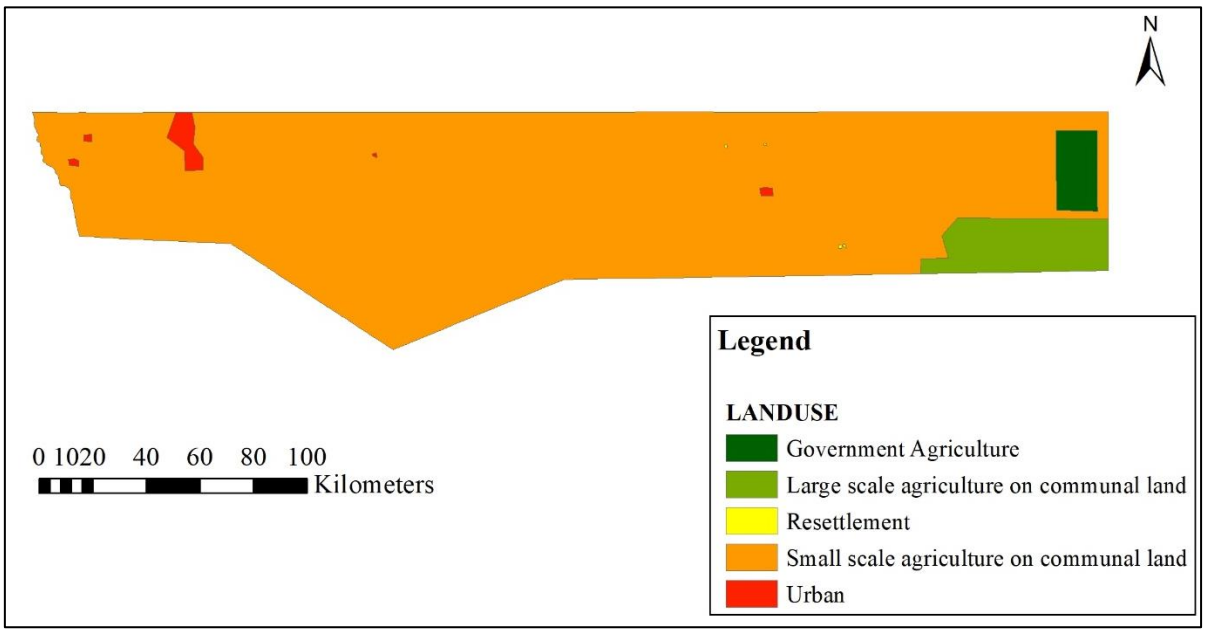

Figure 3.6: Land use/Land cover map of Ohangwena region

Table 3.3: Land use/land cover distribution for Ohangwena region

Land use type	Area (km²)	percentage (%)
Government Agriculture	1010.26	9,41
Urban	852.44	7,94
Resettlement	17.18	0,16
Large scale Agriculture on communal land	3478.46	32,40
Small scale agriculture on communal land	5377.67	50,09
Ohangwena region total area	10736.01	100

According to Figure 3.7 and Table 3.3, the larger area of the region is covered by small scale agriculture on communal land covering an area of 50.09% of the total region area, followed by large scale agriculture on communal land covering 32.4% of the total area, followed by government agriculture covering 9.41% of the total area, followed by urban area which is covering 7.94% of the total area, and lastly, resettlement covering 0.16% of the region area.

3.6.1.3 Lineaments

Lineament's analysis of the study area is part of the important factors for determining groundwater recharge potential zones, as they provide valuable information on subsurface fractures that could impact the groundwater circulation and storage. Due to their size, these fractures are of undeniable hydrogeological interest, as their recharge into aquifers is a priori favourable. This study used the Digital Elevation Model (DEM) data, and ArcGIS to prepare the lineament and lineament density map. The DEM data of Namibia was obtained from the DIVA-GIS portal, and it was then clipped to the study area using the clipping tool, one of the spatial analyst tools in ArcGIS.

The lineaments were formed by four (4) different combinations of hill shade maps, which were prepared in ArcGIS using the spatial analyst tool of hill shade. The first hill shade map was constructed with an azimuth of 315, an altitude of 45, and a z factor of 1. The second hill shade map was constructed with an azimuth of 200, an altitude of 50, and a z factor of 1. The third hill shade map was constructed with an azimuth of 100, an altitude of 60, and a z factor of 1. And the last hill shade map was constructed using an azimuth of 50, an altitude of 90, and a z factor of 1. The z- factor was kept constant throughout, and different azimuth angles and altitudes were used to observe and capture well the fractures of the study area at different angles. In Ohangwena there are only fractures (fault zones), and no mountains, thus, only fractures were used to form up the lineaments. The lineaments were then digitized using polylines from the four hill shade maps produced in ArcGIS. These lineaments were then converted into lineament densities presented in Figures 3.8 and 3.9.

According to Figure 3.8, the lineament density of the Ohangwena region ranges from 0 to 0.90 km/km², with the lowest lineament densities lying in the areas with high elevation, and median to high lineament densities lying in the areas with low elevation. These densities were further reclassified into five (5) classes from very low to very high shown in Figure 3.9. A large part of the Ohangwena region has very low lineament density, while a few areas in the middle of the region and on the western part of the region has low to moderate lineament densities. Very high lineament densities in the range of 0.61 to 0.70 km/km² are found in the river that is on the eastern side of the region, which discharges in the Okavango delta. High lineament densities are mostly found on the river that is passing across the region, which discharges water into the Etosha pan located in the southern direction of the region. The upper east side of the region is classified with few high lineament densities, and a few which are partially distributed on the western side of the region.

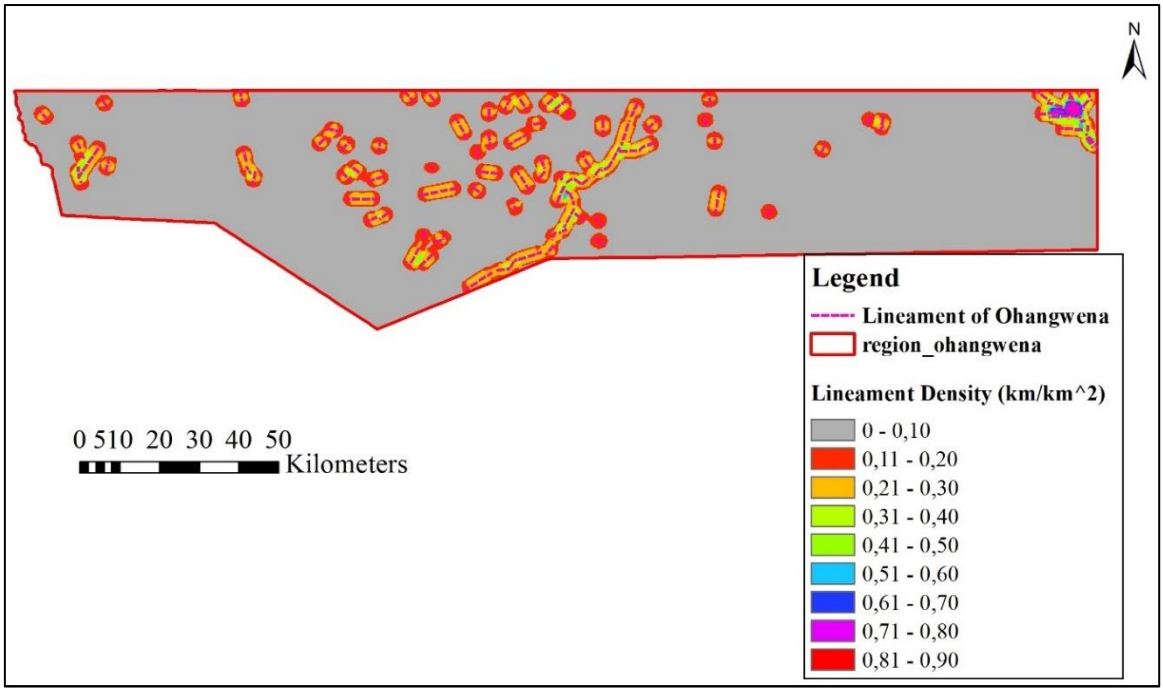

Figure 3.7: Lineament density map for Ohangwena region

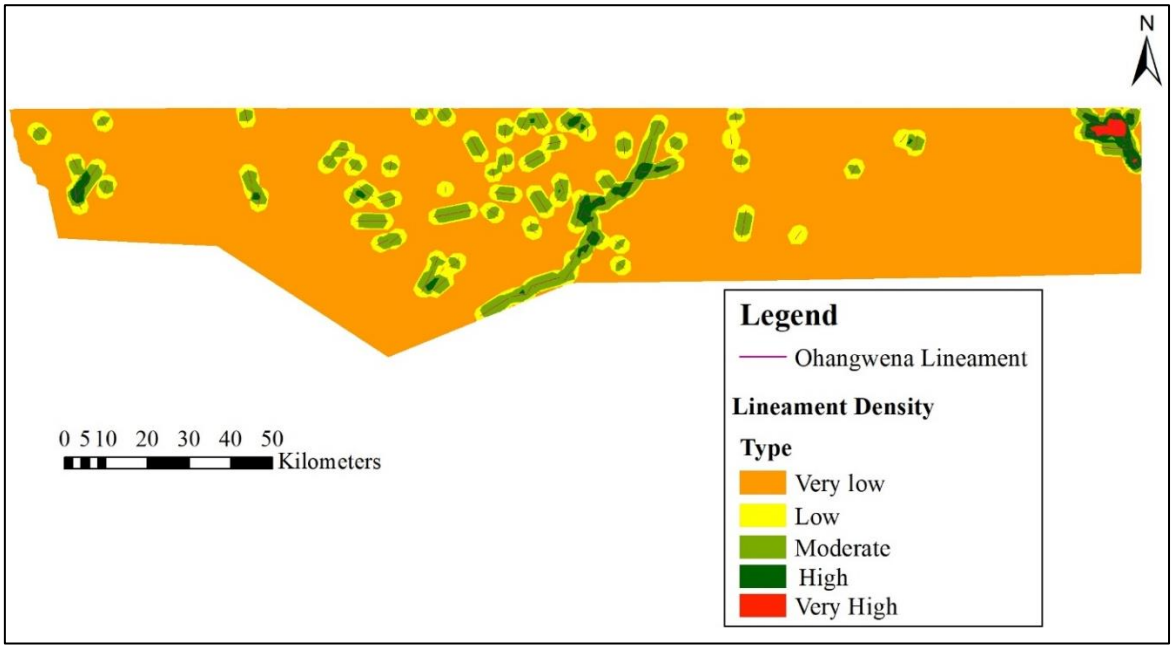

Figure 3.8: Lineament density map re-classified into 5 classes

3.6.1.4 Drainage

Drainage density plays a significant role in visualizing which areas have a high groundwater recharge. The structural analysis of the drainage network helps in assessing the characteristics of the groundwater recharge zones, as they indicate areas with larger and lower runoff. The drainage network of the Ohangwena region was digitized with polylines from the Namibian

streams network map that was obtained from the digital Atlas of Namibia. The drainage was digitized in ArcGIS, and it was then further converted into drainage density, using the spatial analyst tool of line density. ArcGIS used Equation (2) described in Section 2.7 to calculate the drainage density. The drainage density of the region is shown in Figure 3.10.

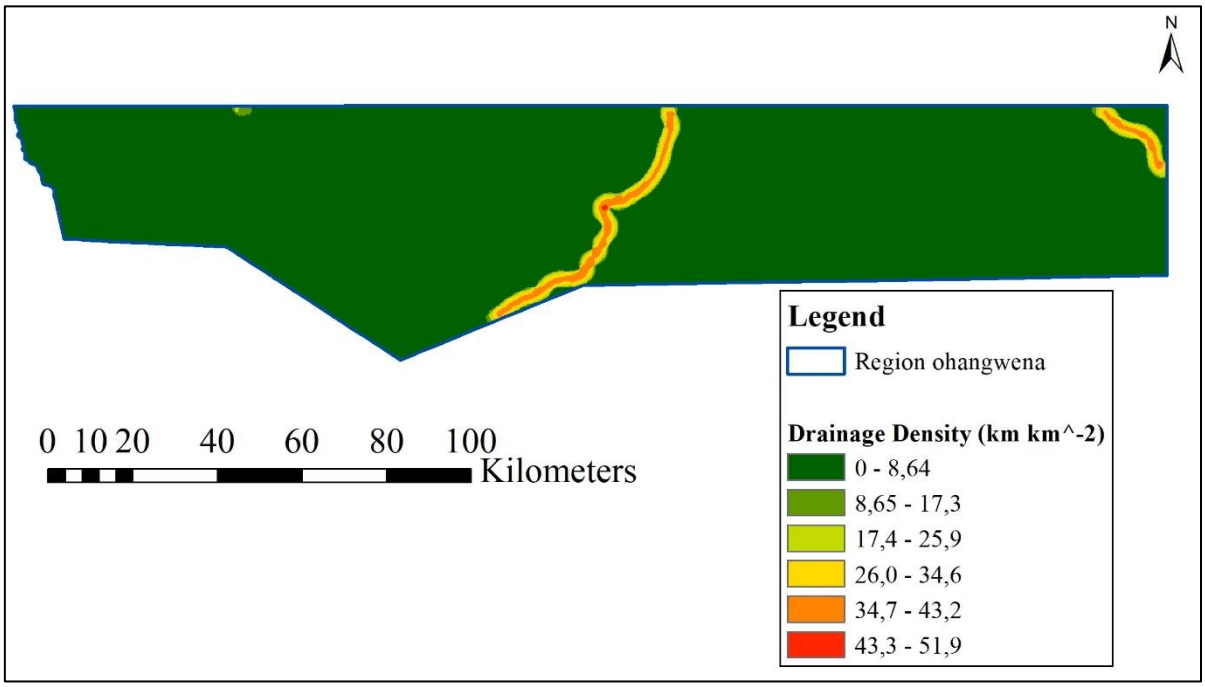

Figure 3.9: Drainage density map for Ohangwena region

According to Figure 3.10, the drainage density in the region ranges from 0 to 51.9 $km\ km^{-2}$. The larger part of the region has a very low drainage density ranging from 0 to 8.64 $km\ km^{-2}$. In the areas where the drainage density is low, the base flow will have a larger contribution to the streams, and a smaller contribution from the overland flow. A high drainage density in the region is found along the river flow paths with a drainage density of 34.7 to 51.9 $km\ km^{-2}$. Higher drainage densities are an indication that these areas collect rainwater more quickly, making the contribution of surface runoff to discharge to be high, and making the lag time shorter. The median drainage density of 17.4 to 34.6 $km\ km^{-2}$ is found close to the river flow paths.

3.6.1.5 Slope

The slope is another important factor in identifying the groundwater recharge zones of watersheds. The slope influences both the speed and retention of runoff on the soil surface as well as the infiltration capacity. The slope of the Ohangwena region was produced from the DEM (SRTM 30m) of the region which was obtained from the DIVA-GIS portal. The surface and slope spatial analyst tools in ArcGIS were used to digitize the slope map of the region shown in Figure 3.11. The slope was further reclassified into 5 classes using the reclassify spatial analyst tool, for better visualization shown in Figure 3.12.

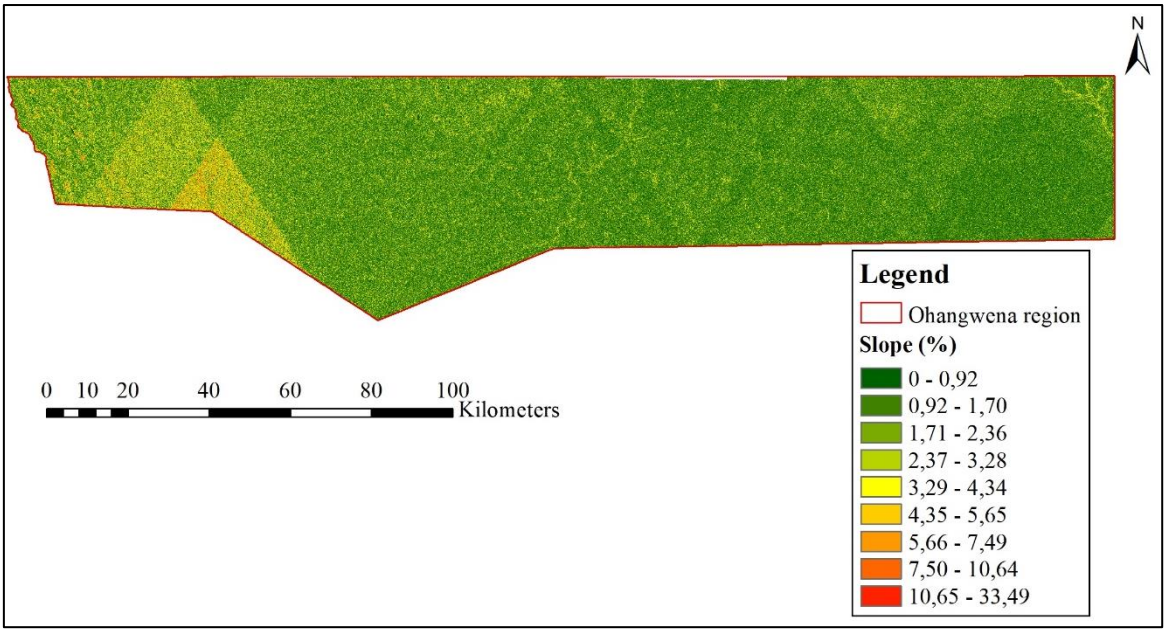

Figure 3.10: Ohangwena region slope analysis map

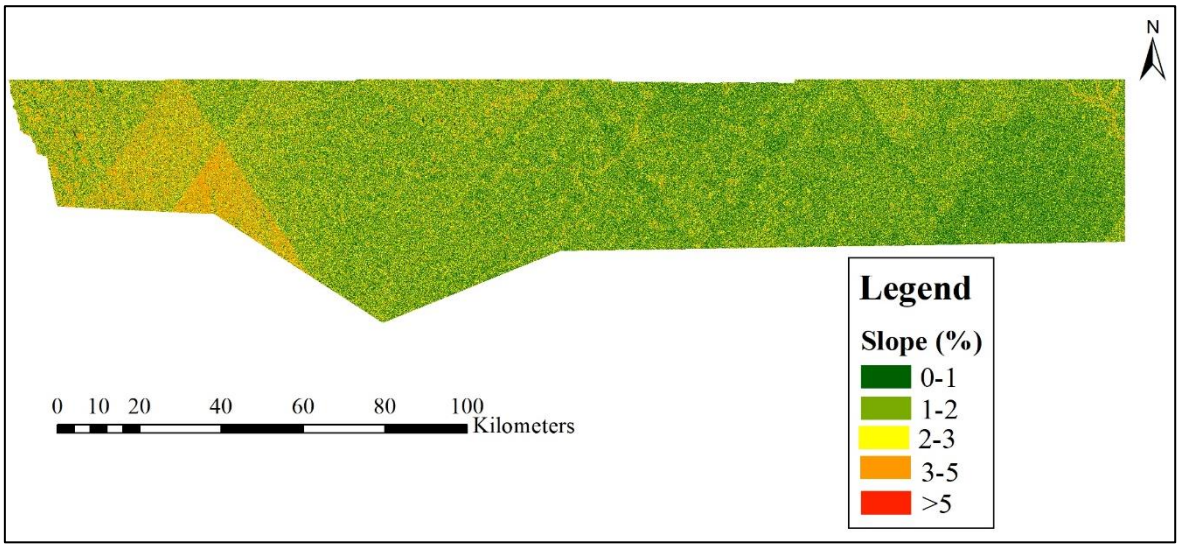

Figure 3.11: Ohangwena region slope analysis map re-classified

According to Figure 3.11, the slope of the region ranges from 0 to 33.49%. A large part of the region has very little slope ranging from 0 to 2.36%, and the highest slope in the region is about 33.49%, which lies on the western side of the region. The flat areas with low slope values are very good for groundwater recharge capability since these types of areas influence high infiltration rates and less generation of surface runoff. However, areas with a steep slope (high slope values) tend to have low groundwater levels, because there is less time for runoff to infiltrate, and rainfall turns easily into the runoff, which rapidly flows down the slope which can be captured in water sources and be used in injection wells for aquifer recharge. There are also areas within the region which has a gentle slope ranging from 2 to 3 according to the classification system of Figure 3.12 and also ranging from 3.29 to 4.34% according to the

classification of Figure 3.11. These areas with a gentle slope are prospects of high groundwater potential since more rainfall can percolate into the subsurface in these areas.

3.6.1.6 Geology

Geology plays a major role in controlling groundwater recharge, and for water to move through an aquifer, the internal voids and fractures must be connected. The geology map of the study was considered in the mapping of the potential groundwater recharge zones, to indicate the distribution of different types of rocks and surficial deposits, and also to show the locations of the geologic structures such as faults and folds. The geology map of the Ohangwena region was developed from the geological map of Namibia, which was obtained from the Digital Atlas of Namibia. This map was digitized in ArcGIS using spatial analyst tools.

There are no rocks in the Ohangwena region, but the entire region is characterized by sands and calcrete. Sandy soil is highly permeable and has high infiltration rates, thus making it ideal for groundwater recharge. Runoff can easily percolate and infiltrate the ground through the sandy soil due to its large pore spaces, and it can be easily captured in water sources for recharge purposes.

3.6.1.7 Soils

The soil plays a crucial role in hydrology, since it influences the partitioning of precipitation into filtration and runoff, and ultimately how water moves through the soil and recharges groundwater. Soil pores determine if water will penetrate the soil and reach groundwater. The soil map for the Ohangwena region was developed from the soils map of Namibia, which was obtained from the Digital Atlas of Namibia. The map was digitized in ArcGIS using the spatial Analyst tools, and it is shown in Figure 3.13.

According to Figure 3.13, the soils in the Ohangwena region are classified into five classes namely, Cambic arenosols, eutric cambisols, ferralic arenosols, haplic calcisols, and Petric calcisols. The Cambic Arenosols and Ferralic Arenosols are types of sandy soil, having a texture that is loamy sand or coarser. Ferralic arenosols cover a large part of the Ohangwena region, especially in the eastern and central parts. The flow of the main river passing across the region has a soil type of Petric calcisols, which is a soil type with the substantial secondary accumulation of lime. These soil type also covers a part of the western part of the region. The upper western part of the region is characterized by Eutric cambisols, which are among the most productive soils on earth that make good agricultural land.

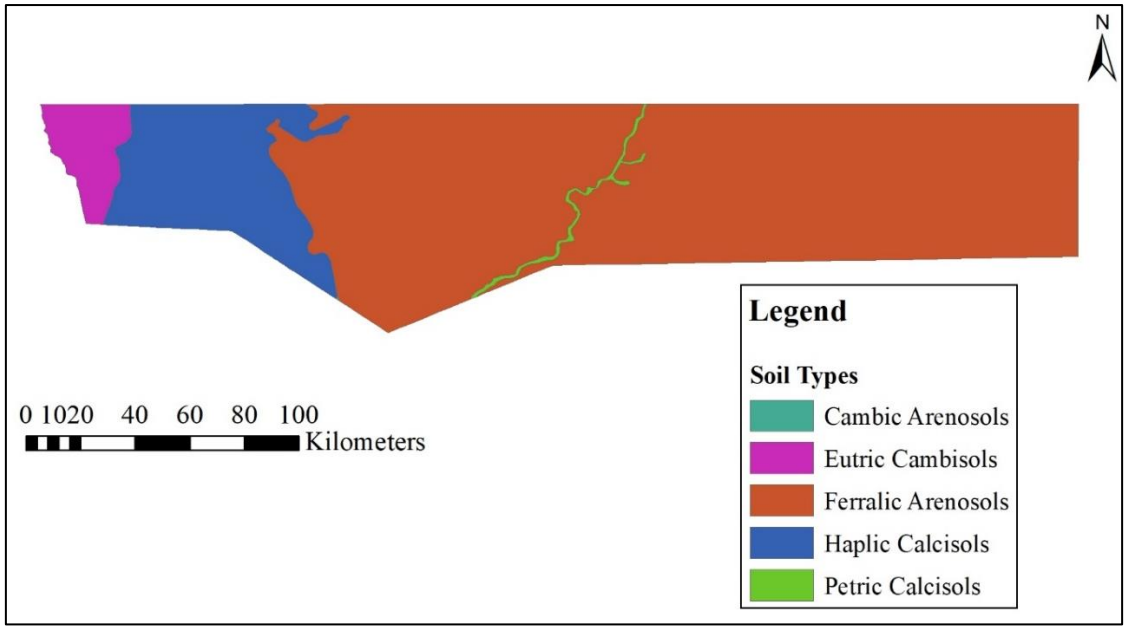

Figure 3.12: Soils map for Ohangwena region

3.6.2 Assigning weights to groundwater recharge factors

Various weights were assigned to the seven (7) important groundwater-related factors, to determine the level of influence of each factor in groundwater recharge. The scale of relative importance used in the weighting system of this study is shown in Table 3.4, as per *(*Singh *et al*., 2013).

Table 3.4: Scale of relative importance (Singh *et al*., 2013)

The scale of relative importance	
1	Equal importance
3	Moderate importance
5	Strong importance
7	Very strong importance
9	Extreme importance
2,4,6,8	Intermediate values
1/3,1/5,1/7,1/9	Values for Inverse comparison

All the factors affecting groundwater recharge were classified into different classes according to the scale of relative importance shown in Table 3.4. The classified factors were then prepared in a pair-wise comparison matrix using the Analytical Hierarchical Processing Method (AHP), shown in Table 3.5.

Table 3.5: Pair-wise comparison matrix for factors influencing groundwater recharge

Factors	Geomorphology	Lineament Density	Lithology	Slope	Soil	LuLc	Drainage Density	Weight
Geomorphology	7	6	5	4	3	2	1	0.38
Lineament Density	7/2	6/2	5/2	4/2	3/2	2/2	½	0.19
Lithology	7/3	6/3	5/3	4/3	3/3	2/3	1/3	0.13
Slope	7/4	6/4	5/4	4/4	¾	2/4	¼	0.10
Soil	7/5	6/5	5/5	4/5	3/5	2/5	1/5	0.08
LuLc	7/6	6/6	5/6	4/6	3/6	2/6	1/6	0.064
Drainage Density	7/7	6/7	5/7	4/7	3/7	2/7	1/7	0.055
Total	18.15	15.56	12.96	10.37	7.78	5.19	2.59	
Total								1

The weights for each factor obtained from the pair-wise matrix (Table 3.5), were used to determine the weights of each sub-category in each map, which was then used to find the overall weight of each shown in Table 3.6.

Table 3.6: Overall weights of different factors influencing groundwater recharge potential

Factors	Weight	Rank	Over All
Geology			
Sands & Calcrete	38	5	190
Lineament Density			
Very high	19	5	95
High		4	76
Moderate		3	57
Low		2	38
Very low		1	19
Lithology			
Sands & Calcrete	13	2	26
Slope			
0-1	10	5	50
1_2		4	40
2_3		3	30
3_5		2	20
>5		1	10
Soils			
Cambic Arenosols	8	2	16
Eutric Cambisols		3	24
Ferralic Arenosols		2	16
Haplic Calcisols		1	8
Petric Calcisols		1	8
LuLc			
Government Agriculture	6,40	3	19,2
Large scale agriculture on communal land		5	32
Resettlement		2	12,8
Small scale agriculture on communal land		5	32
urban		1	6,4
Drainage Density			
Very high	5,5	1	5,5
High		2	11
Moderate		3	16,5
Low		4	22
Very low		5	27,5

The properties of the main factors affecting groundwater recharge were assigned ranks ranging from one to five in Table 3.6, of which the most suitable influential factor was given high weight and the least influential was given the least weight. These ranks were multiplied by the total weight of each factor to determine the overall rank of each characteristic of the factors.

3.6.3 Spatial analysis of the potential groundwater recharge zones

Based on the characteristics of the study area, the weights of different factors for potential groundwater recharge and the scores under various characteristics were evaluated. For each factor, appropriate scores were assigned, and the spatial analysis function was used to determine the potential groundwater recharge zones of the study area. The reclassified factors layers in Table 3.6 from Section 3.6.2, were used as inputs in the spatial analysis tool in ArcMap to generate a groundwater potential recharge map. The potential groundwater recharge zone map developed for the Ohangwena region is shown and discussed in detail in Section 4.1.

3.7 Modeling the relative impact of Aquifer Recharge on groundwater levels

Due to the inadequate data and the existing restrictions on monitoring recharge projects, numerical modelling has been the preferred method for quantitative evaluation of recharge projects. This research also focused on forecasting the groundwater flow in Ohangwena region on the water budget and water table using the MODFLOW mathematical model. This was done to assess the potential of recharging the aquifers in the region. Darcy's equation (5) was used to model the groundwater flow in the porous media of constant density under non-equilibrium conditions in a heterogeneous and anisotropic medium. Figure 3.14 shows the flowchart used in this study to assess the impact of runoff as a water source for Aquifer Recharge on groundwater levels.

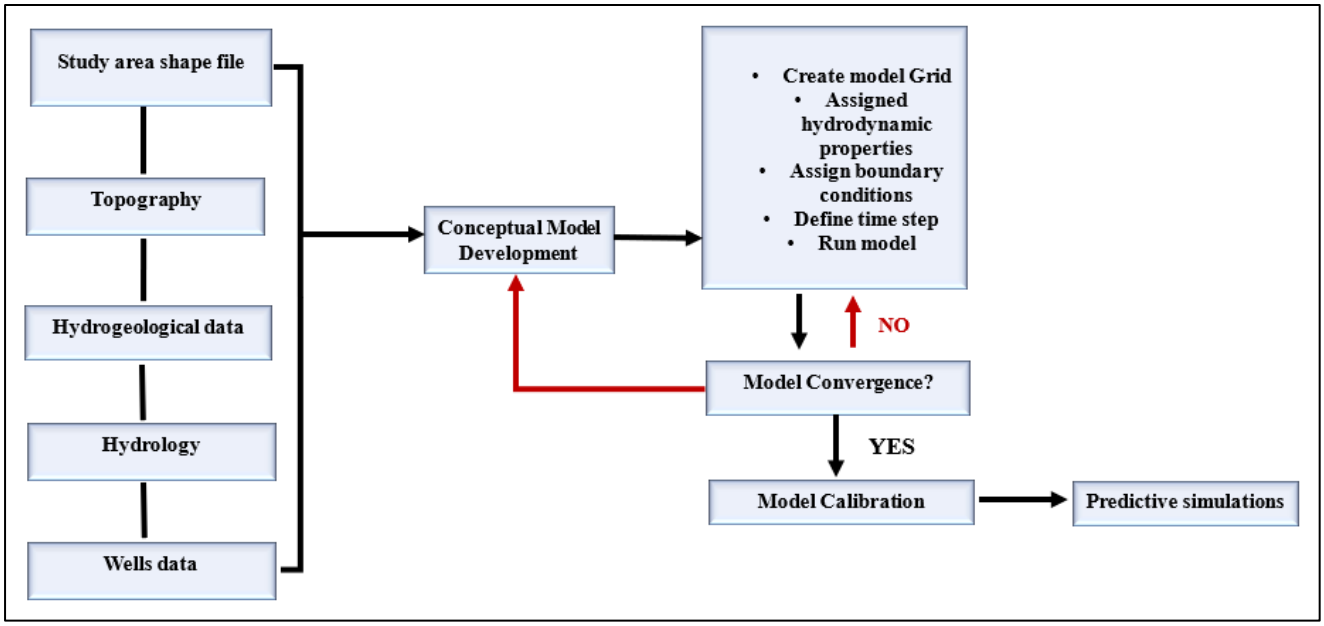

Figure 3.13: Flowchart for assessing the impact of aquifer recharge on groundwater levels

The parameters in Figure 3.14 are discussed further in detail from Section 3.7.1 to Section 3.7.8.

3.7.1 Conceptual model

The conceptual setup of the model was based on the available data obtained from the Namibian Ministry of Agriculture Water and Land Reform (historical groundwater levels), and some previous studies done in the study area. The type of data used in this part of the study are as follows, study area shapefile, topography, Hydrogeological data, hydrology, and wells information. The model domain covered an area of 10736.01 km², and it was set up into five hydrogeological layers respectively (KOH-0, Aquitard 1, KOH-I, Aquitard 2, and KOH-II). The technique of Aquifer Recharge was assessed on the KOH-II aquifer because most boreholes in the region are drilled tapping into this aquifer. The layers were assigned the same storage coefficients, except the hydraulic conductivity which varies in each layer. The inflow to the model domain consists of the recharge flow from precipitation, while the outflow includes existing wells, and evapotranspiration (ET). The model was set up using MODFLOW-NWT code in the ModelMuse graphical user interface. Table 3.7 shows the parameter information used to set up the conceptual model.

Table 3.7: Conceptual model parameters (Reginalda, 2015)

Layers	Depth (m)	Type of Aquifer	Hydraulic Conductivity (Kx)	Specific storage
KOH-0 (Layer 1)	30	unconfined Aquifer	1.20×10^{-4} m/s	9.82×10^{-4}
Aquitard (Layer 2)	10	Convertible	7.00×10^{-11} m/s	
KOH-I (Layer 3)	180	Confined Aquifer	3.15×10^{-5} m/s	
Aquitard (Layer 4)	10	Convertible	7.00×10^{-11} m/s	
KOH-II (Layer 5)	350	Confined Aquifer	4.0×10^{-5} m/s	

The groundwater flow direction is towards the Etosha pan (flowing from the upper north to the south), with the two ephemeral rivers and the Cuvelai streams acting as the base level of drainage. The groundwater flow, natural recharge (average contribution from spills), infiltration at the dams, lakes, river section, and ponds, contribute to the recharge of the Ohangwena Aquifer. The groundwater discharge of the Ohangwena aquifer is the Etosha pan, which outflows to the Atlantic Ocean on the West.

3.7.2 Model Grid and Layering

The finite-difference groundwater numerical flow model of the Ohangwena Aquifer was built using MODFLOW-NWT and UPW (Upstream-Weighting) solver package implemented by

using ModelMuse 3.10. The finite-difference model mesh was made up of 86 rows and 372 columns with a uniform grid size of 700×700 m. The first hydrogeological layer of the aquifer was set to be unconfined, layers two and three are confined, while the two aquitards were set as convertible. The elevation of all the layers was set about the Model top, whose elevation was obtained from the 30×30 m Digital Elevation Model (DEM) of the Ohangwena region. The grid discretization of the Ohangwena region with active cells is shown in Figure 3.15.

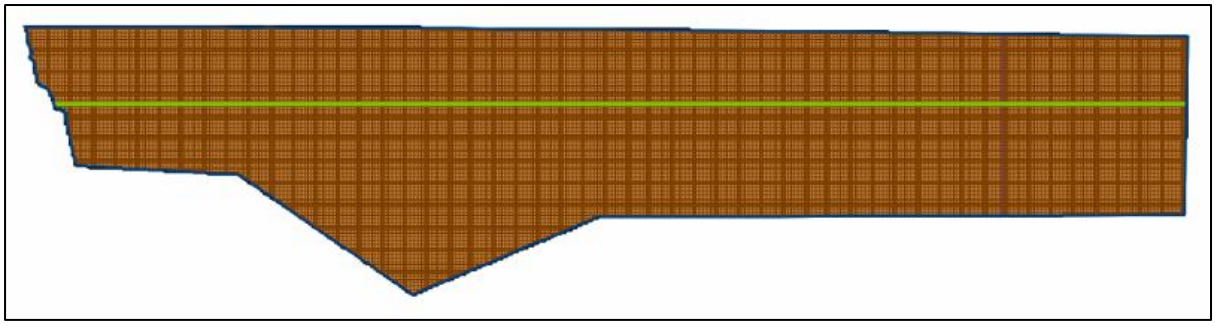

Figure 3.14: Ohangwena region grid discretization with active cells

3.7.3 Boundary conditions

In groundwater modeling, every model requires an appropriate set of boundary conditions to represent the relationship of the system with the surrounding environment. The groundwater flow model's boundary conditions represent locations in the model where water flows into and out of the model region due to external factors.

The different types of boundary conditions used are Constant Head Boundary (CHD), General Head Boundary (GHB), Drainage package (DRN), Recharge package (RCH), Evapotranspiration package (EVT), Well package, Observation head package, and UPW (Upstream Weighting Package). The Newton Solver (NWT) was used to solve the model, with 150 iterations because it is quicker in cases of higher difference on the discretization. These boundary conditions were determined according to the topography of the study area, and the hydro-geological conditions.

The constant head boundary (CHD) was allocated on the Southern boundary of the region, and the General Head Boundary (GHB) was allocated on the Northern boundary of the region, which represents the groundwater flow from the same aquifer but the Angolan side. There were no flow boundaries allocated in the eastern and western directions of the region. The UPW package was used to simulate the groundwater flow of the region. The Constant Head Boundary and the General head Boundary were set to model top, which was defined by the DEM of the Ohangwena region. The constant head boundary condition (CHD) was also used in this study, to fix the head value in selected grid cells regardless of the system conditions in the surrounding cells. It acted as an infinite source of water entering the system. This specified head boundary condition can have a significant influence on the simulation results and may sometimes lead to unrealistic predictions.

The drainage package was used to simulate the influence of the surface water bodies (ephemeral rivers and lakes) on the groundwater flow in the study area. Whereby the two ephemeral rivers passing through the region were simulated as they may contribute to the groundwater system and act as groundwater discharge zones, depending on the hydraulic gradient between the surface water body and the groundwater system. The surface water bodies were assigned to the model top which was defined by the DEM.

The recharge package simulated recharge at the identified potential groundwater recharge zones identified from Section 3.6, and the Well package simulated the wells that withdraw and add water to and from the model (aquifer) at a constant rate during the stress period, regardless of the cell area or head in the cell. The head observation package (HOB) was used to compare the observed water heads and the simulated water heads at the boreholes of the region used in this study, and also the same head observation package was used for calibration which is explained in Section 3.7.8.

Discharge by Evapotranspiration (ET) was simulated with a head-dependent function that decreases linearly with depth. Simulating discharge by evapotranspiration involves specifying in the model the maximum evapotranspiration rate, the elevation of the Evapotranspiration surface, the conductance, and the extinction depth of evapotranspiration. All these were done with the evapotranspiration package in MODFLOW. The maximum evapotranspiration rate for the Ohangwena region is 6.49×10^{-8}, the evapotranspiration depth is 0.5m, and the conductance of 0.001, were used in this model (Wallner *et al*., 2017). The evapotranspiration elevation surface was set to model top, which was defined by the DEM of the study area. The DEM of the Ohangwena region is shown in Figure 3.16.

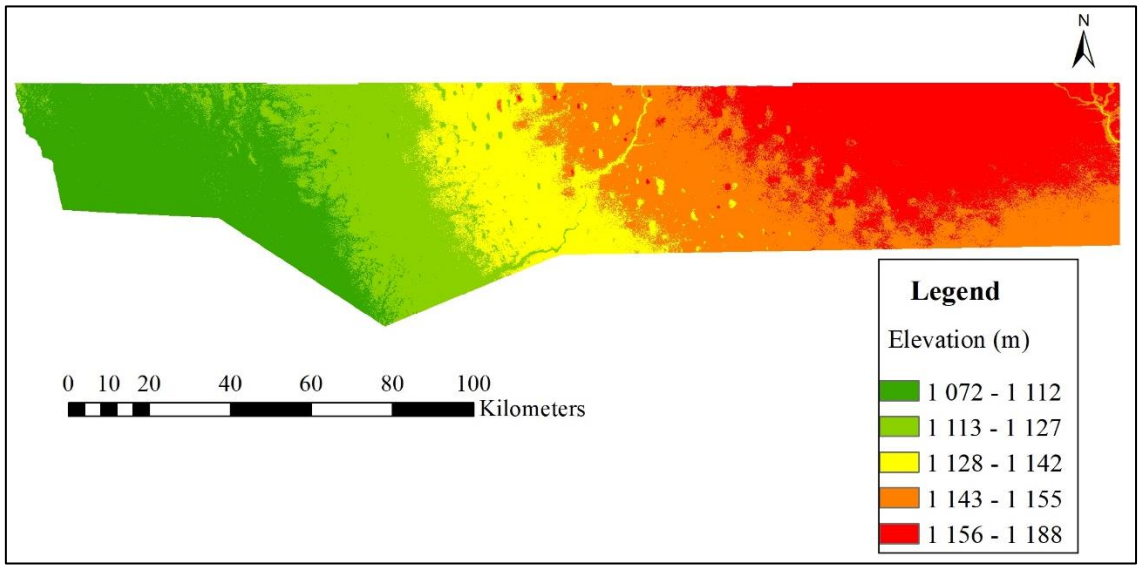

Figure 3.15: Ohangwena region Digital Elevation Model

3.7.4 Initial conditions and Hydraulic properties

The MODFLOW initial head of the model was set to model top, which was defined by the DEM of the study area. The respective Hydraulic properties of the 5 layers set for the model such as the hydraulic conductivities, their depths, and the layer type *i.e* confined/unconfined, or convertible were defined. These were defined with the parameters of the conceptual model in Table 3.7.

The recharge amounts were introduced to the model with the assumption that they are runoff and infiltrate or recharge the aquifer system through enhanced recharge. The recharge rates were assigned according to the groundwater potential zones obtained from the results of Section 3.6. These zones were digitized in ArcGIS from the groundwater potential zones map in Figures 4.1 and 4.2 of Section 4.1. The very high groundwater recharge zones were assigned recharge values from 47 mm/year to 60 mm/year, and the high groundwater recharge zones were assigned values in the range of 40 to 45 mm/year. These recharge values were obtained from previous studies done in the study area by (David, 2013), and they were obtained using the CMB (Chloride Mass Balance Method).

3.7.5 Defining time steps

The time step is one of the important parameters that need to be defined in the model. The model used in this study was run for two different time steps. It was first run for a steady-state to approximate aquifer recharge under controlled conditions, and then transient state for close representation of recharge in reality at the four wells. The steady-state was run with a one-time step, from negative one (-1) to one (1), and the transient state was run for six years with a time step of 40, which is equivalent to 189345600 seconds.

3.7.6 Observation wells

There are several boreholes in the study area, but this study focused on 4 observation wells, of which data was obtained from the Namibian Ministry of Agriculture and Land Reform. The Head Observation Package (HOB), and Well package in ModelMuse were used to simulate these wells, and compare the simulated results obtained at these wells with the observed water levels results at the wells. The observation wells used are namely, WW201045, WW20267, WW201634, and WW201637. These wells' locations in the region are shown in Figure 3.17.

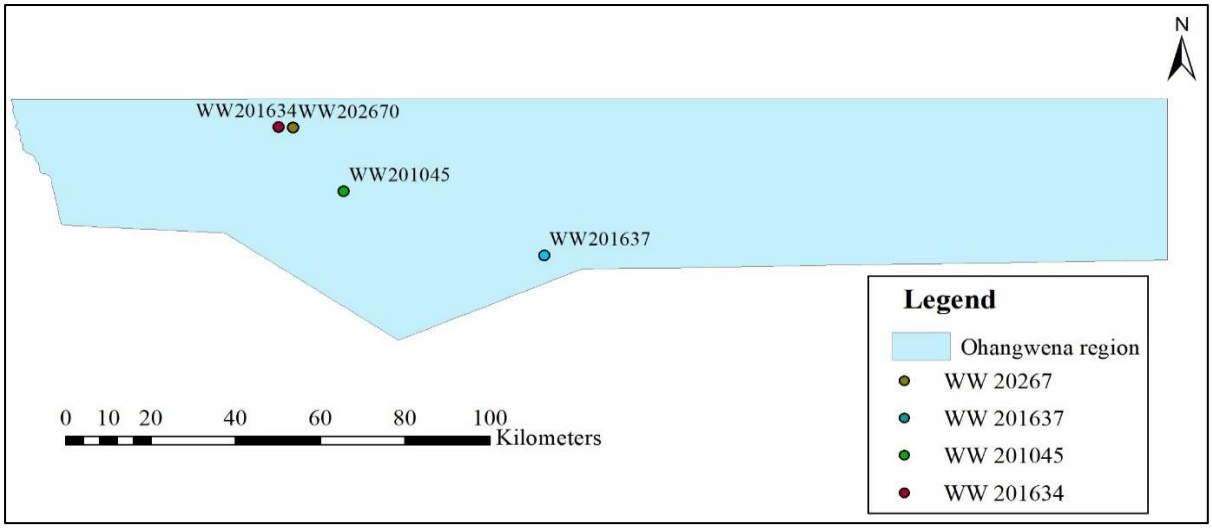

Figure 3.16: Observation wells in Ohangwena region

3.7.7 Model simulations

After assigning and defining all the needed parameters in the model. Each model (steady-state model and the transient state model) was then run with MODFLOW – NWT, whereby both models converged with a percent discrepancy of 0.0%.

3.7.8 Model Calibration

The converged simulated models' results were then checked if the Observed water levels in the four wells were close to the simulated groundwater level results. The closeness of these results is shown by the Root Mean Square Error (RMSE) as described in detail in Section 2.8. The trial-and-error technique was used in this study to calibrate models. The calibration was done based on the obtained RMSE value, if it is greater than one, then there was a need for calibration. The calibration was then done by manually adjusting the assigned hydrogeological parameters within the reasonable range, for the simulated heads to match with the observed heads.

3.8 Modeling the transport of runoff contaminants in the aquifer

Recharging of aquifers is associated with groundwater contamination, by the type of water used in recharge. Therefore, the third part of this study assessed the transport of runoff contaminants in the aquifer. This part looked at how contaminants associated with runoff travel with reference to time in an aquifer if runoff is used as a water source to recharge the aquifer through aquifer recharge technique in the Ohangwena region. This was assessed at two boreholes within the study area serving as injection wells, where the runoff is injected in the aquifer and was assessed with particle tracking and MT3DMS in ModelMuse incorporating MODFLOW 2005.

The method which was adopted to observe the transport of runoff contaminants within the aquifer in the Ohangwena region is shown in Figure 3.18, and it is further explained in detail from Section 3.8.1. to Section 3.8.8.

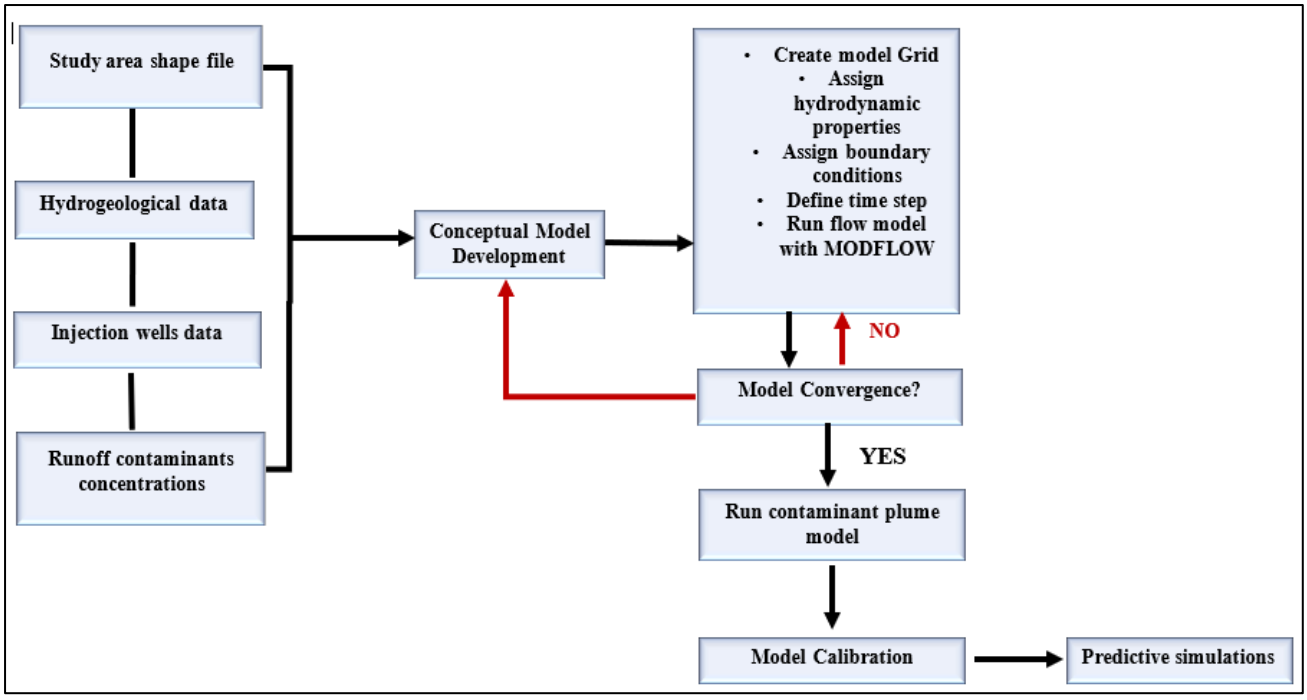

Figure 3.17: Flowchart for tracking the transport of runoff contaminants in the aquifer

3.8.1 Conceptual model

Similarly, to the groundwater flow model in Section 3.7, the Groundwater contaminant plume transport model was also set up based on the available data from the Namibian Ministry of Agriculture Water and Land Reform, and the previous studies that were done in the study area. The model domain covered an area of 10736.01 km², and it was set up into five hydrogeological layers respectively (KOH-0, Aquitard 1, KOH-I, Aquitard 2, and KOH-II). The layers were assigned the same storage coefficients, except the hydraulic conductivity which varies in each layer. The inflow to the model domain consists of the recharge from precipitation runoff, while the outflow includes existing pumping wells, and evapotranspiration (ET). The model was set up in the ModelMuse Graphical User Interface, whereby MODFLOW 2005 was used to simulate the groundwater flow, and Particle tracking and MT3DMS were used to track the movement of the contaminants associated with runoff within the aquifer at different times. The conceptual model of the contaminant plume transport was also set up using the parameters in Table 3.7.

3.8.2 Model grid and layering

The finite-difference model mesh was made up of 86 rows and 372 columns with a uniform grid size of 700×700 m. The three hydrogeological layers of the aquifer are confined while the aquitards are convertible. The elevation of all the layers was set about the Model top, whose elevation was obtained from the 30×30 m Digital Elevation Model (DEM) of the Ohangwena region.

3.8.3 Boundary Conditions

The groundwater contaminant transport model developed for the Ohangwena region is a combination of two models, which consist of the groundwater flow model and the contaminant transport model. The groundwater flow model was simulated using MODFLOW 2005, and it used boundary conditions such as the time-variant specified head package (CHD), well package, and the solver used was the preconditioned Conjugate Gradient Package (PCG). The contaminant transport plume model was simulated using particle tracking and MT3DMS. The boundary conditions incorporated in this model are such as Basic Transport Package (BTN), Advection Package (ADV), Dispersion Package (DSP), Sink and Source Mixing Package (SSM), Transport Observation package, and the solver used was the Generalized Conjugate Gradient Solver (GCG).

3.8.4 Initial conditions and Hydraulic Properties

The MODFLOW initial head of the model was set to model top, which was defined by the DEM of the study area. The respective Hydraulic properties of the 5 layers set for the model such as the hydraulic conductivities, their depths, and their type were defined. These were defined according to the conceptual model shown in Table 3.7. The pumping rates of the wells that serve as injection wells were obtained from the Namibian Ministry of Agriculture Water and Land Reform and are shown in Table 3.8. The runoff contaminants concentrations used in this study were obtained from the University of Namibia undergraduate research projects (unpublished), and these contaminants concentrations are shown in Table 3.9.

Table 3.8: Average pumping rates for the injection wells

Well number	Average pumping rate (m^3/s)
WW201045	0,467
WW201637	0,352

Table 3.9: Runoff contaminants concentrations

Contaminant	Concentrations	units
Chloride	1000,00	mg
Electrical Conductivity (EC)	532,00	mS/s
Total Dissolved Solids (TDS)	478.56	mg/l
E-coli	9.58	Counts/ml

According to the Namibian water act of 1956 (Ministry of Agriculture, 1990), the runoff water concentrations shown in Table 3.9 falls in water group C which is described as water with low health risk. The concentration limits of the group C water are 1200 mg/l of Chloride, 400 mS/m at 25 °C of Electrical Conductivity, *E-coli* concentration's limit is 10 counts per 100 ml, and Total Dissolved Solids should not be more than 500 mg/l. Only chloride, electrical conductivity, Total Dissolved Solids, and *E-coli* data were obtained for the surface runoff for the Ohangwena region, thus the study assessed only four contaminants to show the trend of how contaminants disperse within the aquifer. In comparison with the national concentration standards, the Electrical Conductivity concentrations exceed the limit with 132 mS/s.

3.8.5 Defining time steps

The timestep for the contaminant transport plume model was defined as a transient state, which was a simulation of 6 years (189345600 s), with 40-time steps. This simulation was run for six years to observe the trend of movement of the runoff contaminants within the aquifer.

3.8.6 Injection wells

Among the wells used in the assessment of the impact of Aquifer Recharge on groundwater levels in Section 3.7, two wells were chosen depending on their location in Figures 4.1 and 4.2 (the figures that show the location of potential groundwater recharge zones). The wells chosen were WW201045, and WW 201637. These two wells were chosen because they are the only ones with available data, lying in the zone of very high groundwater recharge potential zones, and they are shown in Figure 3.19.

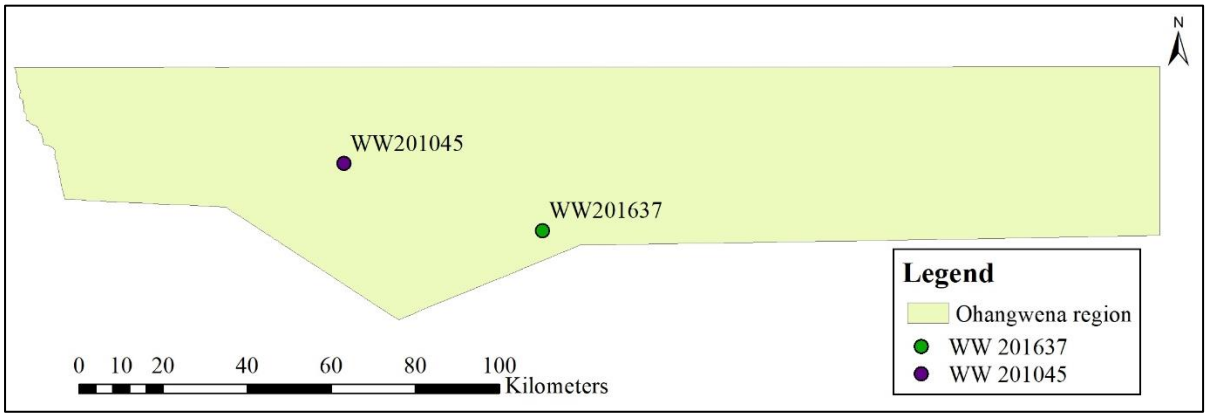

Figure 3.18: Injection wells

3.8.7 Model Simulation

The model simulation was done after all the boundary conditions were assigned and all the parameters defined. The model was first run with MODFLOW 2005, to simulate the groundwater flow using the Darcy equation (5), which after converged with 0.00%

discrepancy. After the flow model converged, the transport model was then also run with particle tracking and MT3DMS as stated earlier, to simulate the dispersion of contaminants concentrations at different times within the aquifer. MODFLOW 2005 was used instead of the latest MODFLOW 6, because there is proper guidance on MODFLOW 2005, to carry out the simulation.

3.8.8 Model Calibration

The model was calibrated to reduce the errors between the simulated values and observed values. The trial-and-error technique that was used to calibrate the model for the impact of aquifer recharge on groundwater levels, was the same method used to calibrate models for contaminant transport. The calibration was done based on the obtained RMSE value, if it is greater than one, then there was a need for calibration. The calibration was then done by manually adjusting the assigned hydrogeological parameters within the reasonable range, for the simulated heads to match with the observed heads.

3.9 Summary of the method

An assessment of groundwater quantity and quality for Aquifer Recharge in Ohangwena region, was undertaken in this study. A Geographical Information System (GIS) approach was first used to identify the suitable locations for recharge in the region. The impact of Aquifer Recharge on groundwater levels was then modeled at some boreholes within the region using MODFLOW. Runoff was used as the source of water in this study, therefore since it is associated with a lot of contaminants, four contaminants (chloride, Electrical Conductivity, *E-coli*, and Total Dissolved Solids) were assessed with particle tracking and MT3DMS on how they disperse within the aquifer.

4. Results and discussion

4.1 Mapping the potential groundwater recharge zones

A Geographical Information System (GIS) approach was used to identify suitable locations for the recharge in the Ohangwena aquifer system in the northern part of Namibia. As described in Section 3.6, the overlay of the seven layers *i.e.*, lithology, land use/land cover, lineaments, drainage, slope, geology, and soil type were integrated with GIS. The results obtained in this part of the study are discussed further in Section 4.1.1.

4.1.1 Potential groundwater recharge zones map

The weights of the potential groundwater recharge factors layers in Table 3.6, were used as inputs in the weighted overlay tool in ArcMap to generate a groundwater potential recharge zones map. The resultant potential groundwater recharge zones map was produced based on the overall weights of influential factors for recharge, and it was reclassified into five regions namely, very low, low, moderate, high, and very high groundwater recharge potential. The produced potential groundwater recharge zone map for the Ohangwena region is shown in Figures 4.1 and 4.2.

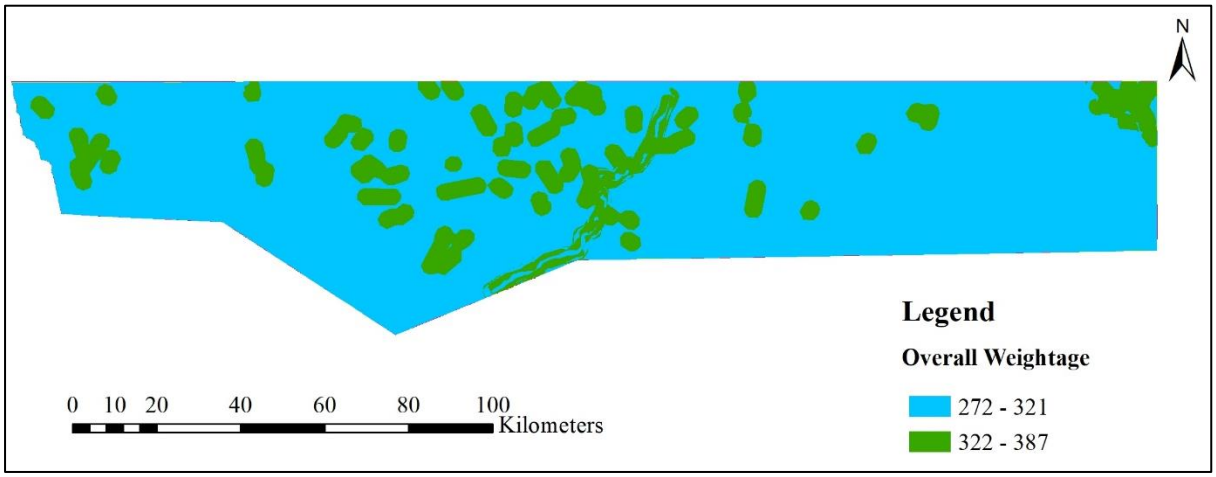

Figure 4.1: Groundwater potential recharge zones map for Ohangwena region

As shown in Figure 4.1, the groundwater recharge overall weightage scores of Ohangwena region are in the range of 272 to 387. The region is classified into two classes of which the first-class overall weightage is in the range of 272 to 321, and the second class has weightage in the range of 322 to 387. These scores were reclassified into five classes with groundwater recharge potentiality from poor to excellent owing to the grading method of equal intervals. The reclassified groundwater recharge scores for the region resulted into two classes namely high and very high shown in Figure 4.2. The range from 272 to 321 is classified as high, and 322 to 387 is classified as very high.

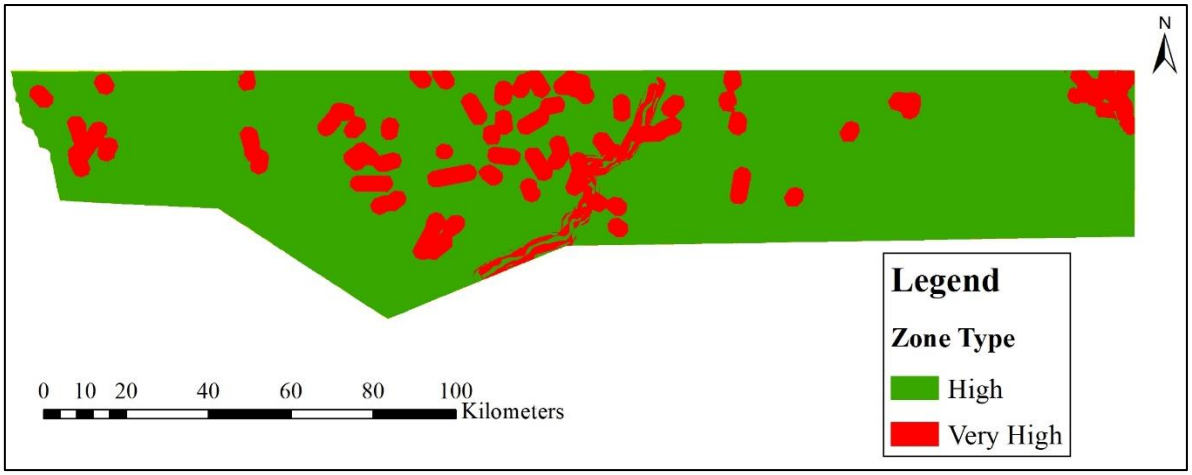

Figure 4.2: Groundwater recharge potential map for Ohangwena region

The analytical results demonstrate that the Ohangwena region is characterized by high and very high groundwater recharge zones. The very high recharge zones are mostly found on the central part of the region, and the far upper west side of the region. Furthermore, these very high recharge zones are mostly found along the river flow paths. Regarding the results in Figures 4.1 and 4.2, the largest part of the region is characterized by a high potential groundwater recharge zone. Approximately 85% of the study area is characterized by a high potential groundwater recharge zone, while 25% is characterized by very high recharge zones.

The recharge scores from 0 to 272, which are attributed as: very low, low, and moderate, were not observed in the region. Therefore, according to the GIS overlay analysis results, the Ohangwena region is classified as a high to very high groundwater recharge potential zone. Incorporating the previous studies done in the study area, it was realized that most of the boreholes in the study area are located in the very high potential groundwater recharge zones shown by Figures 4.1 and 4.2.

The following section 4.2 of this dissertation discusses the impact that aquifer recharge has on groundwater levels.

4.2 Modeling the impact of recharge on groundwater levels

Groundwater numerical simulation has become an important tool in both theoretical and practical aspects of hydrogeology for investigating and managing groundwater resources. Aquifer Recharge was assessed on the study area by analysing its impact on the groundwater levels through modeling using the MODFLOW-NWT and UPW (Upstream-Weighting solver) software package which was implemented in ModelMuse 3.10. The impact of the aquifer recharge was evaluated by hydraulic heads simulation and water budget analysis. Therefore, this section of the dissertation discusses the impact that aquifer recharge has on the groundwater levels, using runoff as the water source of this recharge process.

4.2.1 Groundwater flow model

Stormwater and runoff harvesting are regarded as the cost-effective and easy way to use as a water source to artificially recharge an aquifer. This method is widely used and implemented in rural areas, and it is in most cases accompanied by scientific studies to monitor and manage the structures. Studies using water balance models and rainfall-runoff models described in section 2.8 show that modeling can be useful for estimating the contribution of rainwater and runoff harvesting to the local water balance, and for evaluating the use of recharge structures in catchments. The model was set up in two different time steps, steady-state, and transient state, and the results are shown and discussed in Sections 4.2.1.1 and 4.2.1.2.

4.2.1.1 Steady-state model

The steady-state model which was set up with a time step from a negative one to zero converged with a percent discrepancy of 0.0% which is acceptable. The model was calibrated with a trial-and-error method to reduce the difference between the modeled and measured groundwater head surface. During the model calibration, the hydraulic conductivities of the modeled aquifer and recharge from runoff/precipitation were adjusted, and the Root Mean Square Error (RMSE) was used to measure the accuracy of the model calibration. The model was calibrated from an RMSE value of 6.283 to an acceptable RMSE value of 0.445. The boreholes namely WW201045, WW20267, WW201634, and WW201637 were used in the simulations to depict the change in groundwater levels due to recharge with runoff. The results obtained are shown from Tables 4.1 to 4.2, and from Figures 4.3 to 35.

Table 4.1: Observed vs Simulated heads (uncalibrated)

Borehole #	Observed head (m)	Simulated head (m)
WW201045	1096	1099,2
WW20267	1102	1106,8
WW201634	1103	1106,8
WW201637	1103	1099,0

Table 4.2: Observed vs Simulated heads (calibrated)

Borehole #	Observed Head (m)	Simulated head (m)
WW201045	1096	1095,9
WW20267	1102	1102,2
WW201634	1102	1102,7
WW201637	1103	1103,6

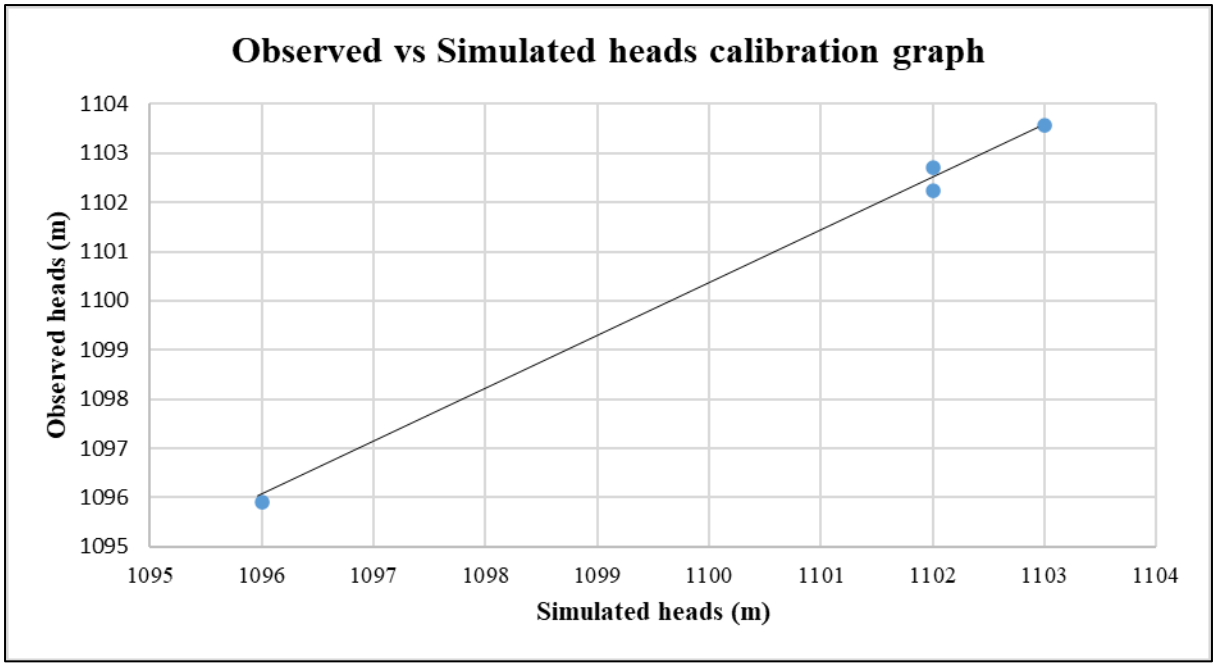

Figure 4.3: Observed vs Simulated heads calibration graph

The results of the uncalibrated model shown in Table 4.1 show that the simulated heads are higher than the observed heads, showing an increase in groundwater levels due to recharge. Due to the RMSE value and high differences between the observed and simulated heads, the model was calibrated to get the results with an RMSE value within the acceptable range. The results of the calibrated model shown in Table 4.2, and Figure 4.3, show that the simulated heads are higher than the observed heads, and the results are not that far from each other, shown by the best fit line between the observed and simulated heads. The increase in the simulated heads is an indication that there is a change in the groundwater levels brought about by the recharge using runoff injected at the simulated wells. The differences in the groundwater levels due to aquifer recharge of the calibrated model of the four simulated boreholes are presented in Table 4.3, and graphically shown in Figure 4.4.

Table 4.3: Comparison of water levels in boreholes with and without recharge

Borehole #	Water level without recharge (m)	Water level with recharge (m)	Difference of water level due to recharge (m)
WW201045	1096	1095,9	-0,1
WW20267	1102	1102,2	0,2
WW201634	1102	1102,7	0,7
WW201637	1103	1103,6	0,6

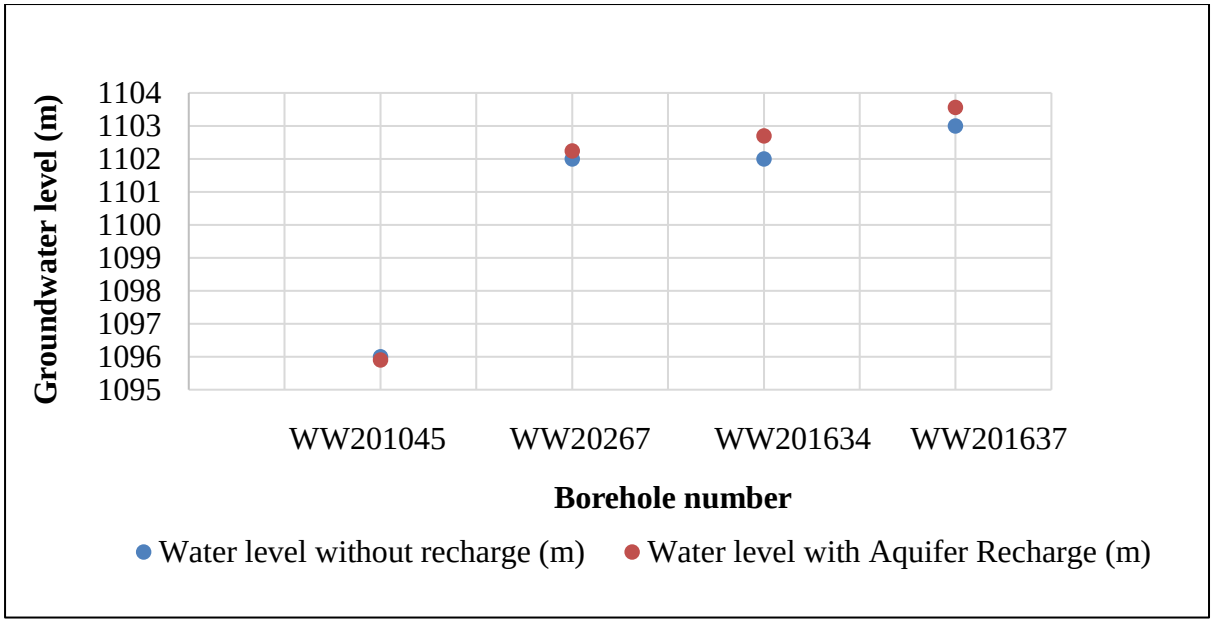

Figure 4.4: Impact of Aquifer Recharge on groundwater levels

According to the results in Table 4.3 and Figure 4.4, there is a rise in groundwater levels in three of the simulated boreholes. Borehole WW20267's water levels increased by 0.2 m due to recharge, borehole WW201634's water level has a great increase of 0.7 m among the four simulated boreholes, and WW201637's water level increased with a depth of 0.6 m. The difference in the groundwater level of borehole WW201045 is -0.1 m, whereby the observed head is greater than the simulated head.

About the location of the boreholes in Figure 3.17, the boreholes with greater simulation heads (WW201634 and WW20267) are located up the region, in the region of very high groundwater recharge zones according to Figures 4.1 and 4.2, and this is where most of the ponds and water bodies are located. Borehole WW201637 is one of the boreholes with high simulated heads, and it is located in the river's drainage path. This borehole is located in the very high groundwater potential recharge zones shown in Figures 4.1 and 4.2. These results show that aquifer recharge in the Ohangwena region is high in the areas of very high groundwater recharge zones, where most ponds and water bodies are located. These areas have high infiltration rates, as discussed in Section 3.4.6.

The hydraulic heads change due to aquifer recharge of the steady-state model are indicated in the five layers of the aquifers that set up the model, which are shown in Figures 4.5 to 4.9, and the water budget analysis which is shown in Table 4.4.

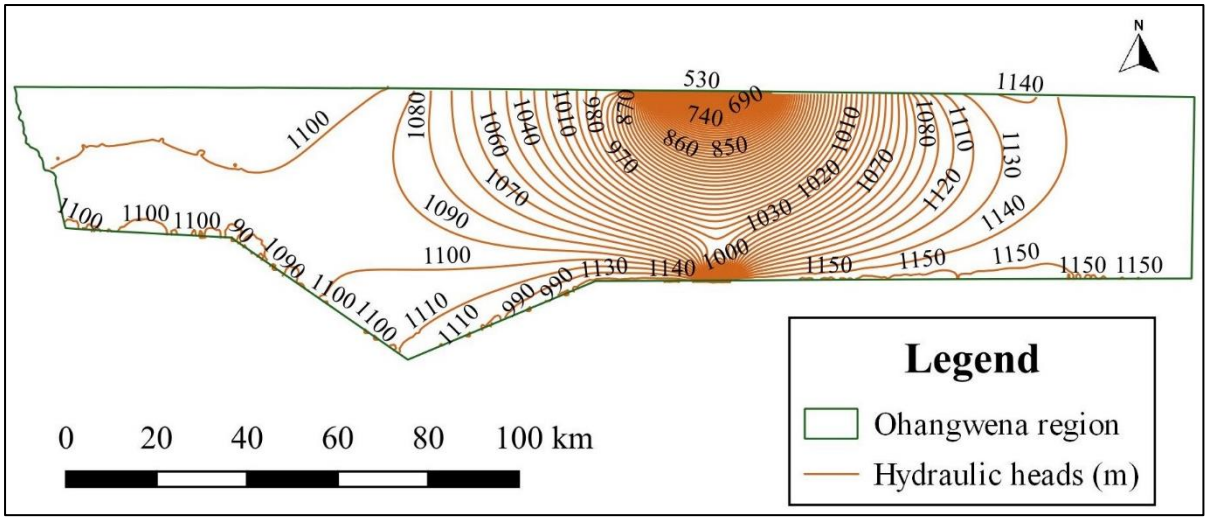

Figure 4.5: Simulated hydraulic heads for layer 1

The simulated heads for the first layer (KOH-0) range from 530 to 1150m, shown by the hydraulic heads in Figure 4.5. The lowest hydraulic heads are located where the main ephemeral river enters the Ohangwena region, from Angola. These lower hydraulic heads show that there is a depression in that area brought by the river. According to Figure 4.5, the hydraulic heads increase as you move in the southern direction of the region, mainly in the river drainage area. Parts of the region excluding the main river drainage area, have high simulated hydraulic heads from 1010 – 1150 meters, due to enhanced recharge with runoff. Apart from aquifer recharge with runoff, the hydraulic heads of layer 1 (KOH-0) of the model, were also influenced by the high hydraulic conductivities of this confined layer.

The simulated hydraulic head results of the first aquitard (layer 2) of the steady-state model are shown in Figure 4.6.

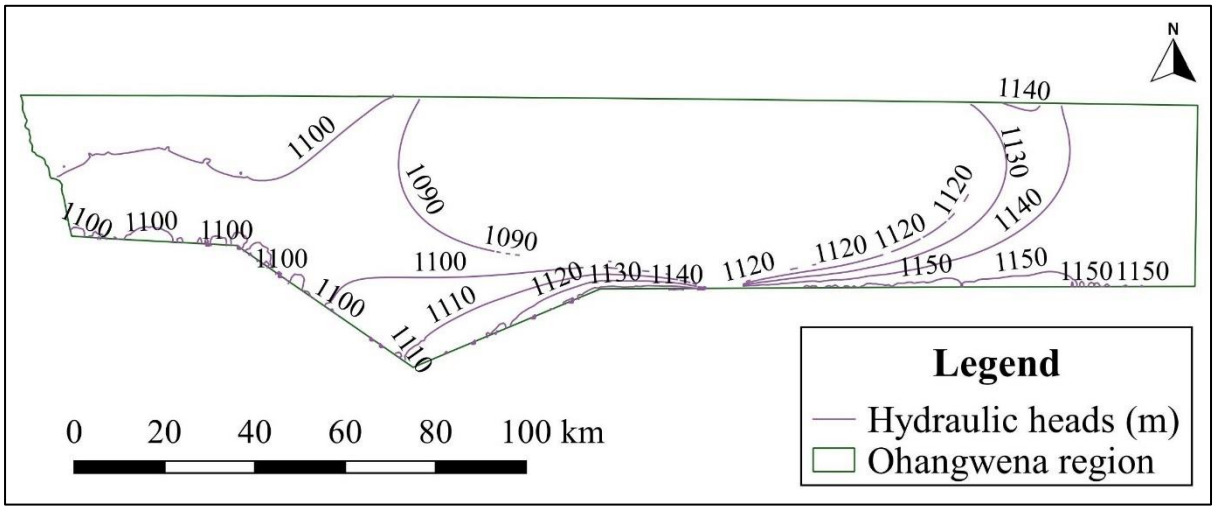

Figure 4.6: Simulated hydraulic heads for layer 2

The unconfined layer 2 which is the first aquitard of the Ohangwena aquifer system, has the simulated heads in the range of 1090 to 1150 m shown by the hydraulic heads in Figure 4.6. According to Figure 4.6, the highest hydraulic heads in the range of 1120 to 1150 are situated on the western side of the region, while the lowest hydraulic heads are situated on the eastern side of the region, due to enhanced recharge with runoff. These hydraulic heads ranges are directly proportional to the Digital Elevation Model of the region shown in Figure 3.16. The high hydraulic heads are highly influenced by the low hydraulic conductivity of the aquitard, which is 7.00×10^{-11} m/s.

The results of the simulated hydraulic head of the steady-state model of layer 3 (KOH-I) are shown in Figure 4.7.

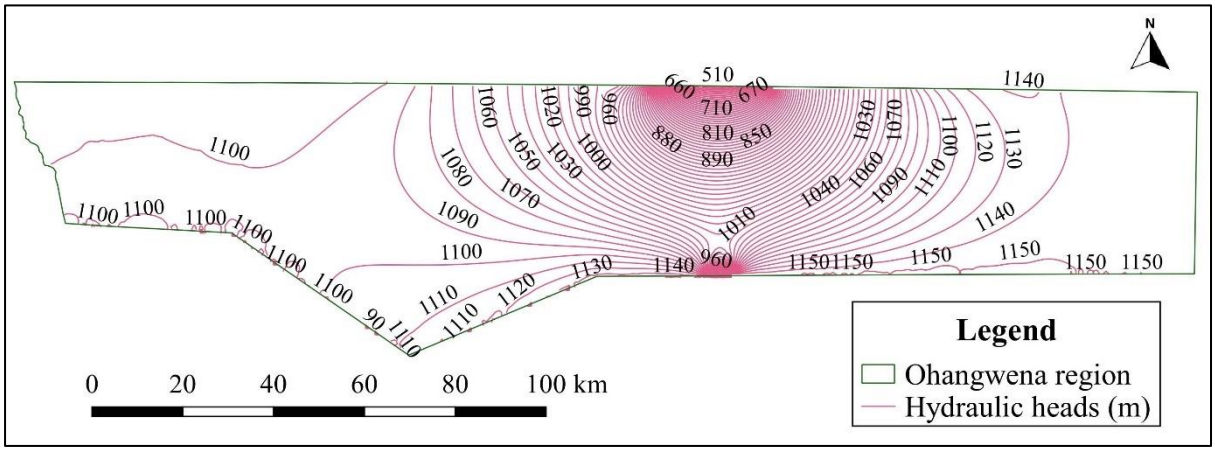

Figure 4.7: Simulated hydraulic heads for layer 3

The simulated hydraulic heads of layer 3 (KOH-I), of the steady-state model shown by Figure 4.7, range from 510 to 1150 m. These hydraulic heads are the same as simulated hydraulic heads of layer 1 shown in Figure 4.7. The lowest heads of 510 to 960 m lie in the area where the main ephemeral river enters the region, from the neighbouring country Angola. These low hydraulic heads show depression in the drainage path of the river. The highest hydraulic heads of 1020 to 1150 m cover a major part of the region, and it is an indication that the groundwater levels increased due to the aquifer recharge simulated.

The hydraulic heads of the second aquitard (layer 4), of the steady-state model, are shown in Figure 4.8.

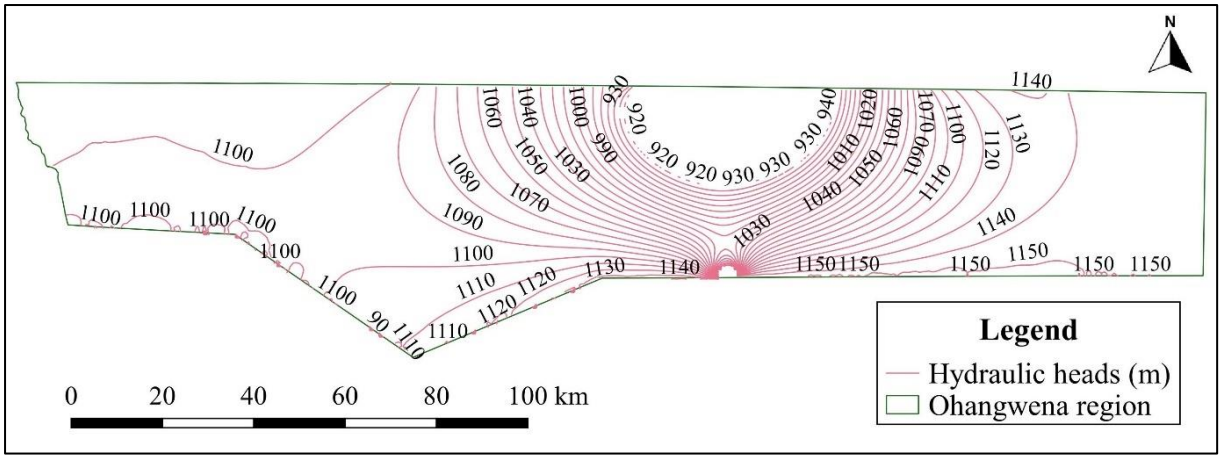

Figure 4.8: Simulated hydraulic heads for layer 4

The simulated hydraulic heads of aquitard 2 (layer 4) of the steady-state model range from 920 to 1150 meters, shown in Figure 4.8. The highest hydraulic heads in the range of 1120 to 1150m are found in the areas with high elevations, mostly on the western side of the region. These high hydraulic heads represent an increment in the groundwater levels of the aquifer due to recharge that was assessed on the aquifer, with model simulation.

The aquifer's layer five (KOH-II) simulated hydraulic heads are shown in Figure 4.9.

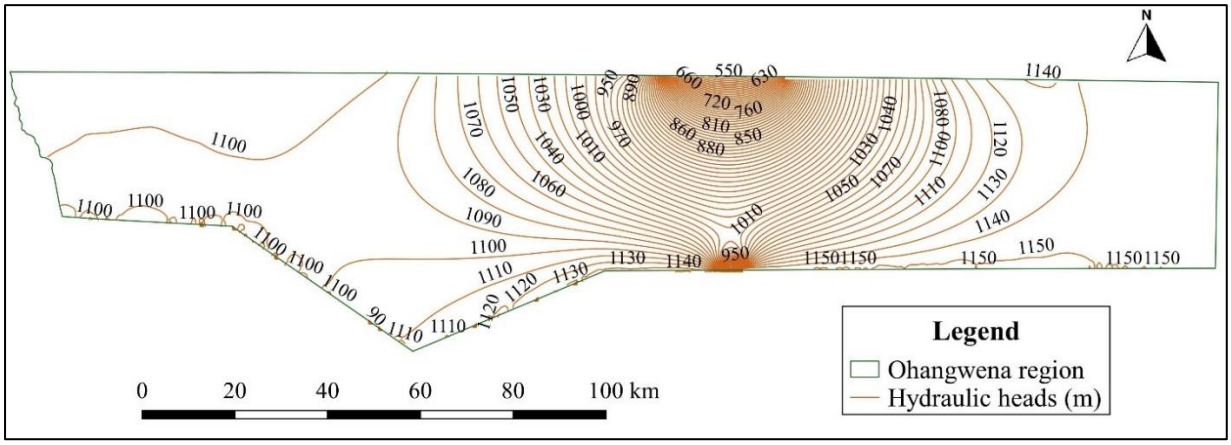

Figure 4.9: Simulated hydraulic heads for layer 5

The simulated hydraulic heads of layer 5 (KOH-II) of the steady-state due to aquifer recharge range from 550 to 1150 m. The pattern of the simulated hydraulic heads for this layer is similar to layers 1 and 3. The low hydraulic heads are found at the point where the river enters the region. And the high hydraulic heads are found on the entire western and eastern sides of the region. The heads for layer five and their locations are similar to that of layer one and layer three.

The water budget of the calibrated steady-state model is shown in Table 4.4 and further discussed.

Table 4.4: Steady state water budget

Item	Inflow (m^3/s)	Outflow (m^3/s)
Storage	0,0	0,0
Constant head	323,1	237,6
Wells	0,0	1,1
Evapotranspiration	0,0	12,8
Head dep Bounds	31,9	104,5
Recharge	1,0	0,0
Total	356,0	356,0
In-Out	$6{,}5918\times10^{3}$	
% Discrepancy	0,0%	

According to the water budget results shown in Table 4.4, the inflows that bring in water into the model are constant heads and recharge, while the outflows responsible for taking water out of the model are constant heads, wells, evapotranspiration, and head-dependent bounds. There is no change of storage under steady-state conditions. The difference between the total inflow and total outflow shows that the inflow is slightly higher than the outflow with a difference of 0.0065918. The percentage discrepancy is 0.00%, which contributes to the calibration's confidence interval. The water balance also shows a greater inflow than outflow at the constant head, which suggests that some water was extracted from the aquifer, some were lost through evapotranspiration, and some were lost via head-dependent bounds.

The simulated water table elevation heads of the steady-state model due to recharge are shown in Figure 4.10.

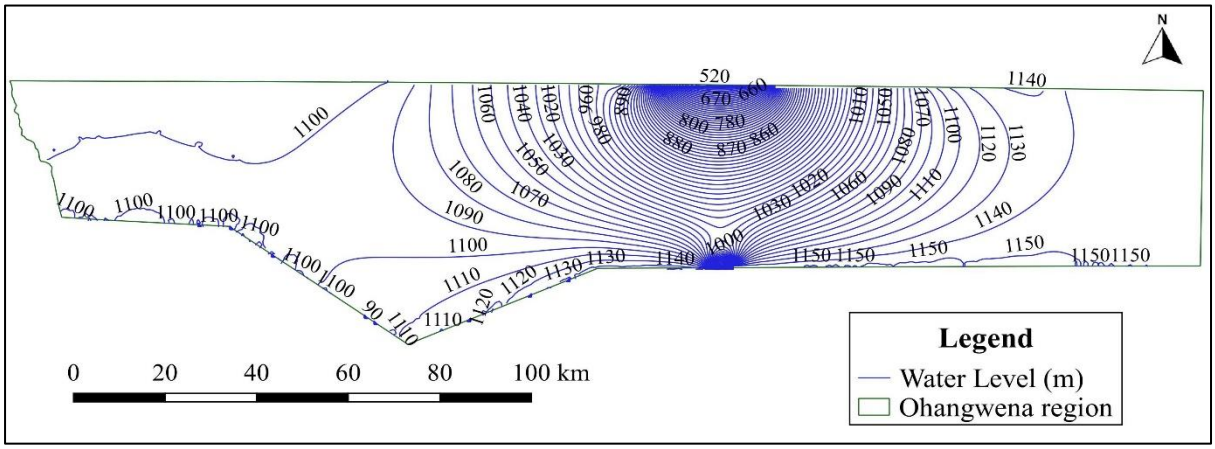

Figure 4.10: Water table heads (steady-state)

According to the water table results in Figure 4.10, it shows that the water table is low at the entrance of the ephemeral river, with the lowest head of 520m, and it also gets lower close to

the southern boundary of the region with the lowest head being 1000m. The entire western and eastern sides of the region have a high-water table to the maximum head of 1150m.

4.2.1.2 Transient state model

The transient state model was set up for a period of 6 years which is equivalent to 189345600 seconds, with a time step of 20. The model converged with a percent discrepancy of 0.0% for all the 20-time steps. The calibration of the transient state model was done using the same method used in the steady-state model, and it was calibrated from an RMSE value of 15.234 to an RMSE value of 7.534. During calibration, the boreholes' water levels without recharge were compared to the simulated water levels of the boreholes due to recharge. The water level without recharge are the recorded boreholes water levels from the Namibian Ministry of Agriculture, Water, and Land Reform. The same boreholes that were used in the steady-state model were the same boreholes used for simulating the impact of recharge on groundwater levels in the transient state model. The impact of aquifer recharge using runoff in a transient state model is presented in Table 4.5 and Figure 4.11.

Table 4.5: Observed vs Simulated heads

Borehole number	Water level without recharge (m)	Water level with Aquifer Recharge (m)	Difference in water level due to recharge (m)
WW201045	1096	1105,2	9,2
WW20267	1102	1112,5	10,5
WW201634	1102	1111,5	9,5
WW201637	1103	1115,1	12,1

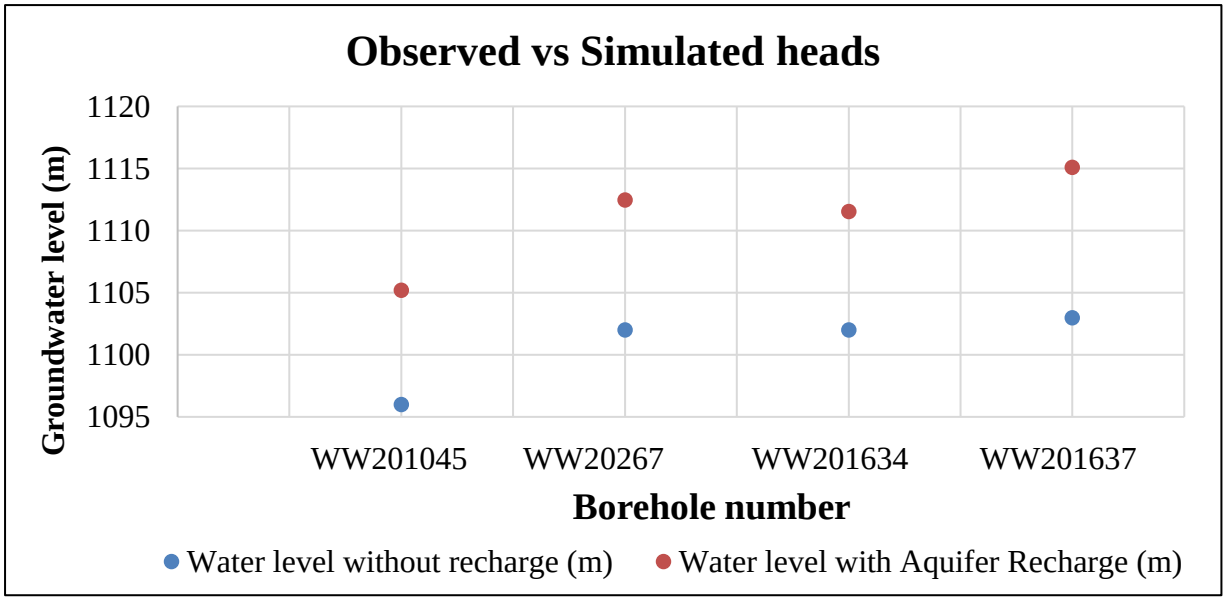

Figure 4.11: Impact of Aquifer Recharge on groundwater levels

According to Table 4.5 and Figure 4.11, there is a significant increase in the groundwater levels due to aquifer recharge, assessed at the four boreholes (WW201045, WW20267, WW201034, and WW201637). Borehole WW201637 which is located down the region on the southern side according to Figure 3.17, has the highest recharge with a difference of 12.1 m in the groundwater levels. Borehole WW201634 and WW20267 which are located in the upper north-western direction of the region shown in Figure 3.17 have a high difference of 9.5 m and 10.5 m respectively in the groundwater levels due to aquifer recharge, while borehole WW201637 which is located almost in the middle of the region on the southwestern direction shown in Figure 3.17, has the low difference of the impact due to aquifer recharge among the four assessed boreholes in the transient state model.

The simulated hydraulic heads of the transient state model for layer one are shown in Figure 4.12.

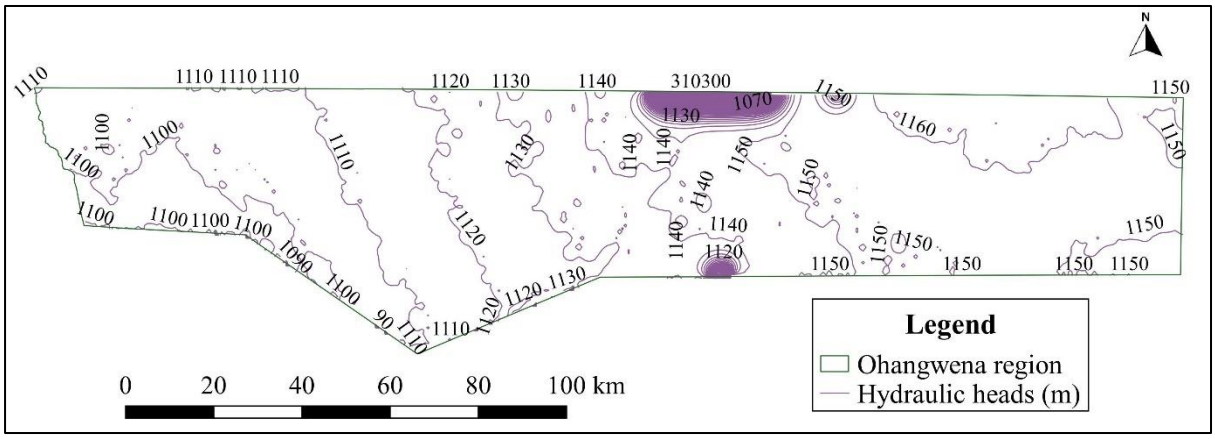

Figure 4.12: Hydraulic heads for layer 1 (transient state)

The results presented in Figure 4.12 are for the 20th time step, which is the last time step of the entire 6 years simulation. The results show that the simulated hydraulic heads for layer one range from 330 to 1160 meters, whereby the lower hydraulic heads cover a small portion of the region, basically where the ephemeral river enters the region. Approximately 98% of the region has simulated hydraulic heads lying in the range of 1100 to 1160 meters. The high hydraulic head values are an indication that there is a gradual increase in the groundwater levels due to enhanced recharge with rainfall-runoff, for the simulated period. The results for the 20th time step presented in Figure 4.12, is an accumulation of the hydraulic heads from time step one to the 20th time step.

The simulated heads for the first aquitard (layer one) of the transient state model are presented in Figure 4.13.

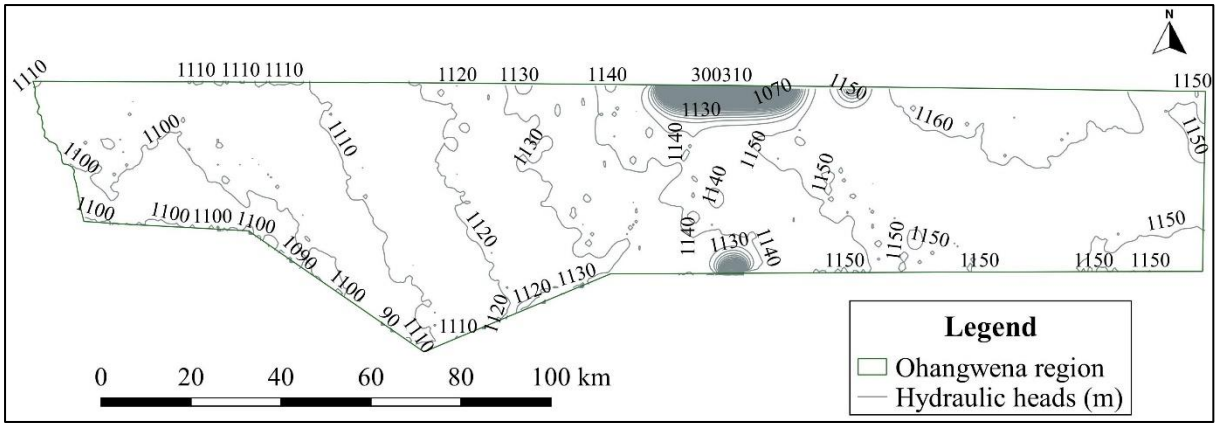

Figure 4.13: Hydraulic heads for layer 2 (transient state)

The simulated hydraulic head results for layer two presented in Figure 4.13, show that the heads for the first aquitard (layer two) lie between 300 and 1160 meters. Similarly, to the first layer, these heads are lower in the area where the main ephemeral river enters the region, showing depression in that area, and the high hydraulic heads in the range of 1100 to 1160 meters cover approximately 98% of the Ohangwena region. These high hydraulic heads are an indication that the is a gradual increase in the groundwater levels, brought by the accumulated recharge for the six simulated years.

The simulated heads for the third layer of the Ohangwena aquifer are shown in Figure 4.14.

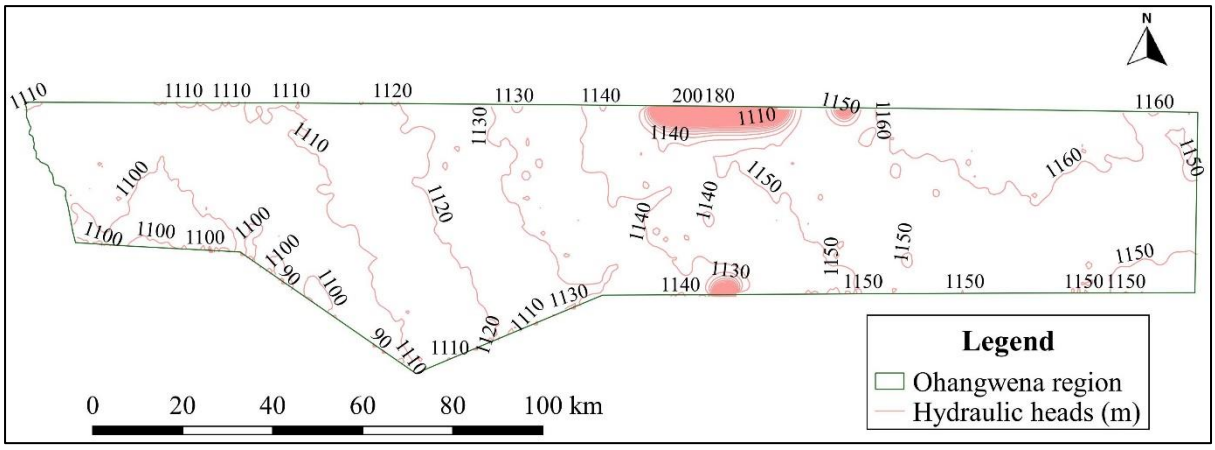

Figure 4.14: Hydraulic heads for layer 3 (transient state)

According to layer two results presented in Figure 4.14, the minimum hydraulic head for the third layer is 180 meters and the maximum is 1160 meters. Compared to layer one and layer two, layer three has the lowest minimum heads. In layer three, the lowest hydraulic heads also cover a very small portion of the region approximately 0.5%, while the entire region is covered with high hydraulic heads lying between 1100 to 1160 meters. Similarly, to layer one and layer two, the high hydraulic heads covering the entire region are an indication that there is a huge impact on the groundwater levels due to Aquifer Recharge.

The heads for the second aquitard (layer four) are presented in Figure 4.15.

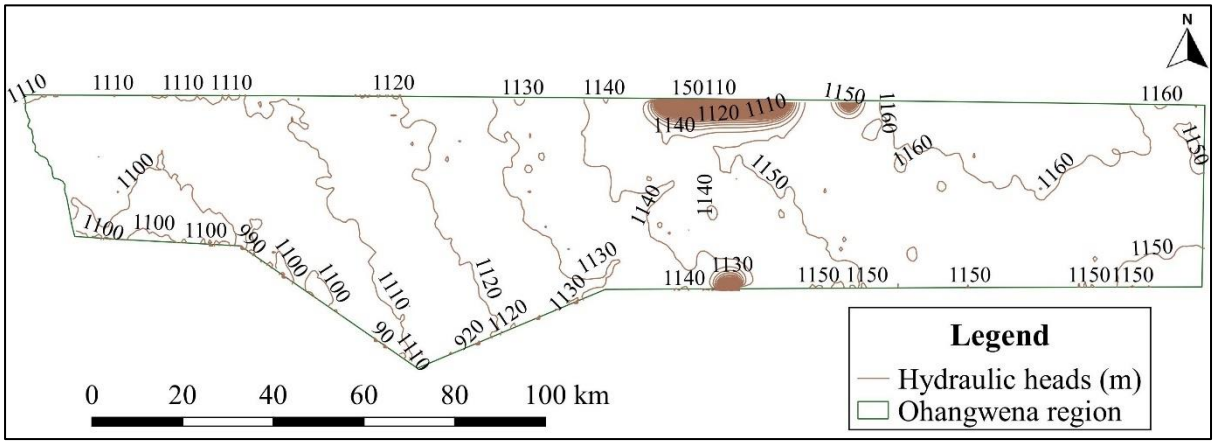

Figure 4.15: Hydraulic heads for layer 4 (transient state)

Figure 4.15 shows that the 20th timestep simulated hydraulic heads for the 4th layer of the transient model lies in the range of 110 to 1160 meters. Approximately 0.5% of the region has low heads, which are located in the middle-upper northern direction of the region, where the main ephemeral river enters the region. These low hydraulic heads are also located down the region almost on the boundary of the region. The low hydraulic heads are located almost on the boundary of the region both in layers one, two, three, and four. The entire region has high hydraulic heads in the range of 920 to 1160 meters. The high hydraulic heads are an indication that there is a gradual increase in the groundwater levels brought by the recharge. Compared to the first aquitard (layer two) hydraulic head results, the low heads in aquitard one covers kind of a large area compared to the second aquitard. This shows that the simulated hydraulic heads decrease as you move down the aquifer's layers.

The simulated hydraulic heads for the last layer (layer five), are shown in Figure 4.16.

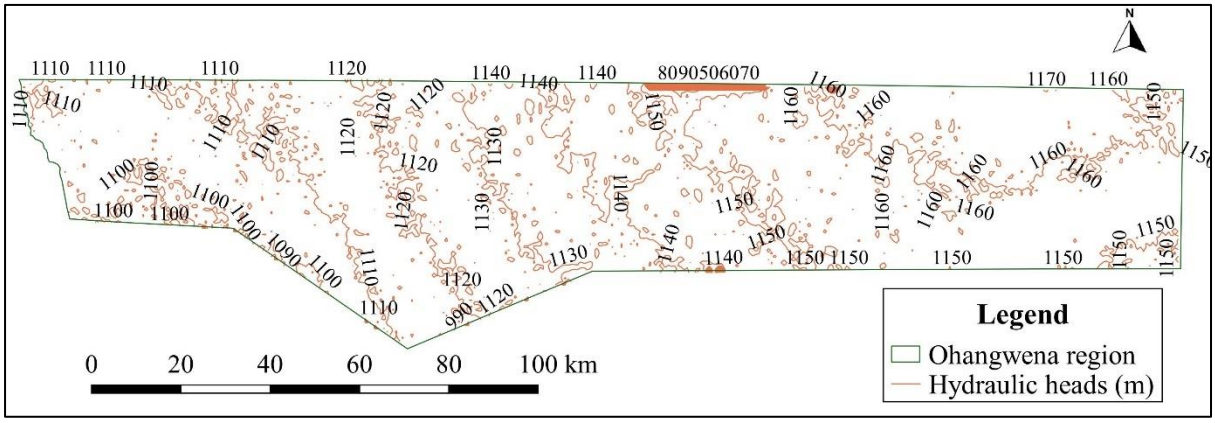

Figure 4.16: Hydraulic heads for layer 5 (transient state)

The hydraulic heads of the 20th time step of layer five for the transient state model shown in Figure 4.16, lie between 41 to 1177 meters. According to these results, the low hydraulic heads lie in the upper northern direction, on the boundary of the region. These hydraulic heads range

from 41 to 230 meters. Approximately 99% of the entire region has high hydraulic conductivities in the range of 1100 to 1170 meters. Overall, the results of this layer show that hydraulic heads increase as you move down the aquifer. They also show that there is a greater increase in the groundwater levels.

The simulations of the impact of Aquifer Recharge with runoff on the groundwater levels of the transient state model also resulted in a water budget for the region. The water budget of the calibrated transient state model's 20th time step is shown in Table 4.6 and further discussed. The water budgets for timestep one to timestep 19 are in the appendices section (chapter 7).

Table 4.6: 20th timestep water budget (transient model)

Item	In (m^3/s)	Out (m^3/s)
Storage	60,9	3,6
Constant head	8,4	8,7
Drains	0,0	0,5
Evapotranspiration	0,0	23,8
Head dep bound	2,6	36,3
Recharge	1,0	0,0
Total	73.0	73.0
In-Out	$1{,}5030\times10^3$	
% Discrepancy	0,0%	

According to the water budget results shown in Table 4.6, the inflows that bring in water into the model are constant heads, recharge, and head-dependent bound. The outflows responsible for taking water out of the model are constant heads, drains, evapotranspiration, and head-dependent bounds. There is a change in storage under transient state conditions, whereby the inflow storage is greater than the outflow storage. This difference in storage is brought by Aquifer Recharge. The difference between the total inflow and total outflow shows that the inflow is slightly higher than the outflow with a difference of 0.0015030 m^3/s. The percentage discrepancy is 0.0%, which contributes to the calibration's confidence interval.

4.3 Modeling the transport of contaminants within the Aquifer

As described in Section 3.8, a part of this study also assessed how the contaminants travel and move within the aquifer. This was assessed at two wells (WW201045 and WW201637) in the region that serves as the injection wells. The assessment was done using particle tracking and MT3DMS in ModelMuse graphical user interface incorporating MODFLOW 2005.

4.3.1 Groundwater flow model and contaminant plume transport

The groundwater flow model (MODFLOW 2005) used in this study simulated the groundwater flow in the region, and particle tracking simulated the migration of the contaminants in this study. The migration of the contaminants was simulated using the transient state model. The contaminants simulated in this model are chloride, electrical conductivity, Total Dissolved Solids (TDS), and *E-coli*. The contaminants' dispersion of the surface runoff within the aquifer were assessed because they are harmful to humans if they are consumed in high concentrations, exceeding the accepted concentrations.

4.3.1.1 Dispersion of chloride as a contaminant within the aquifer

Chloride is one of the contaminants associated with runoff, and its migration within the Ohangwena aquifer system was simulated using the transient state model, with 20-time steps. The simulation was done in such a way that, runoff will be injected into the injection wells (WW201045 and WW201637), as described in Section 3.8, to recharge the aquifer.

The overall combination of chloride dispersion in all directions within the aquifer at the two simulated wells is presented in Figure 4.17. According to these results, the chloride disperses almost equally in all the directions surrounding the simulated injection wells (WW201045 and WW201637). For the simulated six years period, the chloride disperses further with a concentration of 0.0 mg at the 20th timestep of the simulated model. The initial measured chloride concentration of runoff (1000 mg) takes time for it to disperse at the beginning. This is shown by a large area of the red colour region at the two wells in Figure 4.17. The results also show that as the timesteps increase, the concentration of chloride decreases as you move away from the point source, and it takes time for the contaminant to disperse further into the aquifer.

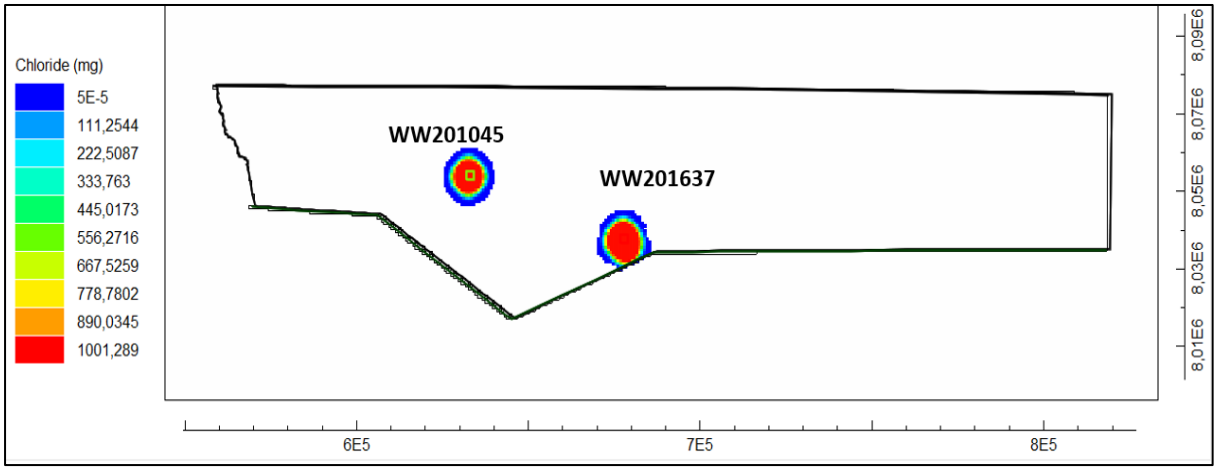

Figure 4.17: Chloride dispersion within the aquifer

The dispersion of Chloride at the two individual simulated wells is shown in Figures 4.18 and 4.19.

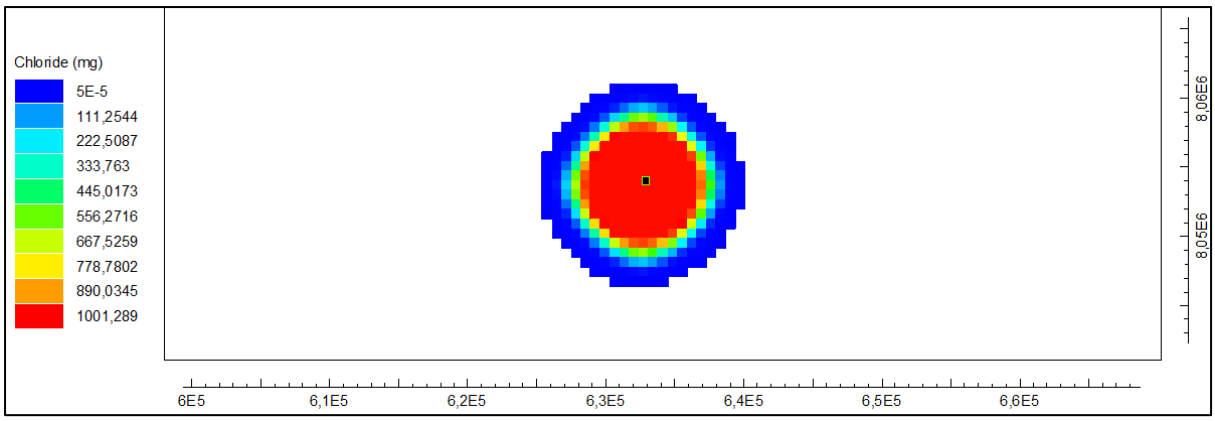

Figure 4.18: Dispersion of Chloride at WW201045

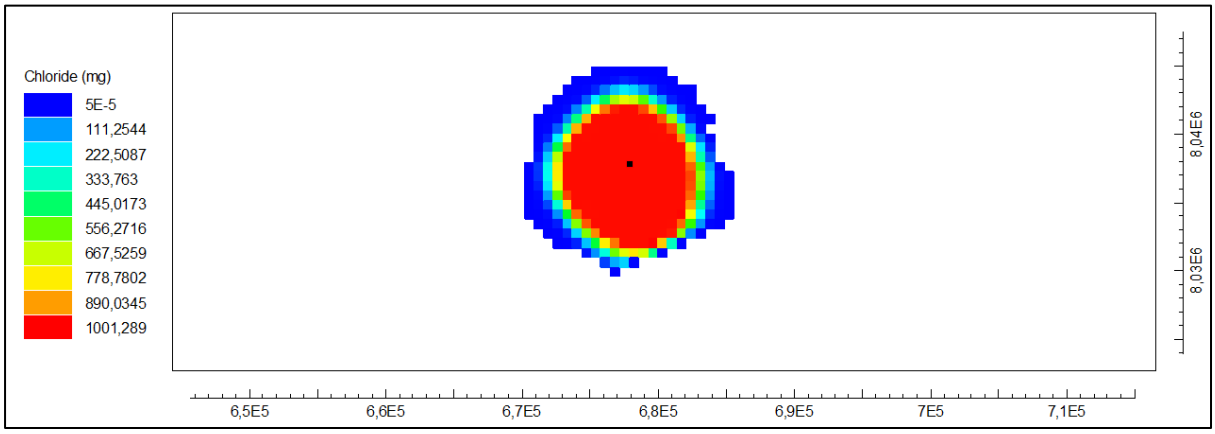

Figure 4.19: Dispersion of Chloride at WW201637

The results for the horizontal migration of chloride in the four directions (North, South, West, and East) within the aquifer due to Aquifer Recharge are shown in Figure 4.20, and in Tables 7.20 to 7.23 in section 7.2.1 of the appendices.

The chloride concentration of surface runoff measured for the year 2017 was 1000 mg, and it was simulated how it disperses across the aquifer. The results simulation in the northern direction shown in Figure 4.20 shows that as the timesteps increase, the concentration of chloride decreases as you move away from the point source. At the last time step (20) the concentration is simulated to be 1.075 mg at well WW201045, and 0.011 mg at well WW201637. These simulation results show that it takes time for the contaminant to disperse further into the aquifer. The dispersion of the contaminant is affected by the different hydraulic conductivities in the aquifer's layers which arises preferential flow paths, and porosity of the aquifer. The aquifer area where well WW201045 is located is much more porous compared to the aquifer area where well WW201637 is located, which also contributed to the Chloride dispersion to be higher in well WW201045 compared to well WW201637, as shown by the last (20^{th}) timestep results, in addition to the different hydraulic conductivities. At both wells, chloride travels almost at the same pace, shown by the closeness of the concentration values at different timesteps. Chloride disperses faster at well WW201637 than at well WW201045.

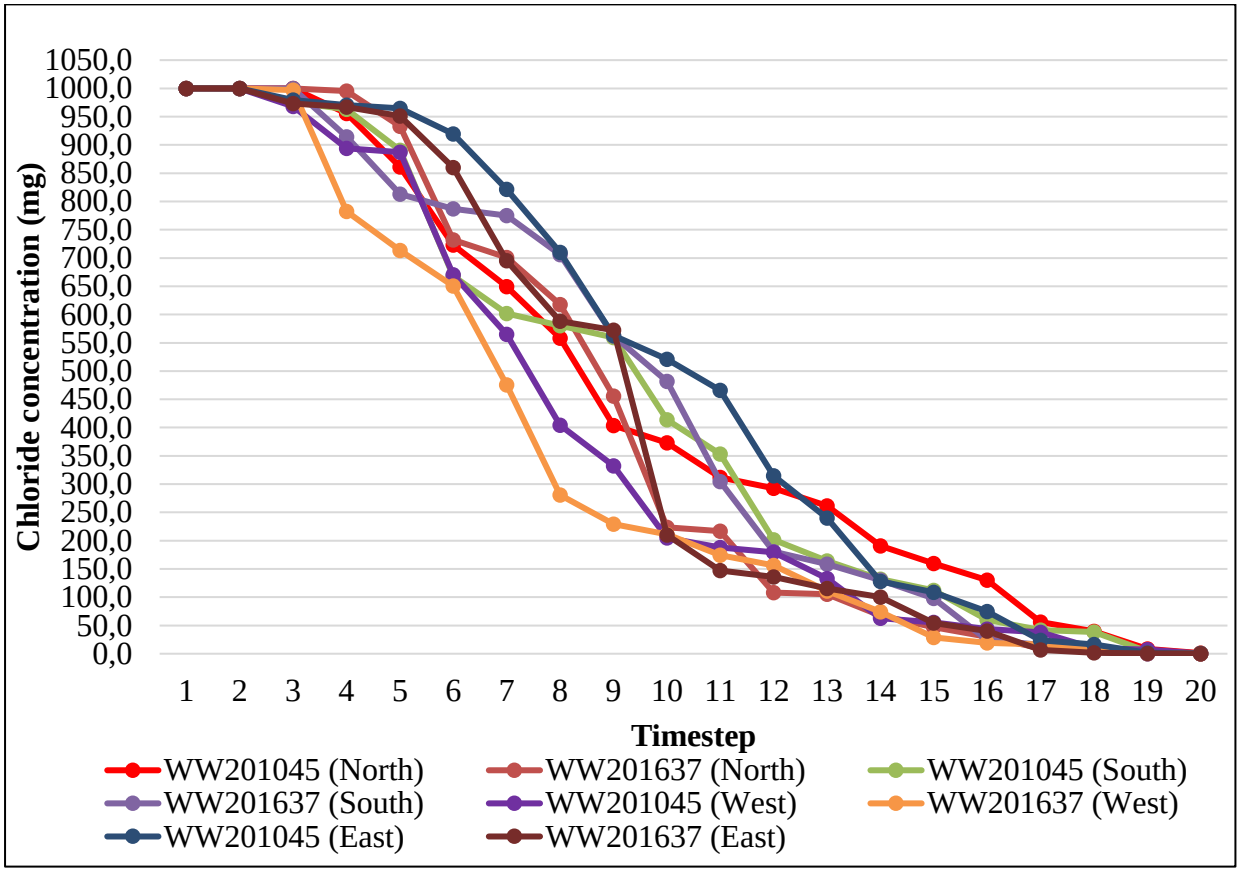

Figure 4.20: Dispersion of Chloride concentration within the aquifer

The results presented in Figure 4.20, shows that chloride concentration decreases in the southern direction of the region at the two wells as timestep increases. The dispersion trend of this contaminant does not move at the same pace at the two wells, although there is a slight difference in the concentration values at the wells at individual timesteps. This is shown at the last time step 20, where the chloride concentration at well WW201045 is higher with 0.5 mg compared to the concentration at WW201637 with 0.1 mg. The results also show that as the timesteps increase, the concentration of chloride decreases in the southern direction as you move away from the point source, and it takes time for the contaminant to disperse further into the aquifer. The dispersion of Chloride within the two wells is mainly affected by the different hydraulic conductivities of the aquifer's layers, and the different porosity of the areas of the aquifer where the wells are located, which caused Chloride concentration dispersion to be higher in well WW201045 at the last (20^{th}) timestep than in well WW201637. According to the simulation, the ability for chloride to migrate and disperse through the aquifer layers in all the timesteps without failing and any error shows that the aquifer's transmissivity is good, and it can allow fluids to flow within it.

The dispersion trend of chloride in the western direction of the region is similar to the dispersion trends in the northern and southern directions discussed earlier. At most time steps,

the chloride concentrations in well WW201045 are higher than the concentration in well WW201637. The chloride concentration decreases in the western direction of the region. Similar to the southern direction, chloride disperses faster in well WW201045 compared to well WW201637. This is shown in the last time step (20), where the chloride concentration is 0.2 mg in well WW201045 and 0.1 mg in well WW201637. The results also show that as the timesteps increase, the concentration of chloride decreases as you move away from the point source, and it takes time for the contaminant to disperse further into the aquifer shown in Figure 4.20.

The results presented in Figure 4.20, shows that chloride concentration decreases in the eastern direction of the region as the timestep increases at the two wells. The dispersion trend of this contaminant does not move at the same pace at the two wells, although there is a difference in the dispersion concentration values at the two wells at individual timesteps. This is shown at the last time step (20), where the chloride concentration at well WW201045 is higher with 0.4 mg compared to the concentration at WW201637 with 0.1 mg. The dispersion concentration of chloride for well WW201045 is higher than the concentrations of well WW201637 for all the timesteps.

The distance travelled by the dispersion of Chloride concentration at different timesteps, and at the two simulated wells is shown in Table 4.7.

Table 4.7: Distance travelled by Chloride dispersion at different times within the aquifer

Timestep	Chloride concentration (mg/l)		Distance travelled (km)	
	WW201045	WW201637	WW201045	WW201637
1	1000,0	1000,0	0,7	0,6
2	999,9	999,8	1,3	1,2
3	980,8	992,6	1,8	1,7
4	945,7	914,9	1,9	2,0
5	900,9	827,5	2,2	2,7
6	745,4	757,2	3,5	3,1
7	659,5	661,8	4,0	3,6
8	563,2	548,3	4,1	4,1
9	464,6	454,9	4,9	4,7
10	378,3	281,6	5,3	5,1
11	329,9	210,8	5,0	5,8
12	247,1	145,2	6,2	6,3
13	199,8	122,5	7,5	6,6
14	128,3	92,8	7,7	7,0
15	108,9	56,9	8,0	7,3
16	77,0	28,4	8,7	6,4
17	40,0	12,2	9,0	7,9
18	26,1	5,1	9,4	8,1
19	5,2	0,4	11,6	9,8
20	0,6	0,1	12,1	10,1

According to the results presented in Table 4.7, it shows that Chloride disperses further into the aquifer reaching a distance of 12.1 km at the last timestep. Chloride dispersion at WW201045 spreads covering a long distance of 12.1 km, compared to dispersion at WW201637 which covers a distance of 10.1 km.

4.3.1.2 Dispersion of Electrical conductivity as a contaminant within the aquifer

Electrical conductivity is another contaminant associated with surface runoff. It is a measure of the ability of a solution to conduct electric current. Although it is not a concentration, it was included in this study because it is related to the ions that are present in the solution, in this case, surface runoff. Its movement within the Ohangwena aquifer system was simulated using the transient state model, for one stress period, six years with 20-time steps similar to the simulation model for Chloride as a contaminant discussed in section 4.3.1.1. The simulation was done in such a way that, the runoff will be injected into the injection wells (WW201045 and WW201637), as described in Section 3.8, to recharge the aquifer, and observe how the electrical conductivity spread within the aquifer.

The overall combination of electrical conductivity dispersion in all directions within the aquifer at the two simulated injection wells (WW201045 and WW201637) is presented in Figure 4.21. The results in Figure 4.21 show that the electrical conductivity disperses slightly evenly in all the directions surrounding the simulated injection wells (WW201045 and WW201637). For the simulated 6 years period, the Electrical Conductivity disperses with the furthest horizontally with a concentration of 0.0 mS/s at the 20th timestep of the simulated transient model. The initial measured Electrical Conductivity of runoff (532 mS/s) takes time for it to disperse at the beginning. This is shown by a large area of the red color region at the two wells in Figure 4.21. It is also shown that the Electrical Conductivity value of 0.0 mS/s covers a large area, although not as large as the area for 532 mS/s. Electrical Conductivity values ranging from 473.8 to 59.2 mS/s cover small areas.

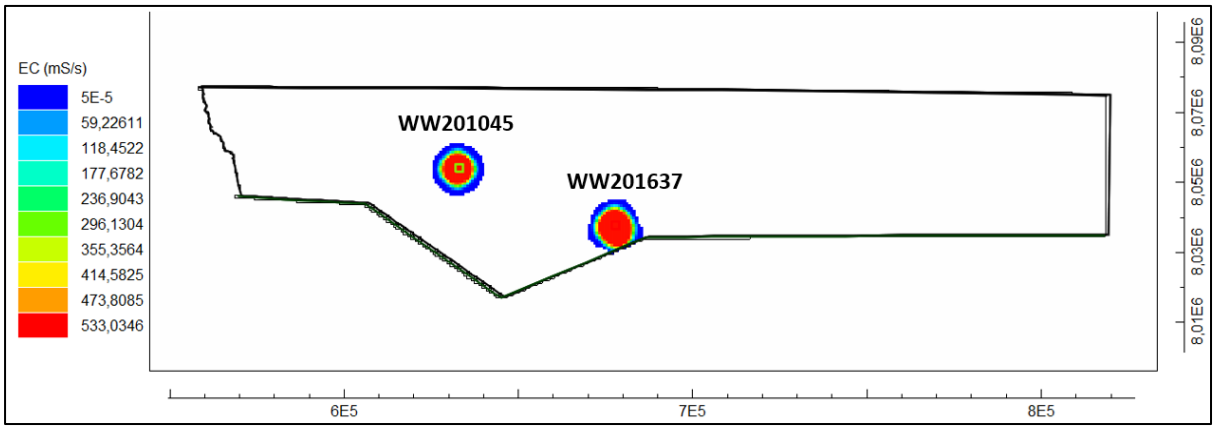

Figure 4.21: Dispersion of Electrical conductivity within the aquifer

The dispersion of Electrical Conductivity at the two simulated wells (WW201045 and WW201637) is shown in Figures 4.22 and 4.23.

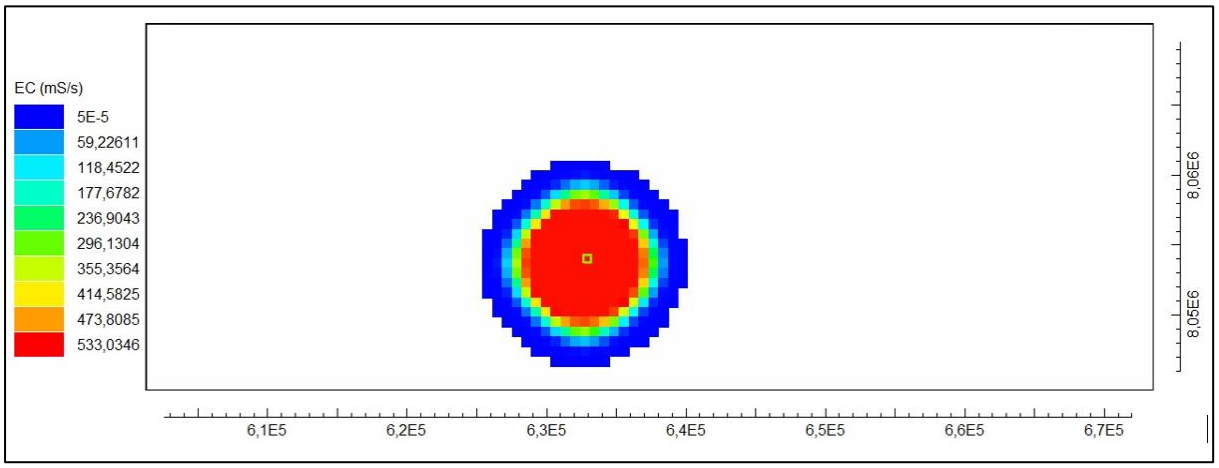

Figure 4.22: Dispersion of Electrical conductivity at WW201045

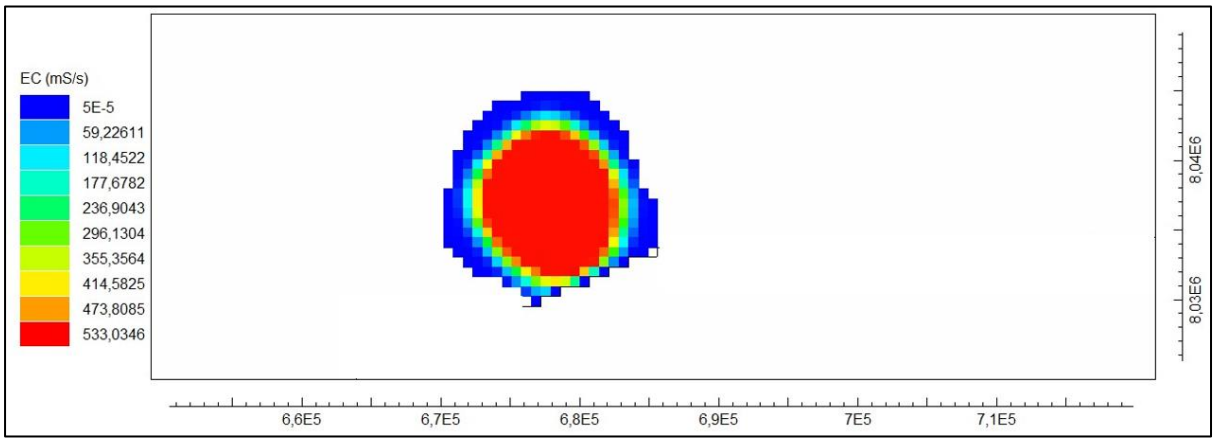

Figure 4.23: Dispersion of Electrical conductivity at WW201637

The results for the horizontal dispersion of Electrical Conductivity in the four directions (North, South, West, and East) within the aquifer due to enhanced recharge are shown in Figure 4.24, and Tables 7.24 to 7.27 in section 7.2.2 of the appendices.

The results in Figure 4.24 shows that overall electrical conductivity decreases as the timesteps increase. The dispersion trend of electrical conductivity in the northern direction moves almost at the same pace at the two wells. This is shown by the slight differences in the dispersion concentration values in the wells at individual timesteps. The last time step (20), shows that the electrical conductivity concentration at well WW201045 is higher with 0.2 mS/s compared to the concentration at WW201637 with 0.1 mS/s. The dispersion concentration trend of the two wells also shows that the Electrical Conductivity concentrations at the two simulated wells are not far from each other in terms of quantity. The results also show that as the timesteps increase, the concentration of Electrical Conductivity decreases as you move

away from the point source, and it takes time for the contaminant to disperse further into the aquifer.

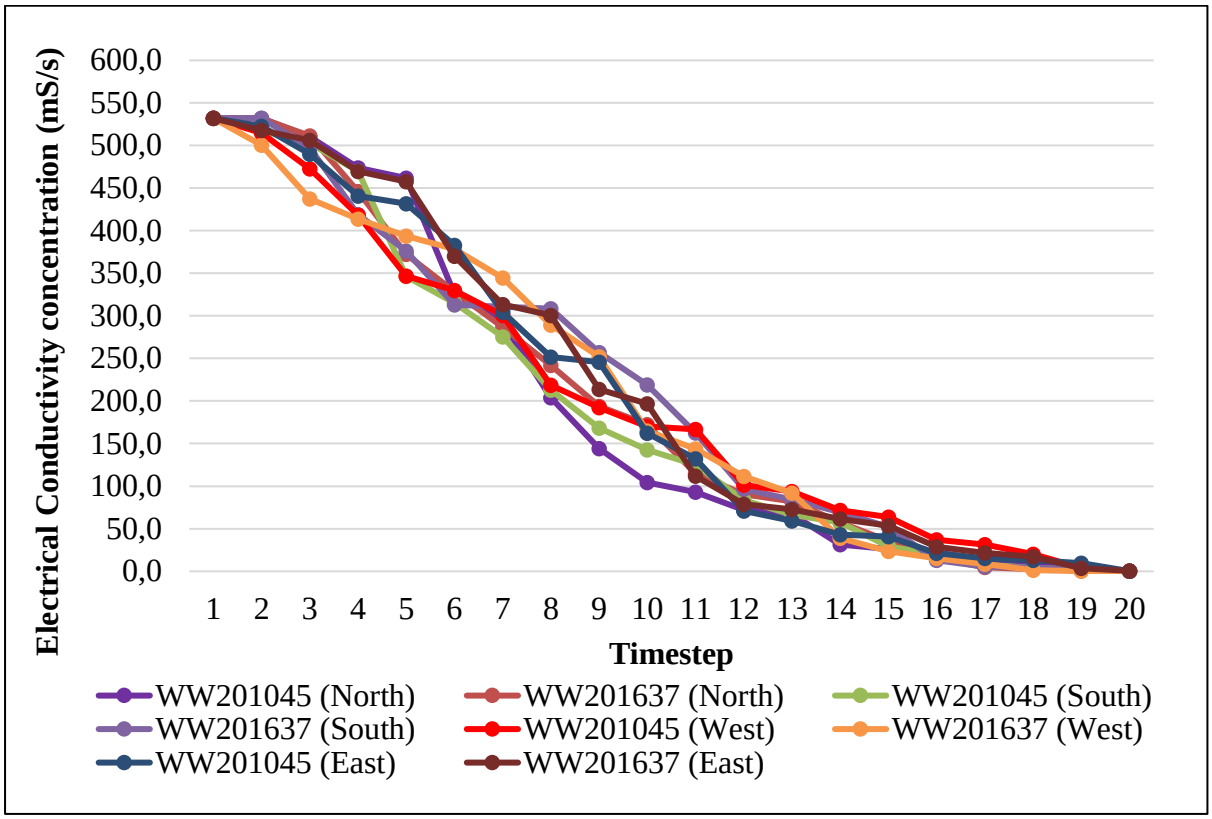

Figure 4.24: Dispersion of Electrical conductivity within the aquifer

The dispersion results of Electrical Conductivity in the southern direction of the region presented in Figure 4.24, show that Electrical Conductivity decreases in the southern direction of the region at the two wells as timestep increases. The dispersion trend of Electrical Conductivity in the southern direction is similar to the dispersion trend in the northern direction of the region discussed earlier. This dispersion does not move at the same pace at the two wells, although there is a slight difference in the concentration values in the wells at individual timesteps. The last time step (20) of the simulation shows that the Electrical Conductivity at well WW201045 is higher with 0.2 mS/s compared to the Electrical Conductivity at WW201637 with 0.1 mS/s. As the timesteps increase, the Electrical Conductivity decreases as you move away from the point source, and it takes time for the contaminant to disperse further into the aquifer. The dispersion of the Electrical Conductivity is affected by different hydraulic conductivities in the aquifer layers. Apart from different hydraulic conductivities in aquifer layers, the higher Electrical conductivity at well WW201045 than at well WW201637 was caused by the high porosity of the aquifer area where well WW201045 is located. The dispersion of this contaminant did not stop at any of the timesteps, which is an indication that the transmissivity of the aquifer at all the two wells allows fluids to migrate through it.

The dispersion of Electrical Conductivity in the western direction of the Ohangwena region presented in Figure 4.24 shows that Electrical Conductivity decreases as the timesteps increase. This is similar to the two directions (north and south) discussed earlier. The dispersion trend of Electrical Conductivity in the western direction moves almost at the same pace at the two wells. This is shown by the slight differences in the dispersion concentration values in the wells at individual timesteps. It is also proved by the last time step (20), which shows that the Electrical Conductivity concentration at well WW201045 is higher with 0.2 mgS/s compared to the concentration at WW201637 with 0.1 mS/s. The dispersion concentration trend of the two wells shown in Figure 4.24 also shows that the electrical conductivity concentration values at the two simulated wells are not far from each other. The results also show that as the timesteps increase, the concentration of chloride decreases as you move away from the point source, and it takes time for the contaminant to disperse further into the aquifer.

The electrical conductivity dispersion in the eastern direction results presented in Figure 4.24 shows that electrical conductivity decreases as timestep increases. The dispersion trend of electrical conductivity in the eastern direction moves at the same pace at the two simulated wells. This is shown by almost similar electrical conductivities for the two wells at individual timesteps. The last time step (20) of simulation, shows that the electrical conductivity concentration at well WW201045 is lower with 0.2 mgS/s compared to the concentration at WW201637 with 0.6 mS/s. There is an indirect proportion between the timestep and the electrical conductivity dispersion or spreading. As the timestep increases, the electrical conductivity decreases as you move away from the point source, and it takes time for the contaminant to disperse further into the aquifer.

The distance travelled by dispersion of Electrical Conductivity at the different timesteps, at the two simulated wells is shown in Table 4.8.

Table 4.8: Distance travelled by dispersion of EC within the aquifer

Timestep	Electrical Conductivity concentration (mS/s)		Distance travelled (km)	
	WW201045	WW201637	WW201045	WW201637
1	532,0	532,0	0,5	0,2
2	521,7	520,6	1,3	0,9
3	494,0	488,0	2,2	1,1
4	450,6	437,1	2,7	1,6
5	396,7	400,0	3,2	1,9
6	338,5	347,5	3,3	2,3
7	293,1	313,9	4,4	2,7
8	221,8	285,0	4,9	3,5
9	187,6	229,1	5,7	3,8
10	144,8	188,2	5,8	4,5
11	129,3	133,3	6,0	4,9
12	81,9	94,3	6,2	5,3
13	71,7	82,8	6,3	5,9
14	50,9	56,8	6,9	6,0
15	39,9	41,2	7,2	6,5
16	25,0	18,2	7,4	6,9
17	17,0	10,1	8,1	7,3
18	11,4	6,4	8,9	7,9
19	5,1	1,6	9,0	8,1
20	0,2	0,2	9,6	8,2

According to the results presented in Table 4.8, it is shown that Electrical Conductivity disperses further into the aquifer covering a distance of 9.6 km. The dispersion is faster at well WW201045 covering a distance of 9.6 km until the last timestep, compared to well WW201637 which covered a distance of 8.2 km until the last timestep. These results show that the location of the well in the region has an impact on the dispersion of the contaminant. Well WW201045 is located in a sloping area, unlike well WW201637 which is located in a more flat area.

4.3.1.3 Dispersion of Total Dissolved Solids within the aquifer

Total Dissolved Solids (TDS) is one of the contaminants associated with runoff, and its migration within the Ohangwena aquifer system was simulated using the transient state model, with 20-time steps. The simulation was done in such a way that, the runoff will be injected into the injection wells (WW201045 and WW201637), as described in Section 3.8, to recharge the aquifer.

Total Dissolved Solids are the amount of organic and inorganic materials such as metals, minerals, salts, and ions dissolved in water. The TDS can affect the water quality; therefore, it

is needed to know the amount of TDS in water, which will allow an informed decision to solve the quality problem, and install the most effective filtration system if it is needed.

The dispersion of Total Dissolved Solids (TDS) within the aquifer is shown in Figure 4.25, while Figures 4.26 and 4.27 show the dispersion of the TDS at individual wells.

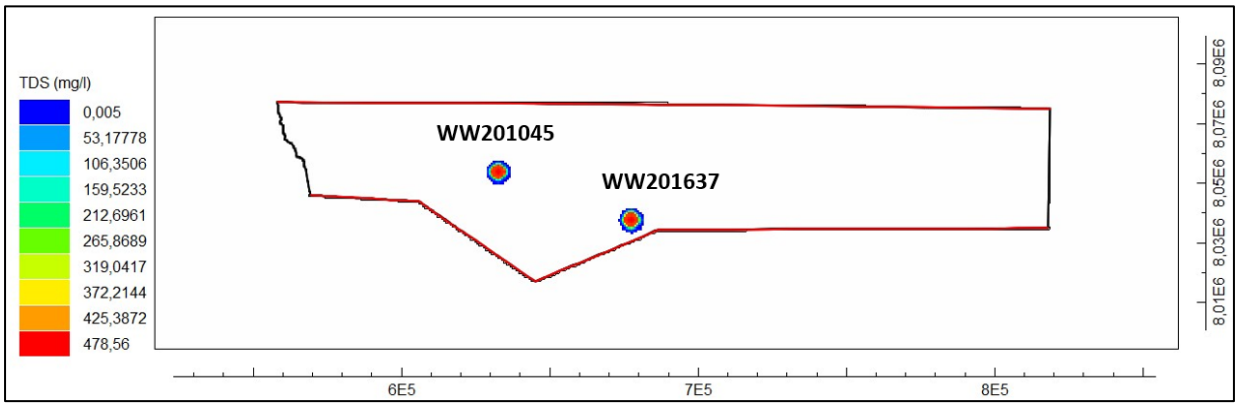

Figure 4.25: Dispersion of Total Dissolved Solids within the aquifer

According to Figure 4.25, the TDS disperse from 478.56 mg/l from the point source to 0.005 mg/l in all directions at the simulated wells. The measured TDS content which is 478.56 mg/l falls in the category of ideal water, according to the TDS water chart. This category of water is the sweet spot for TDS, and the water most likely contains minerals and does not taste flat, thus no filtration process is required for this water category. The Dispersion of the TDS decreases as the timesteps increase in all four directions (North, South, West, and East), similar to the Chloride and Electrical conductivity presented earlier.

The dispersion of the TDS at the individual simulated wells (WW201045 and WW201637) is presented in Figures 4.26 and 4.27.

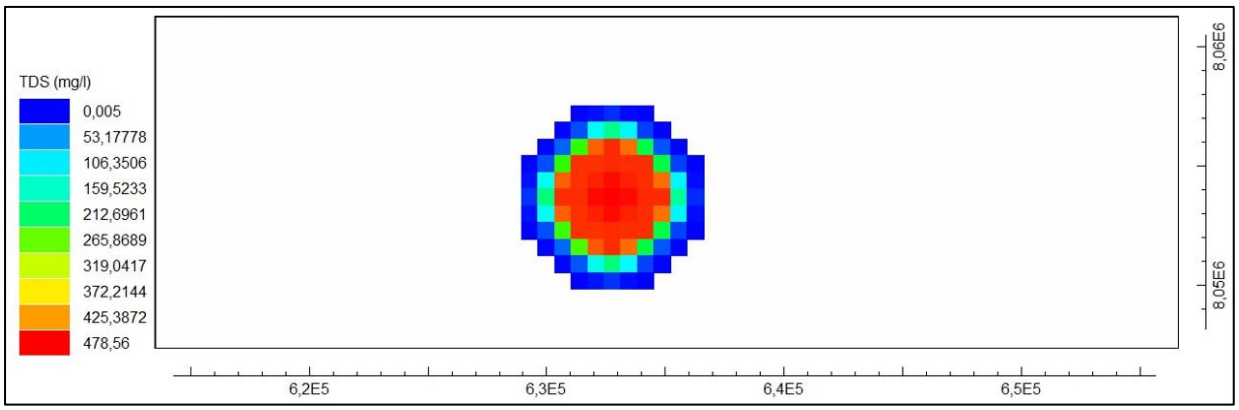

Figure 4.26: Dispersion of Total Dissolved Solids at WW201045

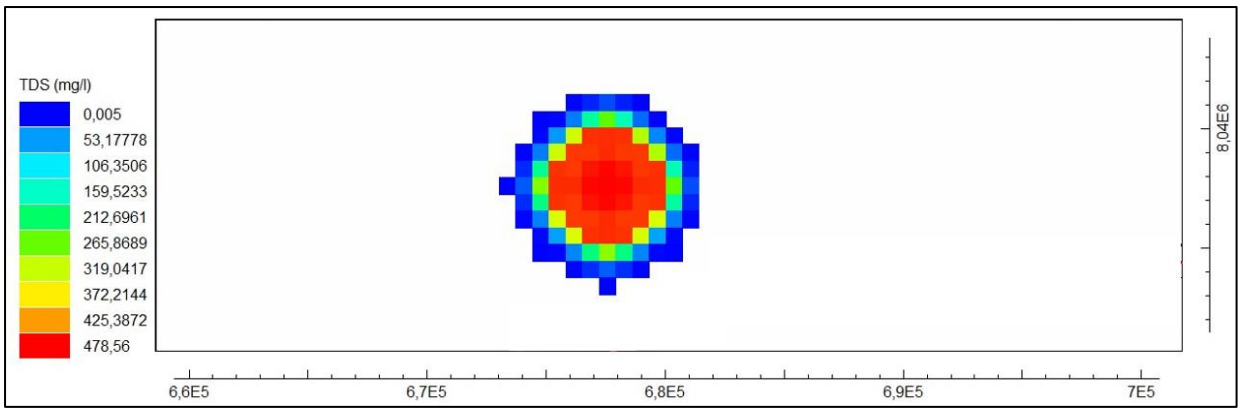

Figure 4.27: Dispersion of Total Dissolved Solids at WW201637

The results for the horizontal dispersion of Total Dissolved Solids (TDS) in the four directions (North, South, West, and East) within the aquifer due to aquifer recharge are shown in Figure 4.28, and Tables 7.28 to 7.31 in section 7.2.3 of the appendices.

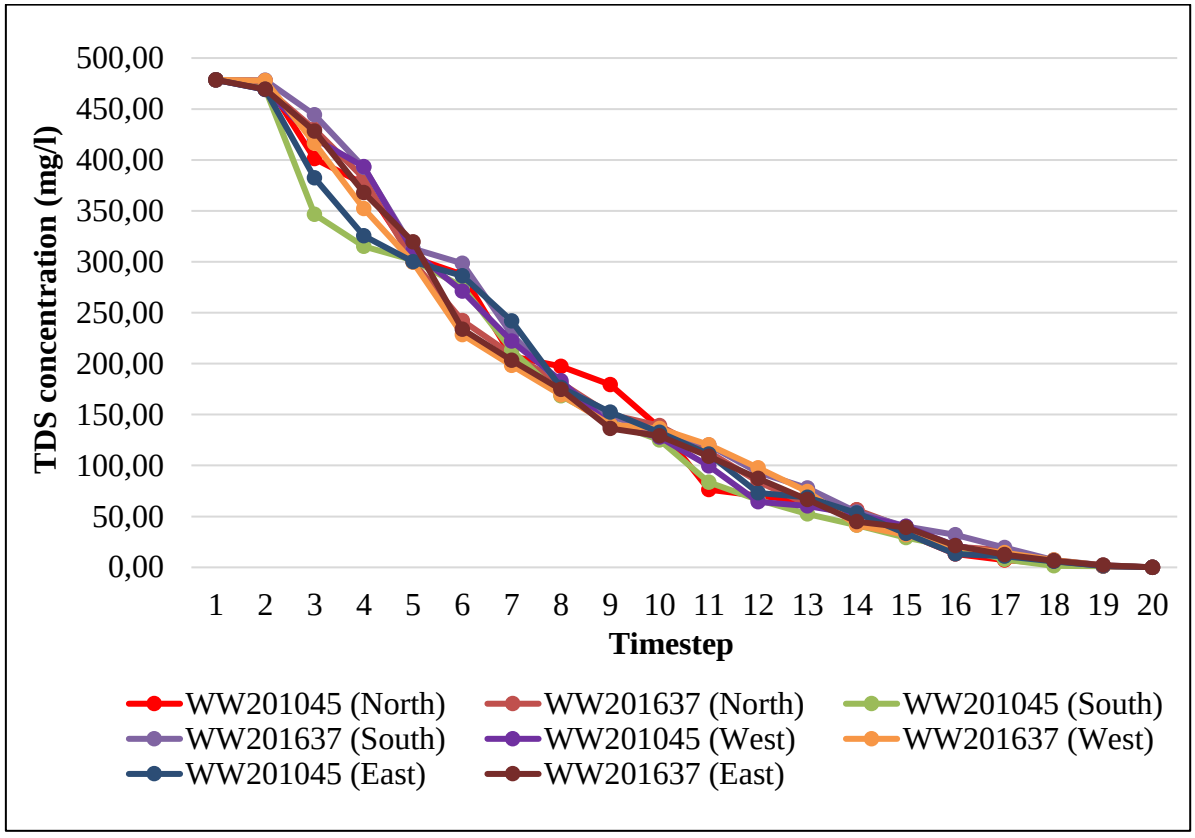

Figure 4.28: Total Dissolved Solids dispersion within the aquifer

The average concentration of Total Dissolved Solids for the simulated years was recorded to be 478.56 mg/l, and it was observed how it spreads in the four directions (North, South, west, and East) at the two injection wells (WW201045 and WW201637) within the aquifer. The dispersion trend shown in Figure 4.28 is the same in the four directions. However, the TDS

spreads faster in all directions at well WW201045 compared to well WW201637. This is shown by the lower concentration values at different timesteps of WW201045 compared to higher concentration values at WW201637. The location of the wells has an impact on the spread of the contaminants. The dispersion trend of Total Dissolved Solids indicates that as time increases, the contaminant (TDS) spreads further in the aquifer, and its concentration decreases as it spreads. The detailed tables of TDS dispersion in the four directions are presented in section 7.2.4 of the appendices (chapter 7).

The concentration of TDS at the last (20^{th}) timestep at all the two wells analysed is similar for all the wells. However, in other timesteps the concentrations vary. Both hydraulic conductivities in different aquifer layers, porosity of the aquifer areas of the well's locations, and transmissivity have an impact on the dispersion of TDS at all the timesteps. At both wells, the transmissivity of the aquifer allowed TDS to disperse through.

The distance travelled by dispersion of Total Dissolved Solids (TDS) at the different timesteps, at the two simulated wells is shown in Table 4.9.

Table 4.9: Distance travelled by dispersion of TDS at the different times within the aquifer

Timestep	TDS concentration (mg/l)		Distance travelled (km)	
	WW201045	WW201637	WW201045	WW201637
1	478,6	478,6	0,2	0,2
2	471,3	474,1	0,3	0,6
3	387,7	429,7	1,4	0,7
4	352,5	373,7	1,8	1,5
5	304,0	308,0	2,0	1,9
6	280,0	250,6	2,8	2,5
7	221,1	209,7	2,9	2,8
8	181,3	176,3	3,4	3,2
9	153,4	143,9	3,6	3,6
10	130,6	134,0	3,9	3,9
11	92,6	115,6	4,0	4,0
12	68,5	90,5	4,5	4,2
13	61,5	70,1	4,7	4,5
14	50,6	49,2	5,1	5,0
15	34,0	37,5	5,7	5,4
16	16,8	23,4	6,5	6,2
17	9,6	15,7	7,3	6,3
18	4,4	6,4	7,7	7,1
19	1,3	1,8	8,1	8,0
20	0,1	0,1	8,7	8,2

According to the dispersion of Total Dissolved Solids results presented in Table 4.9, it shows that TDS moves further into the aquifer reaching a distance of 8.7 km. The most travelled distance of 8.7 km was recorded at well WW201045, while the distance of TDS dispersion at well WW201637 was recorded to be 8.2 km, both of them at the last timestep (20). Similarly, to Chloride and Electrical Conductivity, TDS also dispersed for a long distance at WW201045 compared to WW201637.

4.3.1.4 Dispersion of *E-coli* within the aquifer

E - coli is another contaminant associated with runoff, and its migration within the Ohangwena aquifer system was simulated using the transient state model with 20-time steps. The simulation was done in such a way that, the runoff will be injected into the injection wells (WW201045 and WW201637), as described in Section 3.8, to recharge the aquifer.

E-coli in water is a strong indicator of sewage and animal waste contamination, which can contain many different types of disease-causing organisms. The consumption of a high concentration of *E-coli* beyond the recommended amount may result in severe illnesses. Therefore, the dispersion model of this contaminant is very important to see the extent to which it spreads, and make appropriate recommendations if pre-treatment is required.

The spread of this contaminant is shown in Figure 4.29 and Figures 4.30 and 4.31, which presents the spread of *E-coli* at the individual simulated wells.

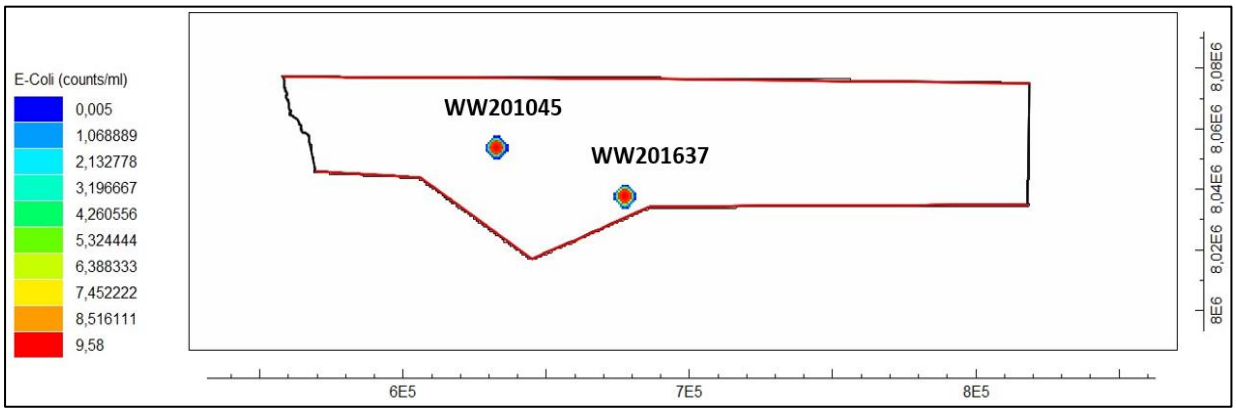

Figure 4.29: Dispersion of *E-coli* within the aquifer

According to Figure 4.29, *E-coli* disperses from the point source with a measured concentration of 9.58 counts/100 ml to 0.005 counts/100 ml, at the two simulated wells. The measured *E-coli* content of the surface runoff is 9.58 counts/100 ml, which falls within the acceptable content of *E-coli* in water in Namibia. The concentration of dispersion decreases as time increases in all three directions (North, South, West, and East). The dispersion of the *E-coli* within the aquifer at the two simulated wells (WW201045 and WW201637) is presented in Figures 4.30 and 4.31.

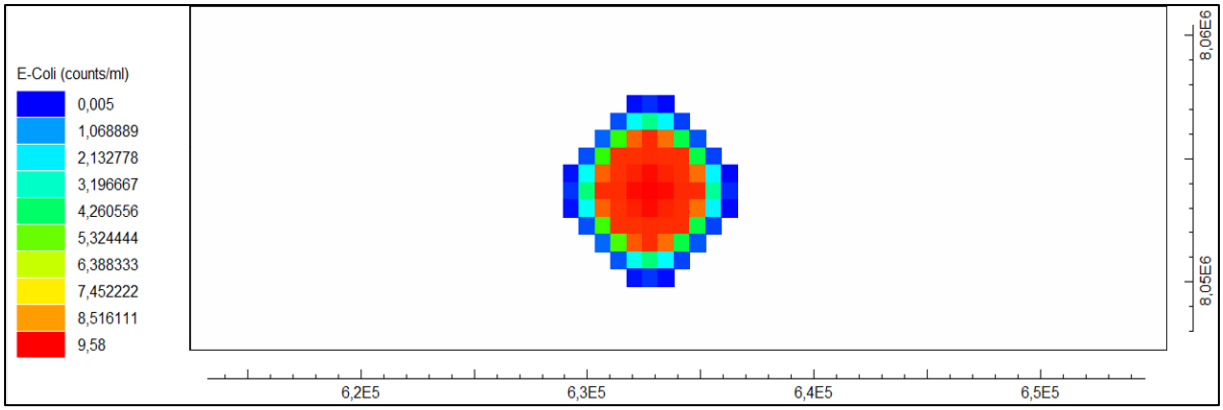

Figure 4.30: Dispersion of *E-coli* at WW201045

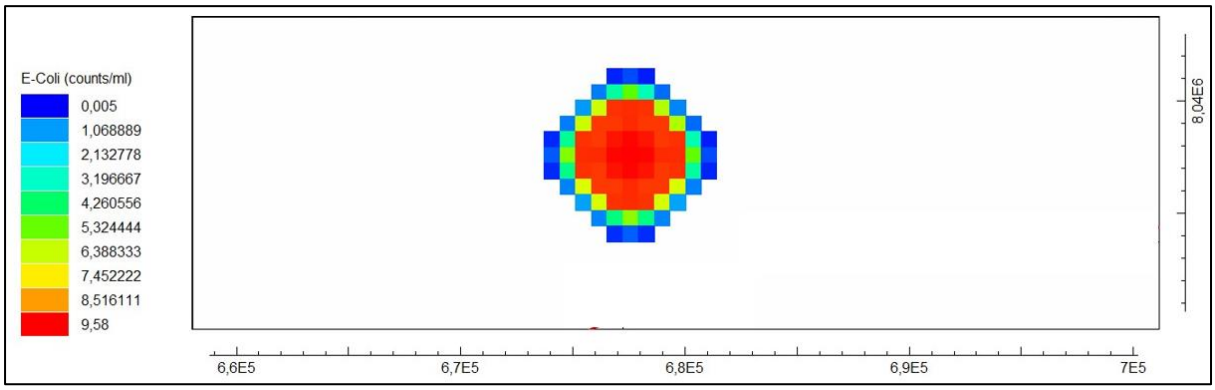

Figure 4.31: Dispersion of *E-coli* at WW201637

The results for the horizontal dispersion of *E-coli* in the four directions (North, South, West, and East) within the aquifer due to aquifer recharge are shown in Figure 4.32, and Tables 7.32 to 7.35 in section 7.2.4 of the appendices.

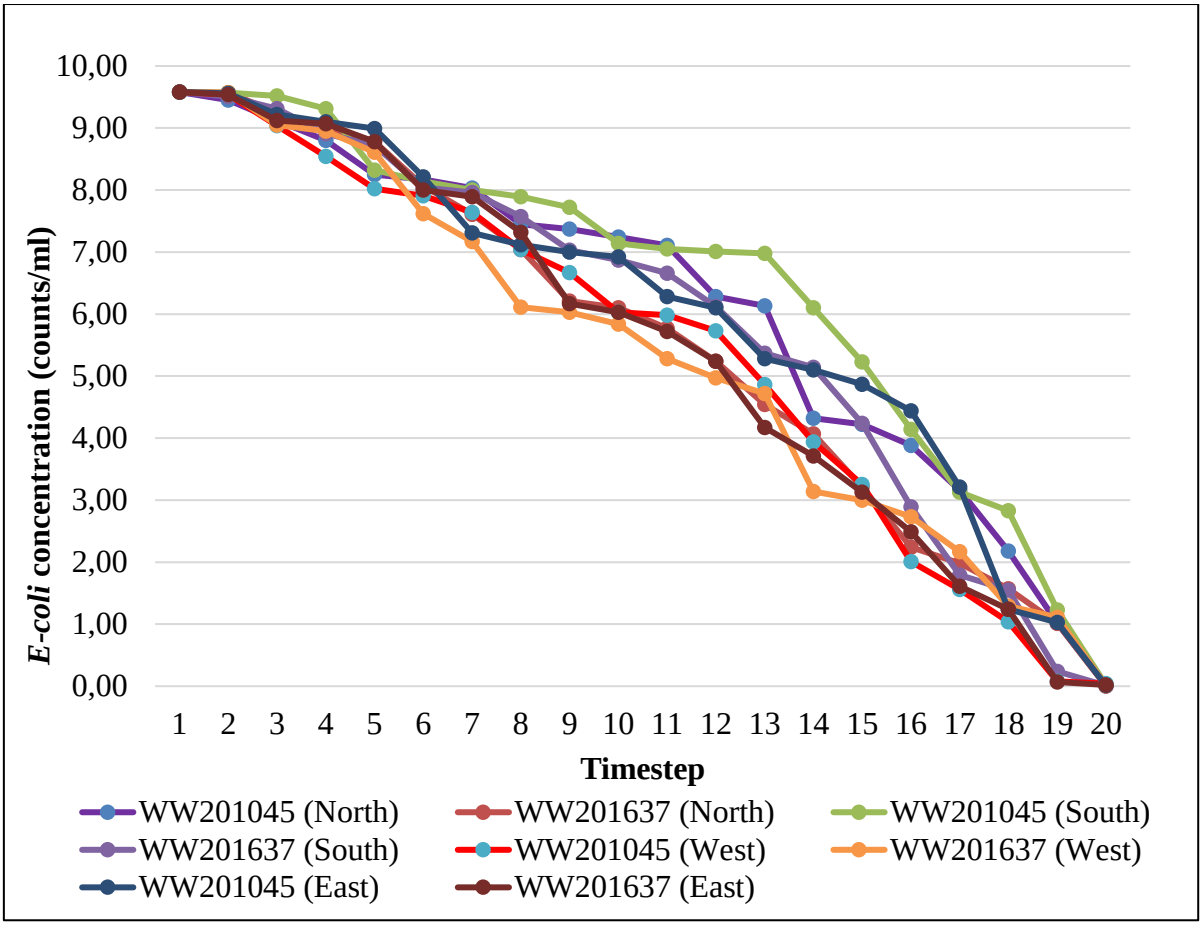

Figure 4.32: Dispersion of *E-coli* with the aquifer

The measured *E-coli* concentration present in runoff for the six simulated years was 9.58 counts/ml. This concentration was then observed how it spreads within the aquifer using a Contaminant transport model in MODFLOW. The results presented in Figure 4.32 shows that *E-coli* concentration disperses up to 0.01 counts/ml at the two simulated wells (WW201045 and WW201637).

According to Figure 4.32, *E-coli* spreads faster in the Western direction reaching 0.01 counts/ml at the 20th timestep at well WW201045 compared to other directions and well WW201637. Similarly, to the previously discussed contaminants (Chloride, Electrical Conductivity, and TDS), the dispersion of *E-coli* is much faster at well WW201045, than at well WW201637. This means that the location influences the dispersion of the contaminant. WW201045 is located in the middle of the region where the elevation is sloping downwards, which makes it easier for the contaminants to disperse, while well WW201637 is located upper the region where the elevation is flat and not sloping. The concentration of *E-coli* decreases as the timestep increases.

In comparison to Chloride, Electrical Conductivity, and Total Dissolved Solids, the aquifer characteristics of different hydraulic conductivities in the aquifer's layers, porosity of the aquifer at different locations (at the two assessed wells) and transmissivity of the aquifer

have an impact on the dispersion of E. coli. According to the simulation results, the transmissivity of the aquifer allows E. coli to disperse through it for all the timesteps analysed. The concentrations of the contaminant at the 20th timestep in all the two assessed wells is the same. However, in other timesteps the concentrations vary, which indicates that the hydraulic conductivities of the layers and porosity of the well location areas, have an impact on the dispersion of E. coli.

The distance travelled by dispersion of *E-coli* at different timesteps, at the two simulated wells is shown in Table 4.10.

Table 4.10: Distance travelled by dispersion of *E-coli* at different times within the aquifer

Timestep	*E-coli* concentration (counts/ml)		Distance travelled (km)	
	WW201045	WW201637	WW201045	WW201637
1	9,6	9,6	0,2	0,1
2	9,5	9,6	0,6	0,3
3	9,2	9,2	0,9	0,9
4	8,9	9,0	1,2	1,2
5	8,4	8,7	1,7	1,5
6	8,1	7,9	2,9	2,7
7	7,8	7,7	3,2	2,7
8	7,4	7,0	3,4	3,1
9	7,2	6,4	3,9	3,5
10	6,8	6,2	4,0	3,7
11	6,6	5,9	4,1	4,1
12	6,3	5,4	4,4	4,8
13	5,8	4,7	4,8	4,9
14	4,9	4,0	5,1	5,0
15	4,4	3,4	5,3	5,1
16	3,6	2,6	5,6	5,3
17	2,8	1,9	5,9	5,7
18	1,8	1,4	6,2	6,2
19	0,8	0,6	6,6	6,4
20	0,1	0,1	6,7	6,5

According to the results presented in Table 4.10, it is shown that *E-coli* disperses further into the aquifer covering a maximum distance of 6.7 km. The dispersion is faster at well WW201045 covering a distance of 6.7 km until the last timestep, compared to well WW201637 which covered a distance of 6.5 km until the last timestep.

4.4 Summary

In summary, the results of this study indicated that the Ohangwena region is characterized by high and very high groundwater recharge zones, making Aquifer Recharge to be most suitable in this area. About 85% of the region is characterized by a high potential groundwater recharge zone, while 25% is characterized by a very high groundwater recharge zone. The very high recharge zones are found on the central part of the region, and the far upper western side of the region.

The steady-state model results analysis of the impact of Aquifer Recharge on groundwater levels in Ohangwena region showed that there is a gradual increase in the groundwater levels brought by the recharge using runoff injected at the simulated wells. The increase is shown by the simulated hydraulic heads that are higher than the observed hydraulic heads. The results also showed that aquifer recharge in the region is high in the areas of very high groundwater recharge zones, where most ponds and water bodies are located.

The results of the analysis of the impact of Aquifer Recharge on groundwater levels simulated with a transient state model show a significant increase in the groundwater levels due to aquifer recharge compared to the steady-state model results. The simulated hydraulic heads of the transient state model are way too higher than the observed heads, which is an indication that there is a gradual increase in the groundwater levels, brought by the accumulated recharge for the six simulated years.

The runoff to be used for Aquifer Recharge is associated with contaminants, that are harmful to humans if they are consumed in high concentrations, exceeding the accepted concentrations. The dispersion simulation of the assessed contaminants (Chloride, Electrical Conductivity, *E-coli,* and Total Dissolved Solids) shows that as time increases, the concentration of the contaminants decreases in all the four directions (North, South, East, and West) as you move away from the point source (which in this case are the two simulated wells WW201045 and WW201637), and it takes time for the contaminants to disperse further into the aquifer. The dispersion of the contaminants is influenced by different hydraulic conductivities in the aquifer's layers, porosity of the aquifer at different areas where the simulated wells are located, and the transmissivity of the aquifer.

Among the assessed contaminants, Chloride disperses further into the aquifer covering a maximum distance of 12.1 km, Electrical Conductivity covers a maximum distance of 9.6 km, *E-coli* covers a maximum distance of 6.7 km, and Total Dissolved Solids cover a maximum distance of 8.7 km. All the maximum distances for all the four contaminants are recorded at well WW201045. The dispersion distances of contaminants at different timesteps at well WW201045 are higher than those WW201637.

5. Conclusion and recommendations

5.1 Conclusion

This study is vital for the long-term use of groundwater resources, thereby improving groundwater levels through proper management. The results of this study indicated that using the GIS technique for groundwater exploration helps to narrow down the target areas for conducting detailed hydrogeological surveys. The results also indicate that the very high groundwater recharge potential zones are located in the central part of the region, the north-western part of the region, and on the upper eastern side of the region. These zones are at the locations where there is a variety of water bodies in the region, which could be turned into infiltration basins for Aquifer Recharge technique to replenish the Ohangwena aquifer. Using the general hydrology characteristics of the Ohangwena region, this study establishes a relationship between groundwater recharge potential factors and the groundwater recharge potential scores. The maps produced in this study can serve as a preliminary guide for the government and water policymakers to select potential groundwater resources management sites.

The results of this study also demonstrated that the groundwater levels can be improved locally by infiltrating surface runoff into the KOH-II aquifer via the injection wells during the rainy season (November to April) when there is plenty of surface runoff and flood in the region. This was proved by the results of both the steady-state and transient state models, which showed that Aquifer Recharge with surface runoff increases the groundwater levels of the aquifer, at the simulated four boreholes. The transient state results which simulated Aquifer Recharge for six years in 20 times steps, showed that there is a huge impact of the recharge in the groundwater levels shown by the very high simulated heads in comparison to the observed head. The huge impact is also portrayed by the water budgets.

The high infiltration rates in the region due to the soil type which is mostly sandy to loam also makes Aquifer Recharge with surface runoff suitable in the Ohangwena region. The various water ponds and water bodies located in the areas with high soil infiltration rates, and very high groundwater recharge zones can be turned into infiltration basins that could be used to artificially recharge the aquifer.

Part of the study also assessed the transport of contaminants associated with surface runoff to be used as a water source for Aquifer Recharge. The assessment of this part of the study was done to observe how these contaminants disperse and spread out within the aquifer. The results of the four assessed contaminants portrayed that it takes time for these contaminants to disperse within the whole aquifer. As time increases, the concentration of the contaminants decreases in all four directions (North, South, East, and West) as you move away from the point source. The results mean if surface runoff is injected into the aquifer via the injection wells *i.e.*, on the western side of the region, these contaminants will take time to reach abstraction

boreholes in other sides of the region. The different hydraulic conductivities in each of the five simulated layers of the aquifer lower the dispersion of the contaminants. These contaminants also disperse further into the aquifer covering a large distance.

5.2 Recommendations

To implement the technique of using surface runoff for Aquifer Recharge in Ohangwena region. The following suggestions and recommendations have been made:

i. Further research should be carried out on assessing the AR technique (method) that is suitable for Ohangwena region, which will use surface runoff as the water source.

ii. Part of future research should also be to carry out this similar study on the other side of the national boundary (in Angola) as this is a transboundary aquifer shared by Namibia and Angola, and study if it influences Ohangwena results.

iii. Research assessing the impact of surface runoff quality on groundwater should also be carried out, to see if the runoff decreases or increases the groundwater-specific concentrations. This is to make sure that runoff is safe to use for Aquifer recharge, or it will require to be pre-treated first before recharging it in the aquifer.

iv. Community awareness needs to be made, to reduce and avoid polluting the surface water sources, and drainage channels. This will reduce the costs involved in pre-treating the surface runoff before it is banked in the aquifer.

6. References

Achu, A. L., Reghunath, R., & Thomas, J. (2020). Mapping of Groundwater Recharge Potential Zones and Identification of Suitable Site-Specific Recharge Mechanisms in a Tropical River Basin. *Earth Systems and Environment*, *4*(1), 131–145. https://doi.org/10.1007/s41748-019-00138-5

Alaa, A., Abdullah, A., & Abdulaziz, A. (2021). Identification of Groundwater Potential Recharge Zones in Flinders Ranges, South Australia using Remote Sensing, GIS, and MIF techniques. *Multidisciplinary Digital Publishing Institute*, *13*(2571). https://doi.org/10.3390/w13182571

Alam, S., Borthakur, A., Ravi, S., Gebremichael, M., & Mohanty, S. K. (2021a). Managed aquifer recharge implementation criteria to achieve water sustainability. *Science of the Total Environment*, *768*, 144992. https://doi.org/10.1016/j.scitotenv.2021.144992

Alam, S., Borthakur, A., Ravi, S., Gebremichael, M., & Mohanty, S. K. (2021b). Managed aquifer recharge implementation criteria to achieve water sustainability. *Science of the Total Environment*, *768*(144992). https://doi.org/10.1016/j.scitotenv.2021.144992

Altchenko, Y., & Villholth, K. G. (2013). Transboundary aquifer mapping and management in Africa: A harmonised approach. *Hydrogeology Journal*, *21*(7), 1497–1517. https://doi.org/10.1007/s10040-013-1002-3

Anthony, J. J., Olivier, B., Randall, J. H., Jean, D. R., & Andrew, R. (2016). *Intergrated Groundwater management; concepts, approaches and challenges*. https://doi.org/10.1007/978-3-319-23576-9_24

Aryanto, D. E., & Hardiman, G. (2018). Assessment of groundwater recharge potential zone using GIS approach in Purworejo regency, Central Java province, Indonesia. *E3S Web of Conferences*, *31*. https://doi.org/10.1051/e3sconf/20183112002

Asmael, N. M., Dupuy, A., Huneau, F., Hamid, S., & Le Coustumer, P. (2015). Groundwater modeling as an alternative approach to limited data in the northeastern part of Mt. Hermon (Syria), to develop a preliminary water budget. *Water (Switzerland)*, *7*(7), 3978–3996. https://doi.org/10.3390/w7073978

Beganskas, S., & Fisher, A. T. (2017). Coupling distributed stormwater collection and managed aquifer recharge: Field application and implications. *Journal of Environmental Management*, *200*(September), 366–379. https://doi.org/10.1016/j.jenvman.2017.05.058

Behroozmand, A. A., Auken, E., & Knight, R. (2019). Assessment of Managed Aquifer Recharge Sites Using a New Geophysical Imaging Method. *Vadose Zone Journal*, *18*(1), 1–13. https://doi.org/10.2136/vzj2018.10.0184

Chenini, I., & Ben , Mammou, A. (2010). Groundwater recharge study in arid region: An approach using GIS techniques and numerical modeling. *Computers and Geosciences*, *36*(6), 801–817. https://doi.org/10.1016/j.cageo.2009.06.014

Chenini, I., Msaddek, M. H., & Dlala, M. (2019). Hydrogeological characterization and aquifer recharge mapping for groundwater resources management using multicriteria analysis and numerical modeling: A case study from Tunisia. *Journal of African Earth Sciences*, *154*(February), 59–69. https://doi.org/10.1016/j.jafrearsci.2019.02.031

Chitsazan, M., Nozarpour, L., & Movahedian, A. (2018). Impact of artificial recharge on groundwater recharge estimated by groundwater modeling (case study: Jarmeh flood spreading, Iran). *Sustainable Water Resources Management*, *4*(1), 79–89. https://doi.org/10.1007/s40899-017-0126-3

David, A. (2013). Groundwater recharge estimation for perched aquifers in the Ohangwena

Region based on soil water balance modeling and chloride mass balance. In *Journal of Chemical Information and Modeling*.

Department of Water Affairs (The republic of Namibia). (1994). *Water Supply and Sanitation Project in Ohangwena region, Namibia* (Issue 1).

Díaz-Cruz, M. S., & Barceló, D. (2018). Trace organic chemicals contamination in ground water recharge. *Chemosphere*, *72*(3), 333–342. https://doi.org/10.1016/j.chemosphere.2008.02.031

Dierkes, K. (2011). *Groundwater investigation of the cuvelai- etosha basin*. 10.

Dillon, P., Pavelic, P., Page, D., Helen, B., & Ward, J. (2009). Managed aquifer recharge. In *National water commission* (Vol. 13). https://doi.org/10.1007/BF01929660

Ebrahim, G. Y., Fathi, S., Lautze, J., Ansems, N., Villholth, K. G., Nijsten, G.-J., Magombey, M., Mndaweni, S., Kenabatho, P., Moehadu, M., Keodumetse, K., Gomo, M., Somolekae, B., Nkile, C., & Kealeboga, D. (2017). *Review of Managed Aquifer Recharge (MAR) Experience in Africa and MAR Suitability Mapping for Ramotswa Transboundary Aquifer Area*. *44*, 56. http://conjunctivecooperation.iwmi.org/wp-content/uploads/sites/38/2019/02/Review-of-MAR-experience-in-Africa.pdf

Ebrahim, G. Y., Lautze, J. F., & Villholth, K. G. (2020). Managed aquifer recharge in Africa: Taking stock and looking forward. *Water (Switzerland)*, *12*(7). https://doi.org/10.3390/W12071844

Fagbohun, B. J. (2018). Integrating GIS and multi-influencing factor technique for delineation of potential groundwater recharge zones in parts of Ilesha schist belt, southwestern Nigeria. *Environmental Earth Sciences*, *77*(3), 1–18. https://doi.org/10.1007/s12665-018-7229-5

Faures, J.-M., Hoogeveen, J., Winpenny, J., Steduto, P., & Burke, J. (2012). Coping with water scarcity: An action framework for agriculture and food security. In *FAO Water Reports* (38th ed.). https://doi.org/10.1097/00010694-199203000-00010

Glass, J., Via Rico, D. A., Stefan, C., & Nga, T. T. V. (2018). Simulation of the impact of managed aquifer recharge on the groundwater system in Hanoi, Vietnam. *Hydrogeology Journal*, *26*(7), 2427–2442. https://doi.org/10.1007/s10040-018-1779-1

Grützmacher, G., & Sajil Kumar, P. J. (2012). *Introduction to Managed Aquifer Recharge (MAR) – Overview of schemes and settings world wide*. *April*, 1–11.

Harbaugh, A. W., Banta, E. R., Hill, M. C., Mcdonald, M. G., Groat, C. G., Harbaugh, B. A. W., Banta, E. R., Hill, M. C., & Mcdonald, M. G. (2000). Modflow-2000 , the U.S. Geological Survey Modular Ground-Water Model User Guide To Modularization Concepts and the Ground-Water Flow Process, Tech. Rep. 00-92. In *U.S. Geological Survey*. https://pubs.usgs.gov/of/2000/0092/report.pdf%0Ahttp://www.gama-geo.hu/kb/download/ofr00-92.pdf%0Ahttp://doi.wiley.com/10.1029/2006WR005839

Inamdar, P. M., Cook, S., Sharma, A. K., Corby, N., O'Connor, J., & Perera, B. J. C. (2013). A GIS based screening tool for locating and ranking of suitable stormwater harvesting sites in urban areas. *Journal of Environmental Management*, *128*, 363–370. https://doi.org/10.1016/j.jenvman.2013.05.023

Izady, A., Davary, K., Alizadeh, A., Ziaei, A. N., Akhavan, S., Alipoor, A., Joodavi, A., & Brusseau, M. L. (2015). Groundwater conceptualization and modeling using distributed SWAT-based recharge for the semi-arid agricultural Neishaboor plain, Iran. *Hydrogeology Journal*, *23*(1), 47–68. https://doi.org/10.1007/s10040-014-1219-9

Jakeman, A. J., Barreteau, O., Hunt, R. J., Rinaudo, J. D., & Ross, A. (2016). Integrated groundwater management: Concepts, approaches and challenges. In *Integrated Groundwater Management: Concepts, Approaches and Challenges* (pp. 1–762).

https://doi.org/10.1007/978-3-319-23576-9

Jasrotia, A. S., Kumar, R., Taloor, A. K., & Saraf, A. K. (2019). Artificial recharge to groundwater using geospatial and groundwater modelling techniques in North Western Himalaya, India. *Arabian Journal of Geosciences*, *12*(24). https://doi.org/10.1007/s12517-019-4855-5

Jovanovic, N., Bugan, R. D. H., Tredoux, G., Israel, S., Bishop, R., & Marinus, V. (2017). Hydrogeological modelling of the atlantis aquifer for management support to the atlantis water supply scheme. *Water SA*, *43*(1), 122–138. https://doi.org/10.4314/wsa.v43i1.15

Khadri, S. F. R., & Pande, C. (2016). Ground water flow modeling for calibrating steady state using MODFLOW software: a case study of Mahesh River basin, India. *Modeling Earth Systems and Environment*, *2*(1), 1–17. https://doi.org/10.1007/s40808-015-0049-7

Kumar, C. . (2003). Introduction to Groundwater Modelling. In *Read* (Vol. 247667).

Kumar, C. P. (2019). An Overview of Commonly Used Groundwater Modelling Software. *International Journal of AdvancedResearch in Science, Engineering and Technology*, *6*(1), 7854–7865. www.ijarset.com

Lachaal, F., Mlayah, A., Bédir, M., Tarhouni, J., & Leduc, C. (2012). Implementation of a 3-D groundwater flow model in a semi-arid region using MODFLOW and GIS tools: The Zéramdine-Béni Hassen Miocene aquifer system (east-central Tunisia). *Computers and Geosciences*, *48*, 187–198. https://doi.org/10.1016/j.cageo.2012.05.007

Lindenmaier, F., Miller, R., Fenner, J., Christelis, G., Dill, H. G., Himmelsbach, T., Kaufhold, S., Lohe, C., Quinger, M., Schildknecht, F., Symons, G., Walzer, A., & van Wyk, B. (2014). Structure and genesis of the Cubango Megafan in northern Namibia: Implications of its hydrogeology. *Hydrogeology Journal*, *22*(6), 1307–1328. https://doi.org/10.1007/s10040-014-1141-1

Liu, J., Yang, H., Gosling, S. N., Kummu, M., Flörke, M., Pfister, S., Hanasaki, N., Wada, Y., Zhang, X., Zheng, C., Alcamo, J., & Oki, T. (2017). Water scarcity assessments in the past, present, and future. *Earth's Future*, *5*(6), 545–559. https://doi.org/10.1002/2016EF000518

Luthy, R. G., Sharvelle, S., & Dillon, P. (2019). Urban Stormwater to Enhance Water Supply. *Environmental Science and Technology*, *53*(10), 5534–5542. https://doi.org/10.1021/acs.est.8b05913

Masule, L. N. (2019). *AGE DATING OF GROUNDWATER IN PERCHED AQUIFERS OKONGO AREA , OHANGWENA REGION* (Issue September).

Ministry of Agriculture, W. (1990). *Namibian water act of 1956* (Vol. 4, Issue 1).

Murray, E. C., & Tredoux, G. (1998). *Artificial Recharge A Technology for Sustainable Water Resources Development*. *842/1/98*. http://www.wrc.org.za/wp-content/uploads/mdocs/842-1-98.pdf

Murray, E. C., & Tredoux, G. (2004). Planning Water Resource Management: The case for managing aquifer recharge. *Proceedings of the 2004 Water Institute of Southern Africa (WISA) Biennial Conference, February*, 430–437.

Murray, R. (2004). *Wise water management for towns and cities - Artificial groundwater recharge*.

Murray, R., Louw, D., van der Merwe, B., & Peters, I. (2018). Windhoek, Namibia: from conceptualising to operating and expanding a MAR scheme in a fractured quartzite aquifer for the city's water security. *Sustainable Water Resources Management*, *4*(2), 217–223. https://doi.org/10.1007/s40899-018-0213-0

Namibia Statistics Agency. (2014). 2011 Population and Housing Census - Ohangwena

Regional Profile. In *Namibia Statistics Agency*.

Page, D., Bekele, E., Vanderzalm, J., & Sidhu, J. (2018). Managed aquifer recharge (MAR) in sustainable urban water management. *Water (Switzerland)*, *10*(239), 1–16. https://doi.org/10.3390/w10030239

Reddy, K. R. (2008). Enhanced Aquifer Recharge. In *Overexploitation and Contamination of Shared Groundwater Resources* (pp. 275–288). https://doi.org/10.1007/978-1-4020-6985-7_13

Ross, A., & Hasnain, S. (2018). Factors affecting the cost of managed aquifer recharge (MAR) schemes. *Sustainable Water Resources Management*, *4*(2), 179–190. https://doi.org/10.1007/s40899-017-0210-8

Russo, T. A., Fisher, A. T., & Lockwood, B. S. (2015). Assessment of managed aquifer recharge site suitability using a GIS and modeling. *Groundwater*, *53*(3), 389–400. https://doi.org/10.1111/gwat.12213

Sallwey, J., Schlick, R., Valverde, J. P. B., Junghanns, R., López, F. V., & Stefan, C. (2019). Suitability mapping for managed aquifer recharge: Development of web-tools. *Water (Switzerland)*, *11*(11). https://doi.org/10.3390/w11112254

Sharma, P. K., Mayank, M., Ojha, C. S. P., & Shukla, S. K. (2020). A review on groundwater contaminant transport and remediation. *ISH Journal of Hydraulic Engineering*, *26*(1), 112–121. https://doi.org/10.1080/09715010.2018.1438213

Singh, Ajay, Panda, S. N., Uzokwe, V. N. E., & Krause, P. (2019). An assessment of groundwater recharge estimation techniques for sustainable resource management. *Groundwater for Sustainable Development*, *9*(100218). https://doi.org/10.1016/j.gsd.2019.100218

Singh, Amanpreet, Panda, S. N., Kumar, K. S., & Sharma, C. S. (2013). Artificial groundwater recharge zones mapping using remote sensing and gis: A case study in Indian Punjab. *Environmental Management*, *52*(1), 61–71. https://doi.org/10.1007/s00267-013-0101-1

Sorensen, P. (2013). The massive Ohangwena II aquifer in northern Namibia. *International Journal of Environmental Studies*, *70*(2), 173–174. https://doi.org/10.1080/00207233.2013.779149

Steinel, A., Schelkes, K., Subah, A., & Himmelsbach, T. (2016). Spatial multi-criteria analysis for selecting potential sites for aquifer recharge via harvesting and infiltration of surface runoff in north Jordan. *Hydrogeology Journal*, *24*(7), 1753–1774. https://doi.org/10.1007/s10040-016-1427-6

Wallner, M., Houben, G., Lohe, C., Quinger, M., & Himmelsbach, T. (2017). Inverse modeling and uncertainty analysis of potential groundwater recharge to the confines semi-fossil Ohangwena II Aquifer, Namibia. *Hydrogeology Journal*, *25*(8), 2303–2321. https://doi.org/10.1007/s10040-017-1615-z

Yeh, H. F., Cheng, Y. S., Lin, H. I., & Lee, C. H. (2016). Mapping groundwater recharge potential zone using a GIS approach in Hualian River, Taiwan. *Sustainable Environment Research*, *26*(1), 33–43. https://doi.org/10.1016/j.serj.2015.09.005

Zhang, H., Xu, Y., & Kanyerere, T. (2019). Site assessment for MAR through GIS and modeling in West Coast, South Africa. *Water (Switzerland)*, *11*(8). https://doi.org/10.3390/w11081646

Zulfiqar, A., Arshad, A., Gulraiz, A., & Iftikhar, A. (2013). Groundwater and Contaminant Hydrology. *Intech*, 13. https://doi.org/10.5772/54732

7. Appendices

7.1 Impact of recharge on groundwater levels (transient state model)

This chapter presents additional results, of water budgets of the transient state model for assessing the impact of aquifer recharge using runoff on groundwater levels, for the time-steps from one to 19. The water budgets are shown in Tables 7.1 to 7.19.

Table 7.1: Water budget for the first timestep (transient state)

Item	In (m^3/s)	Out (m^3/s)
Storage	198,4	76,6
Constant head	4,9	11,2
Drains	0,0	0,7
Evapotranspiration	0,0	84,9
Head dep bound	1,1	31,9
Recharge	1,0	0,0
Total	205,4	205,4
In-Out	$5{,}0354\times10^{3}$	
% Discrepancy	0,0%	

Table 7.2: Water budget for the 2nd timestep

Item	In (m^3/s)	Out (m^3/s)
Storage	134,7	38,9
Constant head	6,1	10,2
Drains	0,0	0,8
Evapotranspiration	0,0	54,8
Head dep bound	1,5	38,6
Recharge	1,0	0,0
Total	143,3	143,3
In-Out	$3{,}3875\times10^{3}$	
% Discrepancy	0,0%	

Table 7.3: Water budget for the 3rd timestep

Item	In (m^3/s)	Out (m^3/s)
Storage	113,8	26,9
Constant head	6,6	9,8
Drains	0,0	0,8
Evapotranspiration	0,0	45,3
Head dep bound	1,7	40,4
Recharge	1,0	0,0
Total	123,1	123,1
In-Out	$2{,}8305\times10^3$	
% Discrepancy	0,0%	

Table 7.4: Water budget for the 4th timestep

Item	In (m^3/s)	Out (m^3/s)
Storage	103,4	20,9
Constant head	6,9	9,6
Drains	0,0	0,7
Evapotranspiration	0,0	40,9
Head dep bound	1,8	41,1
Recharge	1,0	0,0
Total	113,2	113,2
In-Out	$2{,}5558\times10^3$	
% Discrepancy	0,0%	

Table 7.5: Water budget for the 5th timestep

Item	In (m^3/s)	Out (m^3/s)
Storage	96,3	16,5
Constant head	7,1	9,5
Drains	0,0	0,7
Evapotranspiration	0,0	38,2
Head dep bound	1,9	41,4
Recharge	1,0	0,0
Total	106,3	106,3
In-Out	$2{,}4109\times10^3$	
% Discrepancy	0,0	

Table 7.6: Water budget for the 6th timestep

Item	In (m^3/s)	Out (m^3/s)
Storage	90,8	13,2
Constant head	7,3	9,4
Drains	0,0	0,7
Evapotranspiration	0,0	36,4
Head dep bound	2,0	41,5
Recharge	1,0	0,0
Total	101,1	101,1
In-Out	$2{,}2888\times10^{3}$	
% Discrepancy	0,0%	

Table 7.7: Water budget for the 7th timestep

Item	In (m^3/s)	Out (m^3/s)
Storage	86,5	10,7
Constant head	7,4	9,3
Drains	0,0	0,7
Evapotranspiration	0,0	34,8
Head dep bound	2,1	41,4
Recharge	1,0	0,0
Total	97,0	97,0
In-Out	$2{,}2049\times10^{3}$	
% Discrepancy	0,0%	

Table 7.8: Water budget for the 8th timestep

Item	In (m^3/s)	Out (m^3/s)
Storage	82,9	8,9
Constant head	7,5	9,2
Drains	0,0	0,7
Evapotranspiration	0,0	33,6
Head dep bound	2,2	41,3
Recharge	1,0	0,0
Total	93,6	93,6
In-Out	$2{,}1133\times10^{3}$	
% Discrepancy	0,0%	

Table 7.9: Water budget for the 9th timestep

Item	In (m^3/s)	Out (m^3/s)
Storage	79,9	7,5
Constant head	7,6	9,1
Drains	0,0	0,7
Evapotranspiration	0,0	32,4
Head dep bound	2,2	41,0
Recharge	1,0	0,0
Total	90,7	90,7
In-Out	$2{,}0523\times10^3$	
% Discrepancy	0,0%	

Table 7.10: Water budget for the 10th timestep

Item	In (m^3/s)	Out (m^3/s)
Storage	77,2	6,4
Constant head	7,7	9,1
Drains	0,0	0,6
Evapotranspiration	0,0	31,3
Head dep bound	2,3	40,7
Recharge	1,0	0,0
Total	88,2	88,2
In-Out	$1{,}9836\times10^3$	
% Discrepancy	0,0%	

Table 7.11: Water budget for the 11th timestep

Item	In (m^3/s)	Out (m^3/s)
Storage	74,9	5,7
Constant head	7,8	9,0
Drains	0,0	0,6
Evapotranspiration	0,0	30,3
Head dep bound	2,3	40,3
Recharge	1,0	0,0
Total	86,0	86,0
In-Out	$1{,}9150\times10^3$	
% Discrepancy	0,0%	

Table 7.12: Water budget for the 12th timestep

Item	In (m^3/s)	Out (m^3/s)
Storage	73,0	5,3
Constant head	7,9	9,0
Drains	0,0	0,6
Evapotranspiration	0,0	29,4
Head dep bound	2,4	39,9
Recharge	1,0	0,0
Total	84,2	84,2
In-Out	$1{,}8539\times10^3$	
% Discrepancy	0,0%	

Table 7.13: Water budget for the 13th timestep

Item	In (m^3/s)	Out (m^3/s)
Storage	71,2	5,0
Constant head	8,0	8,9
Drains	0,0	0,6
Evapotranspiration	0,0	28,6
Head dep bound	2,4	39,5
Recharge	1,0	0,0
Total	82,6	82,6
In-Out	$1{,}8005\times10^3$	
% Discrepancy	0,0%	

Table 7.14: Water budget for the 14th timestep

Item	In (m^3/s)	Out (m^3/s)
Storage	69,5	4,8
Constant head	8,0	8,9
Drains	0,0	0,6
Evapotranspiration	0,0	27,7
Head dep bound	2,4	39,0
Recharge	1,0	0,0
Total	81,0	81,0
In-Out	$1{,}7548\times10^3$	
% Discrepancy	0,0%	

Table 7.15: Water budget for the 15th timestep

Item	In (m^3/s)	Out (m^3/s)
Storage	67,9	4,5
Constant head	8,1	8,9
Drains	0,0	0,6
Evapotranspiration	0,0	26,6
Head dep bound	2,5	38,6
Recharge	1,0	0,0
Total	79,5	79,5
In-Out	$1{,}7166\times10^3$	
% Discrepancy	0,0%	

Table 7.16: Water budget for the 16th timestep

Item	In (m^3/s)	Out (m^3/s)
Storage	66,4	4,3
Constant head	8,2	8,8
Drains	0,0	0,6
Evapotranspiration	0,0	26,3
Head dep bound	2,5	38,1
Recharge	1,0	0,0
Total	78,1	78,1
In-Out	$1{,}6556\times10^3$	
% Discrepancy	0,0%	

Table 7.17: Water budget for the 17th timestep

Item	In (m^3/s)	Out (m^3/s)
Storage	64,9	4,1
Constant head	8,2	8,8
Drains	0,0	0,6
Evapotranspiration	0,0	25,6
Head dep bound	2,6	37,6
Recharge	1,0	0,0
Total	76,7	76,7
In-Out	$1{,}6327\times10^3$	
% Discrepancy	0,0%	

Table 7.18: Water budget for the 18th timestep

Item	In (m^3/s)	Out (m^3/s)
Storage	63,5	4,0
Constant head	8,3	8,8
Drains	0,0	0,6
Evapotranspiration	0,0	24,9
Head dep bound	2,6	37,2
Recharge	1,0	0,0
Total	75,4	75,4
In-Out	$1{,}5793\times10^3$	
% Discrepancy	0,0%	

Table 7.19: Water budget for the 19th timestep

Item	In (m^3/s)	Out (m^3/s)
Storage	62,2	3,8
Constant head	8,4	8,8
Drains	0,0	0,5
Evapotranspiration	0,0	24,3
Head dep bound	2,6	36,8
Recharge	1,0	0,0
Total	74,2	74,2
In-Out	$1{,}5411\times10^3$	
% Discrepancy	0,0%	

7.2 Contaminants dispersion within the aquifer

7.2.1 Chloride dispersion within the aquifer

This section presents additional results, of chloride's dispersion within the aquifer as a runoff contaminant, and they are presented from Tables 7.20 to 7.23.

Table 7.20: Chloride dispersion in the Northern direction within the aquifer

	Chloride Concentration (mg)	
Timestep	**Well 1 (WW201045)**	**Well 2 (WW201637)**
1	1000,0	1000,0
2	999,9	999,9
3	999,8	999,7
4	955,5	995,1
5	861,1	932,9
6	723,1	731,8
7	649,3	700,9
8	558,2	617,9
9	403,9	455,9
10	373,3	223,4
11	311,8	216,7
12	292,8	107,7
13	261,5	105,1
14	190,5	67,2
15	159,6	47.0
16	130,1	29,7
17	56,1	9,7
18	39,5	8,7
19	8,2	0,2
20	1,1	0,1

Table 7.21: Chloride dispersion in the Southern direction within the aquifer

	Chloride Concentration (mg)	
Timestep	**Well 1 (WW201045)**	**Well 2 (WW201637)**
1	1000,0	1000,0
2	999,8	999,9
3	975,5	999,8
4	963,1	914,4
5	890,5	813,0
6	668,3	786,7
7	601,9	774,8
8	580,2	706,0
9	559,3	562,0
10	413,8	482,0
11	353,5	304,5
12	201,3	180,7
13	164,0	158,4
14	132,2	130,0
15	112,0	97,7
16	59,8	24,3
17	42,0	15,6
18	38,6	2,9
19	3,7	0,2
20	0,5	0,1

Table 7.22: Chloride dispersion in the Western direction within the aquifer

	Chloride Concentration (mg)	
Timestep	**Well 1 (WW201045)**	**Well 2 (WW201637)**
1	1000,0	1000,0
2	999,9	999,9
3	968,2	996,9
4	893,8	782,6
5	887,0	713,1
6	670,6	650,3
7	565,3	475,8
8	404,1	280,8
9	332,5	229,4
10	205,0	211,2
11	188,1	174,6
12	179,6	156,1
13	133,3	111,0
14	62,9	74,0
15	55,4	28,8
16	43,4	19,2
17	38,0	16,6
18	9,7	7,1
19	7,5	0,8
20	0,2	0,1

Table 7.23: Chloride dispersion in the Eastern direction within the aquifer

	Chloride Concentration (mg)	
Timestep	**Well 1 (WW201045)**	**Well 2 (WW201637)**
1	1000,0	1000,0
2	999,9	999,6
3	979,4	973,3
4	970,6	967,3
5	964,8	951,1
6	919,5	859,9
7	821,6	695,5
8	710,1	588,3
9	562,5	572,1
10	520,9	209,8
11	466,2	147,5
12	314,6	136,0
13	240,3	115,5
14	127,7	100,0
15	108,5	54,2
16	74,8	40,3
17	23,8	6,9
18	16,6	1,8
19	1,5	0,3
20	0,4	0,1

7.2.2 Electrical conductivity dispersion within the aquifer

This section presents additional results, of electrical conductivity's dispersion as a contaminant within the aquifer. These results are shown in Tables 7.24 to 7.27.

Table 7.24: Dispersion of EC in the Northern direction within the aquifer

	Electrical conductivity (mS/s)	
Timestep	**Well 1 (WW201045)**	**Well 2 (WW201637)**
1	532,0	532,0
2	531,8	531,9
3	510,3	511,3
4	473,8	445,9
5	461,8	372,4
6	325,9	328,2
7	292,0	286,8
8	203,8	241,8
9	144,0	193,7
10	104,2	172,5
11	92,9	114,9
12	72,0	90,3
13	67,1	82,2
14	31,5	57,3
15	26,2	35,4
16	22,1	15,8
17	13,6	4,6
18	8,5	2,5
19	4,8	0,2
20	0,1	0,1

Table 7.25: Dispersion of EC in the Southern direction within the aquifer

	Electrical Conductivity (mS/s)	
Timestep	**Well 1 (WW201045)**	**Well 2 (WW201637)**
1	532,0	532,0
2	517,3	531,9
3	502,9	497,3
4	469,5	418,9
5	346,5	376,2
6	315,1	312,9
7	275,3	310,6
8	213,1	308,3
9	168,3	256,9
10	142,5	219,1
11	125,1	162,5
12	83,6	96,5
13	66,3	84,5
14	57,2	69,5
15	29,0	52,2
16	19,6	13,0
17	7,8	5,6
18	3,9	4,4
19	1,6	1,6
20	0,2	0,1

Table 7.26: Dispersion of EC in the Western direction within the aquifer

	Electrical Conductivity (mS/s)	
Timestep	**Well 1 (WW201045)**	**Well 2 (WW201637)**
1	532,0	532,0
2	514,8	500,6
3	472,5	437,3
4	418,1	413,7
5	346,8	393,9
6	329,9	378,5
7	300,6	344,6
8	218,6	289,4
9	192,3	251,9
10	170,2	164,7
11	166,9	143,9
12	101,1	111,6
13	93,9	92,0
14	71,7	38,8
15	63,7	23,7
16	37,0	15,2
17	31,4	8,6
18	20,2	1,4
19	4,2	0,2
20	0,2	0,1

Table 7.27: Dispersion of EC in the Eastern direction within the aquifer

	Electrical Conductivity (mS/s)	
Timestep	**Well 1 (WW201045)**	**Well 2 (WW201637)**
1	532,0	532,0
2	522,7	517,9
3	490,1	506,1
4	440,8	469,7
5	431,5	457,6
6	383,0	370,2
7	304,3	313,4
8	251,6	300,4
9	245,8	213,7
10	162,2	196,6
11	132,2	111,8
12	71,0	78,7
13	59,4	72,6
14	43,0	61,6
15	40,7	53,5
16	21,2	28,9
17	15,2	21,5
18	12,9	17,1
19	9,8	3,7
20	0,2	0,6

7.2.3 Dispersion of Total Dissolved Solids within the aquifer

This section presents additional results, of Total Dissolved Solid's dispersion as a contaminant within the aquifer. These results are shown in Tables 7.28 to 7.31.

Table 7.28: Dispersion of TDS in the Northern direction within the aquifer

	Total Dissolved Solids Concentration (mg/l)	
Timestep	**Well 1 (WW201045)**	**Well 2 (WW201637)**
1	478,6	478,6
2	477,6	471,2
3	401,2	430,2
4	376,2	382,0
5	304,1	300,1
6	287,3	242,1
7	207,3	209,0
8	197,2	181,2
9	179,2	150,2
10	137,2	139,0
11	76,4	113,2
12	70,3	83,9
13	64,7	61,7
14	56,1	56,3
15	33,3	38,4
16	13,1	20,4
17	7,2	16,7
18	3,9	5,0
19	1,3	1,3
20	0,0	0,0

Table 7.29: Dispersion of TDS in the Southern direction within the aquifer

Timestep	Total Dissolved Solids Concentration (mg/l)	
	Well 1 (WW201045)	Well 2 (WW201637)
1	478,56	478,56
2	469,53	478,00
3	346,46	444,10
4	315,10	392,65
5	301,41	312,99
6	275,34	298,35
7	213,19	228,64
8	168,28	179,72
9	142,54	148,95
10	125,06	131,94
11	83,55	120,01
12	66,33	93,23
13	52,45	77,91
14	41,22	54,37
15	29,04	40,22
16	19,59	31,82
17	7,83	19,44
18	1,61	7,26
19	0,99	1,99
20	0,01	0,01

Table 7.30: Dispersion of TDS in the Western direction within the aquifer

Timestep	Total Dissolved Solids Concentration (mg/l)	
	Well 1 (WW201045)	Well 2 (WW201637)
1	478,56	478,56
2	469,10	477,90
3	421,04	416,21
4	393,22	352,00
5	310,40	299,40
6	271,02	228,17
7	222,10	198,16
8	183,16	169,40
9	139,42	140,12
10	127,65	136,18
11	99,59	120,22
12	64,21	97,48
13	60,22	74,23
14	51,90	41,23
15	40,24	32,00
16	21,17	20,07
17	12,33	14,23
18	6,24	7,00
19	1,40	1,79
20	0,02	0,03

Table 7.31: Dispersion of TDS in the Eastern direction within the aquifer

Timestep	Total Dissolved Solids Concentration (mg/l)	
	Well 1 (WW201045)	Well 2 (WW201637)
1	478,56	478,56
2	469,10	469,20
3	382,27	428,17
4	325,27	367,93
5	300,04	319,40
6	286,24	233,61
7	241,71	203,19
8	176,36	174,73
9	152,19	136,10
10	132,54	128,92
11	111,02	108,92
12	73,21	87,19
13	68,78	66,43
14	53,30	44,90
15	33,26	39,28
16	13,14	21,14
17	10,78	12,33
18	5,73	6,49
19	1,49	2,01
20	0,03	0,01

7.2.4 Dispersion of *E-coli* within the aquifer

This section presents additional results, of *E-coli's* dispersion as a contaminant within the aquifer. These results are shown in Tables 7.32 to 7.35.

Table 7.32: Dispersion of *E-coli* in the Northern direction within the aquifer

Timestep	*E-coli* (counts/ml)	
	Well 1 (WW201045)	Well 2 (WW201637)
1	9,58	9,58
2	9,45	9,57
3	9,12	9,25
4	8,80	9,01
5	8,25	8,78
6	8,17	8,07
7	8,03	7,61
8	7,45	7,04
9	7,37	6,21
10	7,24	6,10
11	7,11	5,77
12	6,28	5,24
13	6,13	4,54
14	4,32	4,07
15	4,22	3,21
16	3,88	2,24
17	3,16	1,98
18	2,18	1,57
19	1,02	1,01
20	0,01	0,00

Table 7.33: Dispersion of *E-coli* in the Southern direction within the aquifer

Timestep	*E-coli* (counts/ml)	
	Well 1 (WW201045)	Well 2 (WW201637)
1	9,58	9,58
2	9,57	9,51
3	9,52	9,31
4	9,31	8,91
5	8,32	8,72
6	8,14	8,04
7	8,00	7,96
8	7,89	7,57
9	7,72	7,03
10	7,14	6,87
11	7,05	6,66
12	7,01	6,12
13	6,98	5,37
14	6,10	5,14
15	5,23	4,24
16	4,14	2,89
17	3,13	1,79
18	2,83	1,55
19	1,23	0,24
20	0,02	0,01

Table 7.34: Dispersion of *E-coli* in the Western direction within the aquifer

Timestep	*E-coli* (counts/ml)	
	Well 1 (WW201045)	Well 2 (WW201637)
1	9,58	9,58
2	9,54	9,57
3	9,04	9,05
4	8,54	8,95
5	8,02	8,61
6	7,91	7,62
7	7,64	7,17
8	7,04	6,11
9	6,67	6,03
10	6,03	5,84
11	5,98	5,28
12	5,73	4,97
13	4,86	4,72
14	3,94	3,14
15	3,25	3,00
16	2,01	2,73
17	1,56	2,17
18	1,04	1,29
19	0,08	1,11
20	0,04	0,01

Table 7.35: Dispersion of *E-coli* in the Eastern direction within the aquifer

Timestep	*E-coli* (counts/ml)	
	Well 1 (WW201045)	Well 2 (WW201637)
1	9,58	9,58
2	9,56	9,54
3	9,22	9,12
4	9,10	9,07
5	8,99	8,78
6	8,21	8,00
7	7,31	7,89
8	7,12	7,32
9	7,00	6,17
10	6,92	6,03
11	6,28	5,72
12	6,10	5,24
13	5,28	4,17
14	5,10	3,71
15	4,87	3,13
16	4,44	2,49
17	3,21	1,61
18	1,24	1,24
19	1,03	0,07
20	0,01	0,02

7.2.5 Ethics Clearance